NEUROPROTECTIVE ROLE OF LITHIUM-MEDIATED REST RESTORATION TO AMELIORATE OXIDATIVE STRESS IN DOWN SYNDROME CELL MODEL

By

LAM XIN JIEH

Thesis Submitted to the School of Graduate Studies, Universiti Putra Malaysia, in Fulfilment of the Requirements for the Degree of Master of Science

October 2024

FPSK (m) 2024 16

Abstract of thesis presented to the Senate of Universiti Putra Malaysia in fulfillment of the requirement for the Degree of Master of Science

NEUROPROTECTIVE ROLE OF LITHIUM-MEDIATED REST RESTORATION TO AMELIORATE OXIDATIVE STRESS IN DOWN SYNDROME CELL MODEL

By

LAM XIN JIEH

October 2024

Chairman : Associate Professor Cheah Pike See, PhD
Faculty : Medicine and Health Sciences

Caused by an extra human chromosome 21 (HSA21), Down syndrome (DS) is the most common genetic cause of cognitive impairment and early onset of aging. DS individuals usually manifest neurological deficits with neuropsychiatric disorders. Some of the overexpressed genes on HSA21 are responsible for antioxidative events that support and maintain neurogenesis and neuroplasticity. Dysregulation of these genes in DS individuals is likely to cause chronic oxidative stress, which is associated with neuropathologies seen in DS individuals. Repressor Element-1 Silencing Transcription factor (REST), a key player in the neuronal epigenome, has been reported to be dysregulated in the DS brain. Lithium, an FDA-approved drug for bipolar disorder, recently had been re-purposed for its neuroprotective roles against neurodegenerative diseases. Encouragingly, previous studies have proven the ability of lithium to restore REST in aging neurons. However, the

neuroprotective role of lithium in targeting oxidative stress in DS is not extensively investigated. Hence, this study aimed to investigate the neuroprotective potential of lithium to restore nuclear REST and ameliorate oxidative stress in DS *in vitro* model. In this study, 3 pairs of disomic wildtype and trisomic DS-induced pluripotent stem cell (iPSC) lines were procured. The iPSCs were differentiated into neural stem cells (NSCs), and then into neurons. Subsequently, immunocytochemistry (ICC) was performed at each developmental stage to characterize the cells. Prior to lithium treatment, cell viability assay was performed on eight different dosages of lithium (2.5, 5.0, 7.5, 10.0, 12.5, 15.0, 17.5 and 20.0 mM), to establish the range of safety dosage of lithium treatment in neurons. The neurons were then treated with 10 mM of lithium for 24 hours. To evaluate the post-treatment effect, nuclear REST expression in both control and DS untreated and lithium-treated neurons were quantified via ImageJ software. The DCFDA intracellular reactive oxygen species (ROS) assay was performed to measure the cellular ROS level in the lithium-treated and stress-induced neurons. From the ICC results, it revealed a successful characterization of cells in each development stage. Interestingly, the nuclear REST expression level which was found to be significantly lower in the trisomic DS neurons, has been successfully restored after being treated with lithium. When challenged with hydrogen peroxide (H_2O_2), the DS neurons exhibited significantly elevated ROS compared to the untreated ones, demonstrating inherently heightened vulnerability of DS neurons towards oxidative stress. In addition, upon H_2O_2 exposure, the lithium treatment has successfully reduced the ROS levels in control neurons to near-baseline level, proving that lithium can indeed combat oxidative stress. Collectively, these

findings showed a positive association between lithium treatment, REST restoration and oxidative stress. It is indeed exciting to discover that the REST dysregulation in DS neurons can be rescued via lithium treatment. Hence, this study suggested that repurposing lithium could be an impactful contribution towards the discovery of therapeutic strategies in DS neuropathologies.

Keywords: Down syndrome; iPSC-derived neurons; Lithium; Oxidative stress; REST

SDG: GOAL 3: Good health and well being

Abstrak tesis yang dikemukakan kepada Senat Universiti Putra Malaysia sebagai memenuhi keperluan untuk Ijazah Sarjana Sains

PERANAN NEUROPROTEKTIF LITIUM DALAM PEMULIHAN REST UNTUK MENGURANGKAN TEKANAN OKSIDATIF DALAM MODEL SEL SINDROM DOWN

Oleh

LAM XIN JIEH

Oktober 2024

Pengerusi : Profesor Madya Cheah Pike See, PhD
Fakulti : Perubatan dan Sains Kesihatan

Disebabkan oleh tambahan kromosom 21 manusia (HSA21), Sindrom Down (DS) adalah punca genetik paling umum bagi kelemahan kognitif dan permulaan awal penuaan. Individu DS biasanya menunjukkan defisit neurologi dengan gangguan neuropsikiatri. Sesetengah gen yang diekspres berlebihan pada HSA21 bertanggungjawab untuk peristiwa antioksidatif yang menyokong dan mengekalkan neurogenesis dan neuroplastisiti. Disregulasi gen-gen ini dalam individu DS berkemungkinan menyebabkan tekanan oksidatif kronik yang dikaitkan dengan neuropatologi yang dilihat pada individu DS. Faktor Transkripsi Pembisuan Elemen Penindas-1 (REST), pemain utama dalam epigenom neuron, dilaporkan mengalami disregulasi dalam otak DS. Litium, sejenis ubat yang diluluskan oleh FDA untuk merawat bipolar, kini digunakan semula untuk peranan perlindungan saraf terhadap penyakit degeneratif saraf. Secara menggalakkan, kajian terdahulu telah membuktikan keupayaan litium

untuk memulihkan REST dalam neuron penuaan. Walau bagaimanapun, sedikit atau tiada perhatian diberikan kepada peranan neuroprotektif litium dalam mensasarkan tekanan oksidatif dalam DS. Oleh itu, kajian ini bertujuan untuk mengkaji potensi neuroprotektif litium untuk memulihkan REST dan mengurangkan tekanan oksidatif dalam modal *in vitro* DS. Dalam kajian ini, 3 pasang sel stem pluripoten teraruh (iPSC) disomik (sebagai kumpulan terkawal) dan trisomik (sebagai kumpulan DS) telah diperolehi. iPSC dijadikan sel stem neural (NSC), dan kemudian menjadi sel neuron. Seterusnya, imunositokimia (ICC) dilakukan pada setiap peringkat perkembangan untuk mencirikan sel-sel tersebut. Sebelum rawatan litium, ujian kebolehidupan sel telah dijalankan pada lapan dos litium yang berbeza (2.5, 5.0, 7.5, 10.0, 12.5, 15.0, 17.5 dan 20.0 mM), untuk menentukan julat dos keselamatan rawatan litium dalam sel neuron. Sel-sel neuron kemudiannya dirawat dengan 10 mM litium selama 24 jam. Untuk menilai kesan pasca rawatan, ekspresi REST nuklear dalam kedua-dua sel neuron kawalan dan DS yang tidak dirawat dan dirawat dengan litium, dikuantifikasi melalui perisian ImageJ. Ujian spesies oksigen reaktif (ROS) intrasel DCFDA dilakukan untuk mengukur tahap ROS selular dalam sel neuron yang dirawat dengan litium dan diaruh tekanan oksidatif. Daripada keputusan ICC, ia menunjukkan pencirian sel yang berjaya pada setiap peringkat perkembangan sel. Secara mengejutkan, tahap ekspresi REST nuklear yang didapati jauh lebih rendah dalam sel neuron DS trisomik, telah berjaya dipulihkan selepas dirawat dengan litium. Apabila dicabar dengan hidrogen peroksida (H_2O_2), sel neuron DS menunjukkan peningkatan ROS yang ketara berbanding dengan yang tidak dirawat, menunjukkan kerentanan sel neuron DS yang sememangnya tinggi terhadap

tekanan oksidatif. Tambahan pula, selepas pendedahan H_2O_2, rawatan litium telah berjaya menurunkan tahap ROS dalam sel neuron disomik ke tahap hampir garis dasar, memberikan bukti konsep bahawa litium sememangnya boleh melawan tekanan oksidatif. Secara keseluruhannya, penemuan ini menunjukkan hubungan positif antara litium, pemulihan REST dan tekanan oksidatif. Penemuan yang menarik menunjukkan bahawa disregulasi REST dalam sel neuron DS boleh dipulihkan melalui penggunaan litium. Oleh itu, kajian ini mencadangkan bahawa penggunaan semula litium boleh memberi sumbangan berimpak ke arah penemuan strategi terapeutik dalam neuropatologi DS.

Kata kunci: Litium; Neuron daripada sel induk terimbas pluripoten; REST; Sindrom Down; Tekanan oksidatif

SDG: MATLAMAT 3: Kesihatan Yang Baik dan Sejahtera

ACKNOWLEDGMENTS

First and foremost, I would like to express my deepest and most sincere gratitude to my main supervisor, Associate Professor Dr. Cheah Pike See, for her guidance, support, and expertise throughout my research journey. Dr. Pike See has not only been patient and helpful in my Master's journey but has also shown genuine concern for my personal well-being throughout this challenging process. The same goes for my co-supervisor, Dr Sandra Manian, for whom I am profoundly grateful for her mentorship that extends far beyond the laboratory. Both Dr. Pike See and Dr. Sandra have shown their unwavering patience and kindness throughout this journey, and I truly appreciate having them as my supervisors.

Another lecturer to whom I am equally grateful is Professor Dr. Michael Ling King Hwa. Prof. Michael is very patient and always willing to spend time answering my doubts despite having a very tight schedule. His constructive critiques and specialized knowledge have significantly enhanced the quality of this work. The completion of this thesis would not have been possible without his mentorship and dedication.

Next, I am profoundly grateful to my family and friends for their unconditional love, patience, and moral support throughout this challenging academic pursuit. Their belief in me has been a constant source of motivation, especially during the most demanding phases of this research. Special thanks to my fellow friends from the NeuroBiology and Genetics Group (NBGG), for their

continuous support. I would never forget those bittersweet moments that we had throughout the past 2.5 years.

I extend my sincere appreciation to the university faculty, for providing access to laboratory facilities and resources crucial for my research. Staff in the Medical Genetics and Stem Cell Research Laboratory have helped facilitate my experiments and ensure smooth operations. I would also like to acknowledge the suppliers, for their reliable provision of high-quality reagents and consumables essential for my research. Not to forget the fundings that had been received: FRGS grant from the Malaysia Ministry of Higher Education awarded to Dr. Pike See (FRGS/1/2021/SKK06/UPM/02/4), and also the IBRO and ISN Return Home Grants (Vot: 6380075) awarded to Prof. Michael. This study would not have been possible without these fundings.

The thesis was submitted to the Senate of Universiti Putra Malaysia and has been accepted as fulfilment of the requirement for the degree of Master of Science. The members of the Supervisory Committee were as follows:

Cheah Pike See, PhD
Associate Professor
Faculty of Medicine and Health Sciences
Universiti Putra Malaysia
(Chairman)

Sandra Maniam, PhD
Senior Lecturer
Faculty of Medicine and Health Sciences
Universiti Putra Malaysia
(Member)

_____
ZALILAH MOHD SHARIFF, PhD
Professor and Dean
School of Graduate Studies
Universiti Putra Malaysia

Date: 13 January 2025

TABLE OF CONTENTS

LIST OF TABLES

LIST OF FIGURES

LIST OF ABBREVIATIONS

2D	Two dimensional
3D	Three dimensional
AD	Alzheimer's disease
APP	Amyloid-beta precursor protein
ATCC	American Type Culture Collection
ATP	Adenosine triphosphate
Aβ	Amyloid-beta
BD	Bipolar disease
BACH1	BTB and CNC homology 1
BDNF	Brain-derived neurotrophic factors (BDNF)
BrdU	5-bromo-2-deoxyuridine
BRG1	Brahma-related gene 1
C	Control
CAT	Catalase
CO_2	Carbon dioxide
CREB	cAMP-response element binding protein
CRHR1	Corticotropin-releasing hormone receptor 1
CTBP1	Carboxy-terminal binding protein 1
CTDSP1	C-terminal domain small phosphatase 1
DAPI	4′,6-diamidino-2-phenylindole
DCF	2,7-dichlorodihydrofluorescein
DCFDA	2',7'-dichlorofluorescein diacetate
DIV	Days *in vitro*
DMSO	Dimethyl sulfoxide

DNA	Deoxyribonucleic
DPBS	Dulbecco's phosphate buffered saline
DS	Down syndrome
DYRK1A	Dual specificity tyrosine phosphorylation regulated kinase 1A
ESC	Embryonic stem cell
FDA	Food and Drug Administration
FITC	Fluorescein isothiocyanate
GGT	Gamma-glutamyltransferase
GPx	Glutathione peroxidase
GR	Glutathione reductase
GSH	Glutathione
GSK-3β	Glycogen synthase kinase-3β
GST	Glutathione S-transferase
H_2O_2	Hydrogen peroxide
HD	Huntington’s disease
HDAC	Histone deacetylase
HGP	Human Genome Project
HIF-1	Hypoxia-inducible factor 1
HSA21	Human chromosome 21
ICC	Immunocytochemistry
ID	Intellectual disability
IL-β	Interleukin 1 beta
IMP	Inositol monophosphatase
INSM1	Insulinoma-associated 1
iPSC	Induced pluripotent stem cell
IQ	Intellectual quotient

JAK-STAT	Janus Kinase-Signal Transducer and Activator of Transcription
Li_2CO_3	Lithium carbonate
LiCl	Lithium chloride
LPS	Lipopolysaccharide
LSD1	Lysine-specific histone demethylase
Mb	Megabase
MeCP2	Methyl-CpG binding proteins
mGluR5	Metabotropic glutamate receptors 5
Mmu	Mouse chromosome
MPO	Myeloperoxidase
MPP	1-methyl-4-phenyl-1,2,3,6-tetrahydropyridine
mRNA	Messenger ribonucleic acid
MTT	3-(4,5-dimethylthiazol-2-yl)-2,5-diphenyl-2H-tetrazolium bromide
NCARDRS	National Congenital Anomaly and Rare Disease Registration Service
NLS	Nuclear localization sequence
NO	Nitrogen oxide
NPC	Neural progenitor cells
NRF2	Nuclear factor erythroid 2–related factor 2
NRSF	Neuron-restrictive silencing factor
ns	Not significant
NSC	Neural stem cell
OXPHOS	Oxidative phosphorylation
P	Passage
PBS	Phosphate buffered saline
PCR	Polymerase chain reaction

PD	Parkinson’s disease
PDL	Poly-D-lysine
PFA	Paraformaldehyde
PGE_2	Prostaglandin E_2
PRDX2	Peroxiredoxin 2
RCOR1/2	REST corepressors 1 / 2
REST	Repressor element-1 silencing transcription factor
RILP	REST/NRSF-Interacting LIM Domain Protein
ROCKi	Rho-associated protein kinase inhibitor Y-27632
ROI	Region of interest
ROS	Reactive oxygen species
ROUT	Robust regression and outlier removal
SOD1	Superoxide dismutase 1
SVZ	Subventricular zone
TBARS	Thiobarbituric acid reactive substances
TBHP	Tert-butyl hydroperoxide
TBI	Traumatic brain injury
TNF-α	Tumor necrosis factor-alpha
TUJ1	Beta-tubulin III
VEGF	Vascular endothelial growth factor

CHAPTER 1

INTRODUCTION

1.1 Background

Down Syndrome (DS) is a common genetic disorder resulting from an extra copy of chromosome 21. According to the National Congenital Anomaly and Rare Disease Registration Service (NCARDRS) Congenital Anomaly Official Statistics Report in 2020, the live birth prevalence of DS in England was one in 873 live births (NHS England Digital, 2022). In Malaysia, the prevalence of giving birth to a DS baby was 1 in 860 to 1 in 981 (Shabri, 2019). Individuals with DS typically manifest various comorbidities affecting multiple body systems. It is widely recognized as the most common genetic cause of intellectual disability and early onset of aging (Rachidi & Lopes, 2007; Santoro et al., 2021). The pathogenesis of DS phenotypic features can be attributed to the gene dosage imbalance resulting from the triplicated chromosome 21 (Gardiner, 2004). The overexpression of genes on chromosome 21 directly or indirectly influences the expression of genes mapped to different chromosomes. Some of these genes are associated with oxidative stress in DS (Izzo et al., 2018). Consequently, chronic oxidative stress events are strongly linked to neurodevelopmental disorders and early neurodegenerative symptoms observed in DS individuals (Valenti et al., 2018).

Repressor Element-1 Silencing Transcription factor (REST) is a transcription repressor that is a key initiator of epigenetic neuronal gene-expression modification. It plays a crucial role in neural development, function, survival, and stress-resilience (Lam et al., 2023). In a healthy aging brain, REST is upregulated and consolidated within the nucleus to protect aging neurons from various stressors, a process that was found to be aberrant in Alzheimer's disease (Lu et al., 2014). Previous studies reported reduced REST expression in DS models (Bahn et al., 2002; Canzonetta et al., 2008; Lepagnol-Bestel et al., 2009; Lim et al., 2024). However, the relationship between REST levels and its protective function in DS remains unclear.

Encouragingly, the DS brain phenotype can potentially be rescued through pharmacological approaches (Stagni et al., 2015). Lithium, the first-line therapeutic agent for treating bipolar disorders and major depression, has recently gained attention for its neuroprotective roles against neuropsychiatric and neurodegenerative diseases (Puglisi-Allegra et al., 2021; Quiroz et al., 2010). A previous study demonstrated that lithium chloride successfully induced the activation of REST in aging brain neurons (Lu et al., 2014). However, little attention has been given to the neuroprotective role of lithium in targeting oxidative stress in DS, which leads to neuronal impairments. Therefore, an in-depth understanding of the neuroprotective role of lithium in DS is needed as fundamental research towards rescuing the defective homeostatic mechanisms in DS.

1.2 Hypothesis

An optimum dosage of lithium can restore nuclear REST expression and ameliorate oxidative stress in trisomic Down syndrome iPSC-derived neurons.

1.3 Objectives

In general, this study aims to investigate the neuroprotective role of lithium-mediated REST restoration in ameliorating oxidative stress in trisomic DS iPSC-derived neurons.

Apart from that, there are three specific objectives in this study:

1. To establish and characterize the disomic and trisomic neurons derived from DS induced pluripotent stem cells (iPSC).
2. To investigate the restoration of nuclear REST expression levels mediated by an effective lithium dosage, in DS iPSC-derived neurons.
3. To investigate the rescue effect of lithium to reduce reactive oxygen species (ROS) levels in DS iPSC-derived neurons.

CHAPTER 2

LITERATURE REVIEW

2.1 Down Syndrome (DS)

Named after John Langdon Down in 1866, Down syndrome (DS) is the most common genetic cause of intellectual disability. Almost all DS individuals suffer from intellectual disability to some extent that it appears to be the major clinical manifestation of DS (Noble, 1998). According to the Malaysia Ministry of Health, the prevalence of giving birth to DS baby in Malaysia was 1 in 860 to 1 in 981 (Shabri, 2019). With increasing societal awareness, individuals with DS in Malaysia can look forward for better educational opportunities, medical guidance and improved quality of life in the future. DS is a common form of chromosomal abnormality that affects nearly all systems in the body (Patterson & Costa, 2005). The association of DS with the chromosome 21 (HSA21) was established by Dr. Jerome Lejeune in Paris in 1959, where he observed that DS is caused by a partial or full third copy of chromosome 21. Hence, DS is also well known as Trisomy 21 and it is the most prevalent chromosomal abnormality or the most frequently occurring live-born aneuploidy in humans (Akhtar & Bokhari, 2023).

There are three distinct types of DS, each characterized by specific chromosomal anomalies. Distinguishing between these types based solely on chromosomal analysis for accurate diagnosis (Shin et al., 2010; Whitbourne,

2024). The first type is Trisomy 21, which accounts for approximately 95% of DS cases. Each cell in the body possesses three copies of HSA21 instead of the typical two copies in this type. The second type is translocation DS which is less common, affecting about 3% of individuals with DS. Translocation DS arises when an additional part or an entire extra HSA21 is present, but instead of being separate, it is attached or translocated to a different chromosome. The third type which is mosaic DS, is observed in around 2% of DS individuals. In this type, some cells contain three copies of HSA21, while other cells maintain the typical two copies. Individuals with mosaic DS may exhibit fewer characteristics of the condition due to the presence of some cells with normal chromosome count (Shin et al., 2010; Whitbourne, 2024).

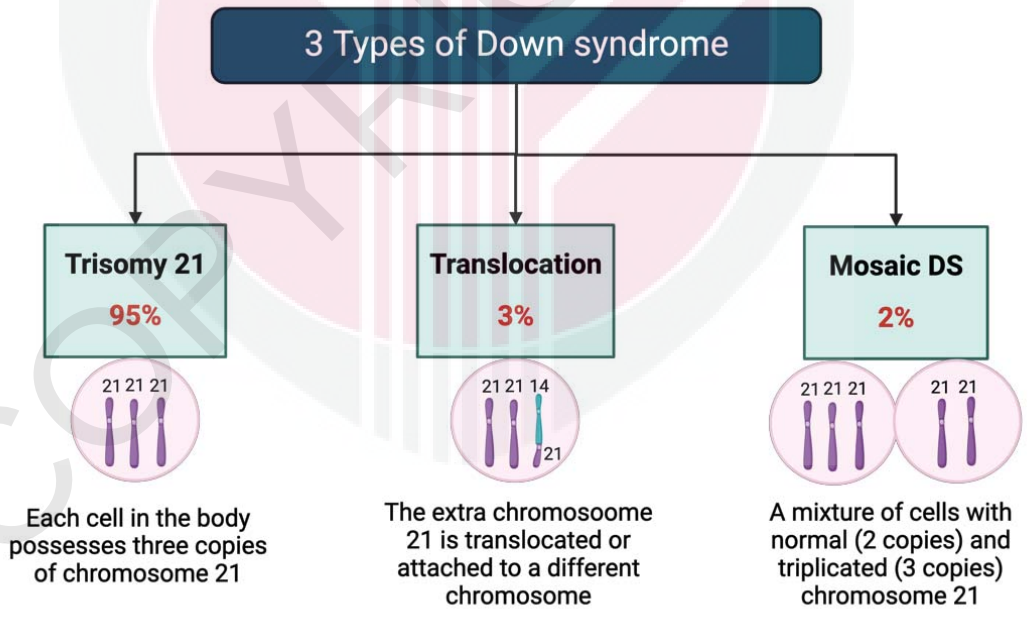

Figure 1: The three types of Down syndrome and their corresponding chromosomal abnormalities.

2.1.1 Clinical Manifestations of DS

The additional HSA21 gives rise to several clinical manifestations and pathologies in DS throughout the pre- and postnatal development (Dierssen et al., 2009). Several typical physical features of a DS individual include reduced muscle tone (hypotonia), shortened neck with excessive skin at the back, flattened facial appearance, upward slanting eyes, short limbs, widened gap between the first and second toes, and a single, deep line across the hand palm (Bull et al., 2011; Kaneshiro, 2023).

In addition, individuals with DS are also presented with several clinical manifestations that have significant impacts on their overall wellbeing and quality of life. For instance, cardiovascular disease which is frequently being described among DS individuals, is the predominant cause of their morbidity and mortality. The most common cardiovascular condition is contributed by congenital heart disease which can be found in almost 50% of DS individuals. (Benhaourech et al., 2016; Dimopoulos et al., 2023). Other than cardiovascular diseases, DS individuals also suffer from endocrinal abnormalities such as dysregulated thyroid function, overweight, diabetes mellitus, vitamin D deficiency, low bone mineral density, and dysregulated gonadal function (Hetman & Barg, 2022; Metwalley & Farghaly, 2022).

Another common pathological condition seen in DS individuals is immune dysregulation. In fact, DS happens to be the most well-known genetic cause of immune defects (Bordon, 2023; Huggard et al., 2020). Previous studies

suggested that the immune system disturbances in DS might arise from the heightened interferon responses or thymic disturbances. This is because the genes encoding for majority of the interferon receptor subunits and the autoimmune regulator transcription factors are located in the HSA21 (Bordon, 2023; Malle et al., 2023). Furthermore, it is also very common in individuals with DS to have defects in the digestive system. Such gastrointestinal symptoms include vomiting, diarrhea, constipation and abdominal discomfort. Parents often face difficulties in feeding their DS children as well (Holmes, 2014; Ravel et al., 2020). Apart from the above-mentioned clinical presentations, some other medical conditions being reported in DS individuals include neurological deficits (Chen & Zuo, 2024; Hasina et al., 2022; López-Hidalgo et al., 2024), hematological complications (Santoro et al., 2016; Triarico et al., 2022), obstructive sleep apnea (Li et al., 2024; Ong et al., 2024), visual impairment (Martin-Perez et al., 2023; Wilton et al., 2021) and auditory impairment (Yam et al., 2008).

2.1.2 Neurological Defects in DS

Since the culprit of DS originates from the triplication of HSA21, it is crucial to investigate the functionality of the HSA21 genes to understand in-depth the causes and mechanisms behind DS pathologies. As per findings of the Human Genome Project (HGP), chromosome 21 was the second chromosome to be fully sequenced following chromosome 22 (International Human Genome Sequencing Consortium, 2001; 2004). By the year 2000, the sequencing of HSA21 revealed 225 genes and 59 pseudogenes (Hattori et al., 2000).

Currently, 202 of the genes were classified as known genes and 23 of them as predicted genes. Among the known genes, 44 are linked to DS disorders, and 35 out of these 44 DS-linked genes were associated with brain disorders in DS. Notably, only 21 genes (10.40%) of HSA21 have been studied in human brains with DS, indicating not all genes associated with brain disorders in DS have been investigated in DS human brains yet (Hasina et al., 2022).

Concerning neurological deficits in DS, intellectual disability (ID) and early onset of Alzheimer disease (AD) have gained much attention from researchers recently. It is postulated that the intelligence quotient (IQ) is highly associated with the total brain volume (McDaniel, 2005). In DS individuals whose IQ is greatly reduced compared to those of the same age, there is evidence that their brain volume is significantly reduced as well. In DS infants that were 2 to 6 months old, their brain weight is 1.2-fold lesser than those similar-aged normal infants (Schmidt-Sidor et al., 1990). In DS children of 7 to 16 years old, they had a 1.1-fold reduction in total intracranial volume compared to the similar-aged normal children (Carducci et al., 2013). A recent study reported that the defects in DS brain development started since gestation period, where reduced cerebellar volume was noticed in the DS fetus since the 21st week of gestation, while deviation in the cortical development was apparent in the third trimester (Patkee et al., 2020).

Moreover, sulci and gyri which make up the brain folding, increase the brain surface area and hence are believed to enhance the behavioural and intellectual ability (Haines & Mihailoff, 2018; Stiles & Jernigan, 2010). In 5 to

24 years old DS individuals, there was a 1.1-fold increment in the cortical thickness and 1.1-fold reduction in the brain total surface area when compared to age-matched normal controls (Lee et al., 2016). Another study also reported a 1.2-fold reduction in the DS superior temporal gyrus of DS 5 to 23 years old individuals (Pinter et al., 2001). Collectively, these reports suggested that DS individuals have smaller brains with fewer superficial sulci and gyri, which in turn causes them to have a lissencephalic or smooth brain surface, eventually resulting in overall cognitive and neurodevelopmental defects (Haines & Mihailoff, 2018).

Any changes to the brain anatomical structure at the cellular level before birth can mirror deviations in the gross anatomy of the foetal brain (Stiles & Jernigan, 2010). Looking into the DS brain development at the cellular level, a study conducted from the 14th week of gestation till birth, observed that the DS population have fewer neurons and disrupted myelination in the cerebral cortex and hippocampal regions (Kanaumi et al., 2013). The balance between the population of astrocytes, oligodendrocytes, microglia and macrophages were also disrupted throughout the prenatal development, which impaired the proper neurogenesis process. This may be the root cause of cognitive impairment in DS individuals (Kanaumi et al., 2013).

Apart from having impaired neurodevelopment which causes intellectual disability, there is also a strong association between early onset of aging and DS. Individuals with DS tend to develop symptoms of AD by the age of 40, and the prevalence increased further in DS elderly over 65 years old (McCarron et

al., 2017; Wiseman et al., 2015). Moreover, it was reported that AD is the main cause of fatality in >30% of the DS population (Hithersay et al., 2019; Landes et al., 2020). DS individuals have a higher risk of developing AD because they have an extra copy of chromosome 21, which contains the amyloid-beta precursor protein (APP) gene responsible for causing AD. The overexpressed *APP* gene in trisomy 21 is the main reason for several amyloid-beta (Aβ) neuropathology seen in DS individuals. The defective Aβ will misfold into amyloid plaques which eventually leads to AD progression (Nistor et al., 2007; Tosh et al., 2021). Besides *APP* gene, other overexpressed genes located at HSA21 contributing to AD progression in DS includes *ETS2, SUMO3, DYRK1A,* and *BACE2* (Gomez et al., 2020; Wiseman et al., 2015). There are elevated levels of Aβ in DS individuals, Further study found that Aβ accumulates mainly in the cells of DS neonates and children. However, as the age increases, deposition of Aβ plaques can be found in the extracellular environment. These diffused Aβ plaques are responsible for the neuroinflammatory responses in DS brains (Aranha et al., 2022; Gensous et al., 2020; Head et al., 2018).

2.1.3 Implications of Oxidative Stress in DS Neuropathology

Oxidative stress plays a critical role in brain development in DS individuals (Buczyńska et al., 2023). A comprehensive meta-analysis of 45 DS-related gene expression studies revealed elevated expression of *SOD1*, which encodes superoxide dismutase, an enzyme responsible for breaking down superoxide radicals (Izzo et al., 2018). According to Buczyńska et al. (2023),

the overexpression of SOD1 eventually leads to excessive H_2O_2 production, overwhelming the antioxidant enzymes catalase (CAT) and glutathione peroxidase (GPx), resulting in cytosolic accumulation and reactive oxygen species (ROS) formation in DS. Due to extensive exposure to oxidative stress during the prenatal period, it is postulated that a decline in the compensatory antioxidant capacity of cells may exacerbate oxidative-related comorbidities, including cognitive phenotypes (Buczyńska et al., 2023).

In addition to *SOD1* overexpression, alterations in other components of the endogenous antioxidant system contribute to ROS accumulation in DS. For instance, reduced expression of peroxiredoxin 2 (*PRDX2*) in DS fetal brain samples affects the redox state comparably to increased *SOD1* expression (Sánchez-Font et al., 2003). A study by Hamed et al. (2011) found that glutathione S-transferase enzyme (GST) activity was reduced to 40.9% in the DS group compared to controls, while glutathione (GSH) concentration decreased to 60.6%. This relative GSH deficiency may increase vulnerability to ROS-mediated diseases and tissue damage.

The impact of oxidative stress on DS brain development has been long recognized. Busciglio & Yankner (1995) first showed that cortical neurons from fetal DS brains exhibited 3 to 4-fold-increase in oxidative stress along with increased lipid peroxidation, which eventually accelerated death in culture compared to control neurons. The degeneration of DS neurons was prevented by treatment with antioxidants. These findings provided initial conclusion that DS neurons have a defect in ROS metabolism that causes neuronal apoptosis,

which may contribute to mental retardation and AD in DS individuals. Lott et al. (2006) also reported that individuals with DS display signs of premature brain aging, including early Alzheimer's-like pathology, potentially linked to chronic oxidative stress.

Oxidative stress also damages mitochondria, causing energy deficits in neurons and exacerbating oxidative damage. Mitochondrial dysfunction in DS is associated with increased oxidative stress, contributing to neuronal impairment (Tan et al., 2023). Mitochondria rely heavily on oxidative phosphorylation (OXPHOS) for energy production, involving four complexes and ATP synthase within the mitochondrial membrane to synthesize ATP (Kühlbrandt, 2015). Studies in DS have reported reductions in mitochondrial complex I enzyme $NADH_3$ in the adult cerebellum (Krapfenbauer et al., 1999), and significant decreases in mitochondrial complex I and ATP synthase in aging cerebrum and DS mouse models (Bambrick & Fiskum, 2008; Valenti et al., 2016). These findings align with recent research indicating dysregulation of OXPHOS machinery proteins following overexpression of *Dyrk1a*, a HSA21 gene potentially overexpressed in DS (Ortega et al., 2022). Given the impaired OXPHOS observed in DS, disruptions in energy production are expected.

Understanding the role of oxidative stress in DS brain development has prompted research into antioxidant therapies as potential interventions. For example, Lockrow et al. (2009) demonstrated that long-term antioxidant treatment in a DS mouse model improved cognitive function and reduced oxidative damage in the brain, suggesting promising avenues for future

therapeutic approaches. Furthermore, Parisotto et al. (2015) examined the effects of vitamin E and C supplementation on oxidative stress in DS individuals over 1.5 years. Results showed significant reduction in oxidative stress markers [SOD, CAT, GPx, glutathione reductase (GR), gamma-glutamyltransferase (GGT), myeloperoxidase (MPO) and thiobarbituric acid reactive substances (TBARS)], with benefits persisting even after stopping supplementation. While antioxidant enzymes decreased, GSH and vitamin E levels increased, and lipid peroxidation reduced. The findings suggest antioxidant supplementation may be beneficial for managing oxidative stress in DS (Parisotto et al., 2015).

2.2 Repressor Element-1 Silencing Transcription (REST)

During the process of brain development, neural progenitor cells need to progress through multiple crucial phases to become fully functional mature neurons eventually (Alberts et al., 2002). Concurrently, it is vital to have a neuroprotective mechanism in place to shield the neurons from different stressors. This protective function is facilitated by a zinc finger repressor referred to as repressor element-1 silencing transcription factor (REST) or neuron-restrictive silencing factor (NRSF), which is integral to this entire process (Lam et al., 2023). Given that REST expression is significantly downregulated in DS *in vivo* models (Lepagnol-Bestel et al., 2009; Lim et al., 2024), understanding its neuroprotective role and potential therapeutic implications makes it a compelling target for the current study.

2.2.1 REST and its Cofactors

REST itself does not solely accomplish the regulation exerted by REST over the neurogenic lineage program, it relies on the recruitment of a series of corepressors and the involvement of several regulatory factors. The complete protein structure of REST consists of three primary functional domains: at the N-terminal and C-terminal respectively, there are two repressor domains at each side, and near the N-terminal, there is a DNA binding domain housing a cluster of eight zinc fingers (Chong et al., 1995; Tapia-Ramírez et al., 1997). Interaction between REST and its RE-1 binding site prompts the repressor domains to recruit corepressors and epigenetic regulatory factors, leading to a cascade of transcriptional inhibitory processes mediated by REST.

When REST binds specifically to its binding site, the N-terminal repressor domain recruits the corepressor mSin3A, creating a platform for histone deacetylase (HDAC) binding. Consequently, localized histone deacetylation at the promoter region induces nucleosome compaction, inhibiting the transcriptional activation machinery and resulting in transcriptional repression (Grimes et al., 2000; Naruse et al., 1999). Conversely, the C-terminal repressor domain recruits another corepressor, coREST, which attracts regulatory factors crucial for the transcriptional epigenetic modification process. These cofactors include HDAC, methyl-CpG binding proteins (MeCP2), histone methyltransferase G9A, lysine-specific histone demethylase 1A (LSD1), carboxy-terminal binding protein 1 (CTBP1), and the ATP-dependent chromatin-remodeling enzyme brahma-related gene 1 (BRG1), all

of which stabilize the REST-RE1 interaction. This complex of epigenetic regulatory cofactors is crucial to ensure a proper function of REST transcriptional regulation (Ballas et al., 2001; Mari´a et al., 1999). The complete protein structure of REST is illustrated in **Figure 2**.

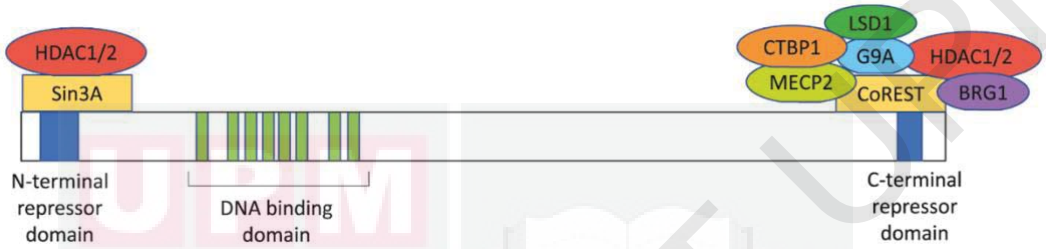

Figure 2: The complete protein structure of REST. The complete protein structure of REST consists of three primary functional domains: N-terminal and C-terminal repressor domains, and a DNA binding domain near the N-terminal that houses a cluster of eight zinc fingers. The N- and C-terminal repressor domains recruit cofactors to form a complex of epigenetic regulatory cofactors (Mampay & Sheridan, 2019).

2.2.2 Nuclear Localization of REST

As a transcription factor, REST's presence in the nucleus is crucial for its role in regulating transcription. Initially, researchers identified a nuclear localization sequence (NLS) in REST C-terminal and proposed that this sequence is responsible for REST nuclear trafficking and binding to its site (Chong et al., 1995; Grimes et al., 2000). Surprisingly, even a truncated splice variant of REST, known as REST4, can still be transported into the nucleus. Further exploration indicates that signals for nuclear trafficking may lie within zinc fingers 2 to 5 (Shimojo et al., 2001). Another variant, REST1, which has only four zinc fingers, is found predominantly in the cytosol, suggesting that the NLS for nuclear targeting is located within zinc finger 5 of REST (Shimojo, 2006).

Moreover, the group of researchers investigated further and discovered the REST/NRSF-Interacting LIM Domain Protein (RILP) that refreshed our understanding on the mechanism of REST's nuclear trafficking. RILP, positioned at the outer nuclear membrane, acts as a receptor for nuclear translocation for both REST and REST4, with specific motifs essential for its function. The interaction between REST and RILP facilitates nuclear translocation of REST, while mutations in RILP motifs lead to the cytosolic localization of REST (Shimojo & Hersh, 2003, 2006).

Nuclear translocation of REST is essential for its neuroprotective function in the brain. Whenever there is a stress event in a healthy aging brain, REST will be triggered to translocate into the nucleus to exert neuroprotection by repressing genes that promote cell death and inducing stress response genes. However, in the diseased aging neurons, REST localization is dysregulated resulting in impaired neuroprotection (Lam et al., 2023). Comparing Alzheimer's and Parkinson's disease brains to healthy aging brains reveals a lack of nuclear REST, indicating a loss of neuroprotection and stress resilience (Kawamura et al., 2019; Lu et al., 2014; Mampay et al., 2021; Meyer et al., 2019). Conversely, aging brains affected by Huntington's disease exhibit abundant nuclear REST due to mutant huntingtin proteins in the cytoplasm unable to sequester REST, leading to an over-repression of neuronal genes like brain-derived neurotrophic factors (BDNF) and constraining neuroprotection (Zuccato et al., 2003).

In a healthy adult brain, REST exhibits neuroprotective functions through insulin-like growth factor- and protein kinase C-mediated regulation of μ-opioid receptor expression, thereby promoting neuronal survival during stress and injury (Bedini et al. 2008, 2010). Whereas in healthy aging brains, REST levels increase in the prefrontal cortex and hippocampus, upregulating stress response genes while downregulating cell death genes (Lu et al., 2014). Study by Lu and colleagues showed that REST knockout in SH-SY5Y cells led to in dysregulation of FOXO1 (a transcription factor known for its role in oxidative stress resistance) followed by increased ROS and oxidative DNA damage. When the condition was reversed, REST overexpression had reduced neuronal death and enhanced nuclear localization, highlighting its crucial role in protecting against oxidative damage and maintaining cognitive function during aging (Lu et al. 2014).

2.2.3 Role of REST in the Developing Brain

The expression of REST is closely associated with the different stages of neuronal cell development. Within the central nervous system, REST is notably present in undifferentiated neural stem cells (NSCs) and differentiated non-neuronal cell types but not in mature neurons (Chong et al., 1995; Mori et al., 1992; Schoenherr & Anderson, 1995). Recent research highlights heightened REST expression during embryonic brain development, with its regulation mediated by corticotropin-releasing hormone receptor 1 (CRHR1)-induced cAMP-response element binding protein (CREB) activity (Kwon et al., 2023). This suggests that REST may uphold NSC stemness through the

repression of neuronal genes. Indeed, protein expression analyses of cortical progenitors and neurons support an inverse correlation between REST and TUJ1, a marker for differentiated neurons (Ballas et al., 2005). Conversely, REST expression is elevated in both developing hippocampal progenitors and mature neurons (Sun et al., 2005), indicating varied functions of REST across neural developmental stages and neuronal populations.

Downregulating REST is imperative for proper neuronal development. As a suppressor of neuronal differentiation, REST must be inactivated or silenced to facilitate the differentiation process. NeuroD2 protein, part of the neurogenic program, plays a pivotal role in REST inactivation during neuronal differentiation. NeuroD2 activates the transcription repressor Zfhx1a, which in turn suppresses REST, initiating neuronal differentiation (Ravanpay et al., 2010). Introducing REST into differentiating neurons significantly increases axon guidance errors in commissural neurons (Paquette et al., 2000) and disrupts neuronal differentiation in the hippocampus (Ravanpay et al., 2010). Upregulated REST expression in neural progenitor cells (NPC) results in disrupted radial migration during neurogenesis (Mandel et al., 2011).

Despite its role in prompting neuronal differentiation, REST is also crucial for promoting the self-renewal and pluripotency of NPCs. Deleting REST from E12.5 NPCs reduces the number and size of neurospheres compared to control NPCs (Covey et al., 2012). Premature elimination of REST from NPCs leads to catastrophic DNA damage during the S-phase of the mitosis cycle, causing premature cell cycle exit—a phenomenon termed precocious neuronal

differentiation. This condition is marked by abnormal chromosome division, cell apoptosis, and a depleted progenitor pool (Nechiporuk et al., 2016). Mice lacking REST exhibit smaller brains, reduced cortical thickness, and hippocampal size, along with disorganized cell arrangement in the subgranular zone and spinal defects, underscoring the importance of REST in postnatal development (Kim et al., 2015; Wang et al., 2021). Thus, REST remains crucial during neurogenesis to safeguard genomic integrity until the terminal stages of neuronal differentiation. In summary, downregulation of REST is vital to initiate neuronal differentiation while maintaining minimal levels of REST is essential for neuronal integrity and survival. Hence, regulating REST expression levels is critical for achieving an optimal balance between neural progenitor proliferation and differentiation.

The regulation of REST during neurogenesis is controlled by two main pathways. The first pathway determines whether REST is stabilized or degraded: CTDSP1 stabilizes REST in stem cells to maintain self-renewal, while ERK phosphorylation and Pin1 activation trigger REST degradation to promote neuronal differentiation (Burkholder et al. 2018; Nesti et al. 2014). The second pathway involves the INSM1-RCOR1/2 complex, where its absence leads to REST upregulation and causes severe brain developmental defects, characterized by excessive neural progenitors and reduced mature neurons (Monaghan et al. 2017). MicroRNAs, including miR-26, miR-124, and miR-9 families, provide additional regulation of REST during neuronal differentiation (Birtele et al. 2019; Sauer et al. 2021). Understanding these regulatory

mechanisms offers potential therapeutic targets for REST modulation in brain development.

2.2.4 Implications of REST Dysregulation in DS Neuropathology

Since DS is a medical condition mainly evident through neurodevelopmental defects, it would be interesting to find out the association between DS neuropathology and REST. The first discovery of REST dysregulation in DS was initially identified by Bahn et al., who noted a significant decrease in REST and its spliced variants in DS NPCs. These cells, when differentiated into neurons, displayed heightened apoptosis and exhibited abnormal morphology such as shortened and convoluted neurites, along with excessive side branching (Bahn et al., 2002). Similarly, two DS mouse models, Tc1 and Ts1Cje, showed reduced REST expression (Canzonetta et al., 2008). However, in the embryonic 152F7 DS mouse model, REST was upregulated compared to wildtype mice, whereas in postnatal mice, it was downregulated (Lepagnol-Bestel et al., 2009). The expression of REST across different DS models appears inconsistent in these studies. A recent study by Lim and colleagues who conducted a comprehensive spatiotemporal profiling of REST in the Ts1Cje DS mouse model, reported significantly reduced REST expression in both DS cultured neurospheres and adult DS mice brains. This study also reported REST nuclear mislocalization in the DS model for the first time (Lim et al., 2024).

The dysregulation of REST in DS arises from imbalance expression of the dual specificity tyrosine phosphorylation regulated kinase 1A (DYRK1A) gene located on HSA21 (Canzonetta et al., 2008; Lepagnol-Bestel et al., 2009). *DYRK1A* interacts with a SWI/SNF complex recruited by REST. This interaction appears to be tightly regulated because both over-activation and inhibiting *Dyrk1a* lead to persistent suppression of *Rest* in all DS adult mice models. Notably, this phenomenon was absent in DS embryonic samples, suggesting a connection between chromatin status (expected to differ between embryonic and adult mice) and *Rest* expression (Lepagnol-Bestel et al., 2009). Another study by Lu et al. (2011) proposed a negative feedback loop between DYRK1A and REST: REST activates DYRK1A by binding to its promoter, while an imbalance in DYRK1A dosage deactivates REST by promoting its ubiquitination and subsequent degradation. This close relationship between DYRK1A and REST is crucial for nervous system development (Lu et al., 2011).

2.3 Lithium

Being approved by the United States Food and Drug Administration (FDA) in 1970, lithium serves as the first line drug for bipolar or manic diseases (Ruffalo, 2017). Despite maintaining as the gold standard drug for bipolar disorders, the administration of lithium has been gradually reduced for the past few years due to its potential side effects such as nausea, diarrhea, weight gain and tremor (Nall, 2024). Once committed to the lithium prescription, the patient's serum markers need to be monitored to ensure safe therapeutic doses (Baldessarini et al., 2019; Tondo et al., 2019). Apart from its application in treating

neuropsychiatric diseases, lithium has also been proven for its positive therapeutic effects towards neurodegenerative diseases such as AD and PD.

2.3.1 Neuroprotective Potential of Lithium

In the past 30 years, emerging research evidence has demonstrated the neuroprotective potential of lithium from both preclinical and clinical aspects. In preclinical studies, it was reported that the presence of lithium has greatly reduced tau phosphorylation in neuronal cell culture (Hong et al., 1997; Muñoz-Montaño et al., 1997; Tajes et al., 2008) and also facilitates amyloid-beta clearance in AD transgenic mice brains (Pan et al., 2018; Zhang et al., 2011), in which both are the key pathological hallmarks of AD. Interestingly, chronic low dose lithium treatment in AD transgenic mice have shown positive outcomes in the mice behavioural studies such as improvement in spatial learning and memory capabilities (Liu et al., 2020; Pan et al., 2018). In addition, an earlier study discovered that when lithium was treated together in the presence of another drug known as rosiglitazone, the AD transgenic mice showed improved spatial memory, reduced amyloid-beta plaques, and also reduced activation of astrocytes and microglia. It was suggested that the positive neuroprotective outcomes of both drugs are possible due to the activation of the Wnt signaling pathway (Toledo & Inestrosa, 2010). Apart from AD, lithium was also found to be potentially useful against post-traumatic memory impairments. In a traumatic brain injury (TBI)-induced mouse model, lithium treatment tends to attenuate the TBI-induced amyloid-beta load and subsequently improves spatial memory (Yu et al., 2012).

Lithium treatment is not only effective against AD, but its therapeutic potential has also been tested in PD. In human SH-SY5Y cells induced with MPP (1-methyl-4-phenyl-1,2,3,6-tetrahydropyridine, PD inducer), lithium is able to exert neuroprotection towards the cells by inhibiting caspase-3 activation and thus preventing cell death (King et al., 2001). Another study also reported similar findings whereby chronic lithium treatment in PD transgenic mice not only prevented PD-induced alpha-synuclein aggregation in several brain regions of the mice, but also protected the neuron cells against oxidative stress-induced neurodegeneration (Kim et al., 2011). In more recent findings, the positive rescue effect of lithium against PD has extended to: (1) modulating PD-induced impaired autophagy by acting on the metabotropic glutamate receptors-5 (mGluR5) (Puglisi-Allegra et al., 2023); (2) regulating the miRNA-mediated alpha-synuclein methylation which further reduces alpha-synuclein aggregates in PD mice brains (Zhao et al., 2019); and (3) promoting the neural stem cells proliferation and differentiation towards dopaminergic neurons in PD mice brains, which overall improves neuronal function and cognitive behaviours in the PD transgenic mice (Qi et al., 2017).

Putting aside preclinical studies, the neuroprotective potential of lithium was also investigated in several clinical studies involving human subjects. In bipolar patients administered with chronic lithium treatment, the risk of developing AD-associated dementia is relatively lower compared to those bipolar patients without lithium exposure (Nunes et al., 2007; Terao et al., 2006). Furthermore, when AD patients were given a microdose (300 µg) of lithium once daily for 15 months, the treated patients showed consistency in the mini-mental state

examination test performance, as compared to those untreated patients whose performance was lower. This study suggested that providing lithium treatment in microdose can prevent cognitive loss in neurodegenerative diseases (Andrade Nunes et al., 2013).

A very common pathology seen in nearly all brain disorders is inflammation. Hence, a drug must be able to modulate the inflammatory responses. A previous study has shown the potency of lithium for its anti-inflammatory effect. In rat primary glia cells induced with lipopolysaccharide (LPS), pre-treatment with 10 mM of lithium for 6 and 24 hours has significantly reduced the expression of pro-inflammatory markers nitrogen oxide (NO), tumor necrosis factor-alpha (TNF-**α**), interleukin 1 beta (IL-β) and prostaglandin E_2 (PGE_2) (Nahman et al., 2012). Moreover, a recent study elaborated on the anti-inflammatory properties of lithium chloride (LiCl) in LPS-induced retinal neuron injury, whereby six weeks of LiCl treatment has prevented microglial activation by regulating the PI3K/Akt/NF-κB pathway, showcasing its neuroprotective effects (Wu et al., 2023). In fact, lithium is capable of increasing the expression of brain-derived neurotrophic factor (BDNF) and vascular endothelial growth factor (VEGF), further supports its neuroprotective potential (Guo et al., 2009; Tunca et al., 2014; Yasuda et al., 2009). Whereas in cultured neurospheres derived from iPSCs, 7 days of treatment with 1 mg/mL of LiCl led to enhancement in the neurospheres formation and sizes, increased cell proliferation and reduced apoptotic cells (Tafreshi et al., 2015).

2.3.2 Application of Lithium to Ameliorate Oxidative Stress

Across past studies exploring lithium's therapeutic potential, researchers also uncovered its ability to rescue oxidative stress. Lithium treatment in both bipolar patients and normal controls showed a reduction in the superoxide dismutase/catalase (SOD/CAT) ratio (Khairova et al., 2012; Machado-Vieira et al., 2007). Besides, six weeks of lithium administration also resulted in significantly increased serum levels of glutathione peroxidase and malondialdehyde in the treated bipolar patients compared to normal controls (Wang et al., 2019). Whereas in human SH-SY5Y cells, the lithium-treated cells displayed reduced ROS production with increased anti-apoptotic markers and reduced pro-apoptotic markers, indicating higher resilience in the cells towards oxidative damage (Alural et al., 2015; Nciri et al., 2013).

Interestingly, it was discovered that the anti-oxidative and anti-apoptotic properties of lithium are modulated through two mechanisms: (1) activation of the nuclear factor erythroid 2–related factor 2 (NRF2) and (2) inhibition of the microRNA 34a (Alural et al., 2015). Collectively, these reports reflect lithium as a potential neuroprotective therapeutic approach targeting oxidative stress. However, to date, the application of lithium in ameliorating oxidative stress in DS has not yet been discovered.

2.3.3 Application of Lithium in DS Studies

While it's widely understood that there is no specific treatment or cure for DS itself, individuals with DS may require medication to manage associated medical conditions. To date, efforts have been made to focus on addressing cognitive deficits in DS individuals. Lithium, known for its neuroprotective properties, is a promising candidate for this purpose.

In a DS Ts65Dn transgenic mouse model, lithium treatment has been proven to reduce the levels of brain metabolite myo-inositol which was initially significantly increased in the DS mice model compared to control mice (Huang et al., 2000). Using the same DS Ts65Dn mice model, lithium treatment was used to investigate its efficacy against the impaired neurogenesis in DS mice brains. Surprisingly, after being fed with the lithium-supplemented diet for one month, the DS mice showed a drastic restoration in neuronal cell proliferation in the subventricular zone (SVZ) of brain, evident through the quantification of 5-bromo-2-deoxyuridine-positive (BrdU+) cells in the SVZ (Bianchi et al., 2010). Subsequently, the same group of scientists reported a lithium-mediated improvement in the mice behavioural performance such as novel object recognition tests, fear conditioning, and object location, alongside the restored hippocampal cell population. They inferred that the lithium treatment has an enhancement effect on the DS brain synaptic plasticity and memory (Contestabile et al., 2013). Apart from that, it is also interesting to find that the 1-month chronic lithium treatment in Ts65Dn DS mice can rescue age-dependent olfactory impairment. There was increased neurogenesis in the

olfactory bulb followed by restored olfactory performance (Guidi et al., 2017). These findings suggest enhancing cognitive and olfactory deficits in DS individuals by restoring a functional neuronal cell population in the DS brains, which can be achieved through lithium.

2.3.4 Lithium and REST

Given that lithium demonstrates high potential for neuroprotective properties, we are eager to uncover the mechanism behind its actions and investigate its association with REST transcriptional regulation in the central nervous system. The first mechanism of action for lithium's neuroprotective action is achieved through the inhibition of glycogen synthase kinase-3β (GSK-3β). Upon suppressing GSK-3β activities, it has a direct regulatory effect on APP processing, resulting in significantly reduced tau phosphorylation and amyloid-beta plaque formation, which eventually causes improvements in memory deficits (Diniz et al., 2013; Engel et al., 2006; Noble et al., 2005). Apart from GSK-3β, lithium also exerts inhibitory effects onto the inositol monophosphatase (IMP) activity which in turn activates the autophagy process thus enhancing the effective clearance of hyperphosphorylated tau protein and amyloid-beta plaques in the brain (Li et al., 2010; Sarkar et al., 2005; Shimada et al., 2012).

Following GSK-3β inhibition, previous studies reported that the Wnt signalling pathway will be activated. Several modulatory effects of lithium have been reported associated with the activation of Wnt/β-catenin signalling pathway

(Junde et al., 2023; Liu et al., 2024; Xia et al., 2017). Moreover, it is noteworthy that the lithium-mediated Wnt activation directly contributes to the induction of REST, which plays a crucial role in brain development and its protective mechanisms. An interesting study reported the Wnt signalling-induced REST that leads to increased REST-RE1 site binding and augmented nuclear translocation, through the lithium-mediated inhibition of GSK-3β (Lu et al., 2014).

Apart from that, lithium-mediated REST upregulation was also reported in a prion disease model, where lithium has restored nuclear REST expression and protected the neuron cells against synaptic damage and neuronal death (Song et al., 2017). Whereas in a recent study using bipolar disease (BD) cerebral organoids, there was a significant reduction in the nuclear REST levels accompanied with abnormal neural development in the organoids. Surprisingly, two weeks of lithium treatment in the diseased organoids were able to rescue the defective development seen in BD cerebral organoids. This study has once again proven the neuronal impairment effect of REST dysregulation in a neuro-related disease model, which can potentially be rescued by lithium (Meyer et al., 2023).

2.4 Down Syndrome Models

To date, research on DS has primarily focused on experiments conducted with rodents and cell models. However, introducing trisomy of human chromosome 21 into rodent models has proven to be quite challenging due to limitations in

genetically modifying mouse chromosomes (Gupta et al., 2016). Additionally, while primary neuron cells and embryonic stem cells (ESCs) have been advantageous, their availability is restricted, and ethical concerns arise as ESCs are typically obtained from discarded embryos from *in vitro* fertilization procedures (Gough et al., 2020). To address these challenges, researchers have turned to generating DS-induced pluripotent stem cells (iPSCs) from somatic cells taken from individuals with DS. These iPSCs share similar characteristics with ESCs in terms of their ability to differentiate into various cell types and their capacity for self-renewal in laboratory settings (Gough et al., 2020; Wang et al., 2023).

2.4.1 Various DS Rodent Models and the Limitations

Like many human diseases, mice have been extensively used as research models. However, adequately modelling DS in mice presents greater challenges compared to many other human conditions (Gupta et al., 2016; Herault et al., 2017). Due to the fact that DS is a genetic condition spanning approximately 35 megabases (Mb) of the HSA21q, areas of similarity between HSA21q and the mouse genome include portions of 3 chromosomes: approximately 28 Mb from the telomeric end of mouse chromosome (Mmu) 16, a central segment of about 1.5 Mb from Mmu17, and another internal segment of about 3 Mb from Mmu10 (Davisson et al., 2001). This has undoubtedly created a huge challenge as it requires trisomy of all three 3 segments to create a complete DS mouse model.

Earlier attempts of creating DS mice models began with trisomy of Mmu16 and these mice had several developmental deficits such as cardiovascular and urinary tract anomalies. However, these mice usually exhibit very low survival rates since birth, rendering it unfeasible to study this DS model beyond that developmental stage (Gropp et al., 1975; Miyabara et al., 1982; Webb et al., 1999). The Ts65Dn DS mouse model was created from trisomy of the 12-15 Mb regions of Mmu16, a segment that displays perfect conserved linkage with HSA21 (Reeves et al., 1995). This model is known as the first viable postnatal DS mouse model, and it is the most widely studied mouse model in DS research. The Ts65Dn DS mouse model has been proven to display several phenotypic features of DS, such as hippocampal-associated cognitive impairment (Giacomini et al., 2018; Hyde et al., 2001), synaptic deficits in the prefrontal cortex (Thomazeau et al., 2023), heart defects (Polk, 2014; Williams et al., 2008) and motor dysfunction (Costa et al., 1999; Hampton et al., 2004). However, a challenge of using this model is the infertility in Ts65Dn males, which limits the DS transmission through the maternal germline. This is not commonly seen in humans as the mothers are trisomic, and it might indirectly affect the phenotype of both trisomic and disomic progenies (Davisson et al., 2007; Moore et al., 2010).

On the other hand, Ts1Cje serves as another mouse model of DS that has also made huge contributions to understanding DS (Sago et al., 1998). Several developmental deficits especially impairments in the neurodevelopment and cognitive behaviors have been investigated in this mouse model (Ishihara et al., 2010; Lim et al., 2024; Ling et al., 2014; Siarey et al., 2005). Nevertheless,

similar to Ts65Dn, the generation of Ts1Cje was by chance instead of design, and the possibility of imposing unforeseen genetic modifications could impact the DS phenotypes (Herault et al., 2017; Sago et al., 1998). Furthermore, there were also other DS mouse models such as Tc1, Ts2Cje, Ts1Rhr, Df1Rhr, Dp2Yey, Df2Yey and Df4Yah. These varying DS mouse models were engineered using different approaches such as chromosome transfer, duplications, deletions, transposon-mediated insertion and selection, and CRISPR/Cas9-mediated chromosome rearrangement (reviewed in Herault et al., 2017). Despite the revolutionary advancements in engineering DS mouse models, comparing outcomes from these studies is challenging due to the variations in mice age, and notably, in the different protocols or genetic backgrounds employed. Hence, there is a compelling necessity to enhance the standardization of experimental protocols to facilitate more equitable comparisons across laboratories.

There has been an effort to create alternative DS *in vivo* models. The first genetic model of DS in rats was created in 2022, by Kazuki and colleagues. The transchromosomic rat model for DS named TcHSA21rat, was developed by inserting HSA21 with an enhanced green fluorescent protein (EGFP) marker into rat embryonic stem cells. This model retains over 93% of HSA21 protein-coding genes, simulating the gene dosage imbalance seen in DS. Compared to mouse models, TcHSA21rat exhibits unique DS characteristics, like reduced cerebellar foliation and robust anxiety and hyperactivity behaviors. TcHSA21rat has notable advantages, such as more human-like organ size, greater ease in performing surgical and physiological procedures, and

enhanced cognitive and behavioural assessments compared to mouse models. However, limitations include technical challenges in maintaining human chromosome stability within rat cells and mosaicism in some animals, though approximately 80% achieve a high HSA21 retention rate (Kazuki et al., 2022).

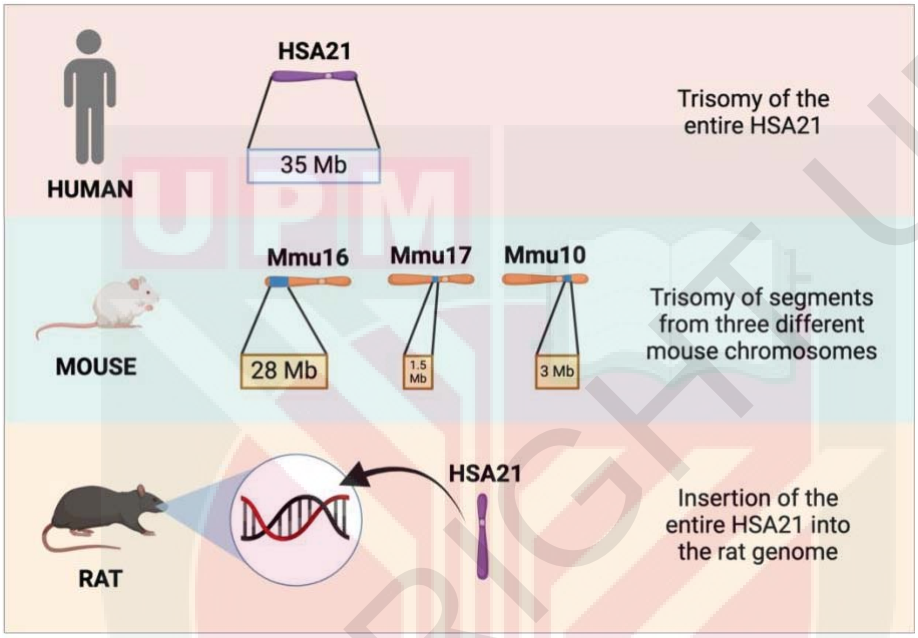

Figure 3: The key chromosomal differences between DS humans, mice and rats. HSA21 = human chromosome 21; Mmu = mouse chromosome; Mb = megabase.

2.4.2 DS-iPSCs Recapitulates Defective Homeostatic Mechanisms seen in DS Individuals

The extensive utilization of rodent models has undeniably enhanced our comprehension of DS. Nevertheless, substantial genetic and physiological distinctions exist between animal models and humans, constraining the translation of findings from animal studies to humans. Employing primary cells and tissues is preferable and more promising, yet ethical and practical concerns arise, such as the accessibility of samples from patients and the

feasibility of experimental manipulation (Rueda et al., 2020; Wang et al., 2023). The emergence of induced pluripotent stem cell (iPSC) technology offers a valuable asset to delve into the DS cellular and molecular pathologies (Wang et al., 2023; Wu et al., 2022). Application of iPSCs would be able to eliminate ethical concerns as the source of iPSCs originates from somatic cells like fibroblasts retrieved from DS or healthy individuals. Reprogramming fibroblasts into iPSCs can be achieved through various methods, including the introduction of Yamanaka factors via retroviral integration or non-integrating techniques like Sendai virus, episomal vectors, or mRNA (Aguirre et al., 2023). Notably, these DS-derived iPSCs retain their complete genomic sequence, including the genetic culprits, making them suitable for disease study, molecular mechanism investigation, treatment development, and drug testing (Kim, 2015; Liu et al., 2018).

For the past three decades, iPSCs derived from DS individuals have been widely utilized in DS research. The first successful case of generating DS-iPSCs occurred in 2008 where cells were obtained from two DS individuals (Park et al., 2008). In earlier DS-iPSC applications, the trisomic iPSCs were usually compared to disomic iPSCs derived from sex- and age-matched healthy individuals. However, challenges arise as there was huge phenotypic variability being observed in the group of disomic iPSCs itself, resulting in questions being raised regarding the reproducibility and reliability of the study (Anderson et al., 2021; Hu et al., 2010). Subsequently, this limitation was addressed by creating isogenic pairs of trisomic and disomic iPSCs from mosaic DS individuals (Kawatani et al., 2021; Murray et al., 2015; Suginobe et

al., 2023). Still, this approach encounters another limitation as mosaicism of DS is uncommon and it only occurs in 2-4% of DS individuals. Hence, researchers came out with strategies to silent one copy of the triplicated HSA21 in the trisomic iPSCs. This strategy was proven useful as the trisomy correction has reversed the developmental defects seen in trisomic iPSCs (Jiang et al., 2013; Li et al., 2012). Overall, these approaches offer a more promising DS cell model in gene expression studies without the confounds of genetic and epigenetic background.

Throughout the revolution of DS-iPSC approaches, efforts have been made to investigate DS-associated pathological features in the engineered DS cell models. In the NPCs and neurons differentiated from trisomic iPSCs, the cells exhibited defects in proliferation, differentiation and migration (Hibaoui et al., 2014; Huo et al., 2018; Meharena et al., 2022; Ponroy Bally et al., 2020; Weick et al., 2013). Furthermore, a few studies revealed a higher tendency of DS-iPSCs to differentiate towards the glial lineage rather than the neural lineage, suggesting impaired neurogenesis (Bhattacharyya et al., 2009; Chen et al., 2014; Kawatani et al., 2021). Indeed, a single-cell RNA sequencing performed on neural stem cells derived from DS-iPSCs, revealed abnormalities during neural differentiation of the cells (Qiu et al., 2023). Intriguingly, the phenomenon of neurogenic-to-gliogenic shift was also reported in a previous *in vivo* DS study (Lee et al., 2016). Besides, it was also noticed that the trisomic iPSC-derived neurons have reduced synaptic development when compared to the isogenic control iPSC-derived neurons (Araujo et al., 2018; Weick et al., 2013).

Overall, some advantages of using DS iPSC-derived neurons in this study include it represents a powerful tool by offering access to human neuron cells that maintain the full chromosomal complement of trisomy 21, allowing for the investigation of cellular phenotypes, synaptic function, and molecular mechanisms in a disease-relevant context (Bhattacharyya et al., 2009; Chen et al., 2014; Kawatani et al., 2021; Qiu et al., 2023). These iPSC-derived neurons can be produced in large amounts, making them practical for many types of experiments. However, iPSC-derived neurons present significant limitations, including their potential variability in differentiation efficiency between cell lines, and the absence of complex neural circuit interactions that exist in the intact brain. Additionally, the simplified *in vitro* environment fails to capture the influence of other cell types and systemic factors that contribute to DS neuropathology (Chiaradia & Lancaster, 2020; Rizzuti et al., 2024).

A significant breakthrough in the regenerative medicine field is the generation of a three-dimensional (3D) cell culture system known as organoids derived from stem cells (Mulaudzi et al., 2023). Using 3D organoids as a disease model holds great advantages over the typical 2D cell culture because it enables investigation of numerous processes that are impossible to be seen in homogenous 2D cell culture or spheroids (Nikonorova et al., 2023). It is exciting to explore the possibility of utilizing this 3D organoid model in DS studies. In fact, researchers have been differentiating DS-iPSCs into cerebral organoids. They have also proven several neurodevelopmental impairments in the DS organoids similar to those observed in DS individuals (Czerminski et al., 2023; Tang et al., 2021; Xu et al., 2022; Xu et al., 2019).

In conclusion, DS-iPSCs exhibit distinct developmental abnormalities that recapitulate the defective regulatory mechanisms observed in DS individuals thus offering a promising avenue for DS research. Stem cell-based DS studies are believed to be important tools for translation into therapies for future DS research.

CHAPTER 3

GENERATION AND CHARACTERIZATION OF DISOMIC AND TRISOMIC NEURONS DERIVED FROM DS-iPSC

3.1 Introduction

The process of differentiating DS neurons from iPSCs represents a cutting-edge approach to understanding the intricacies of DS pathology. Created by reprogramming somatic cells, iPSCs can transform into various cell types, including neurons, mimicking the natural *in vivo* development (Wang et al., 2023; Wu et al., 2022). This allows researchers to create patient-specific neuronal models, reflecting the unique genetic and molecular traits of individuals with DS. By guiding iPSCs to become neurons, we can explore how genetic alterations associated with DS, such as trisomy 21, influence neurodevelopmental processes, including synaptogenesis, neuronal maturation, and network formation (Kim, 2015; Liu et al., 2018).

Despite being informative and may offer valuable insights, DS mouse models inevitably entail interspecies differences. Hence, iPSC-derived neurons offer a more accurate representation of human cells compared to DS mouse models. While mouse models have contributed significantly to our understanding of DS pathophysiology, they may not fully capture the complexity of human neural development and function (Gupta et al., 2016; Herault et al., 2017). On the other hand, iPSC-based models offer a more personalized and clinically

relevant platform for studying DS, allowing us to investigate disease mechanisms in a human-specific context.

3.2 Details of the Cell Lines

A total of 6 iPSC cell lines (control / disomic, n=3; DS / trisomic, n=3) were procured in this study. Out of the 3 pairs of cell lines, 2 pairs are isogenic while the other is not. Isogenic cell lines refer to a group of cells that are genetically identical to each other. These cells are designed to possess the same genetic makeup, which makes them highly valuable in scientific research. Especially when studying genetic disorders, isogenic cell lines enable us to analyse the impacts of specific genetic modifications in a controlled environment. Isogenic cell lines are hence renowned as a powerful tool in exploring genetic disorders, particularly in therapeutic drug discovery (DeWeirdt et al., 2020; Liu et al., 2005).

Throughout this thesis, the 6 lines of iPSCs will be described as C1, C2, C3, DS1, DS2, and DS3. “C” stands for ‘control’ which represents the disomic control group, whereas “DS” stands for ‘Down syndrome’ which represents the trisomic DS group. Among the 6 cell lines, C1-DS1 and C2-DS2 are the two pairs of isogenic cell lines, while C3-DS3 is the non-isogenic pair. C2, DS2 and DS3 iPSC cell lines were procured from the WiCell Research Institute at the University of Wisconsin. The isogenic pair of C1 (HPS4272) and DS1 (HPS4270) were procured from the RIKEN BioResource Center in Japan. Both cell lines originated from skin fibroblasts of a male Trisomy 21 individual aged

below 10 years. Since the donor origin was a fully Trisomy 21 individual, the disomic control line was induced by elimination of the maternal origin of the chromosome 21 from DS1. Both iPSCs cell lines were reprogrammed through non-integrating episomal vectors.

The second isogenic pair of C2 (WC-24-02-DS-A) and DS2 (WC-24-02-DS-M) cell lines originated from skin fibroblasts of a 25-years-old female mosaic DS patient, and the cells were reprogrammed using non-integrating episomal vectors. In contrast, another DS cell line, DS3 (UWWC1-2DS3), were originated from skin fibroblasts of a male Trisomy 21 neonate. The reprogramming method of this cell line was through non-integrating episomal vectors. Moreover, C3 (ATCC-DYS0100) was procured from the American Type Culture Collection (ATCC) and the source of this cell line was from skin fibroblasts of a healthy male neonate. This iPSC cell line was reprogrammed through the Sendai viral transfection system. A summary of details for all the 6 cell lines were tabulated in **Table 1**.

Table 1: Details of the disomic control and trisomic DS iPSC lines

Cell label	Cell line	Donor origin	Reprogramming method	Provider
C1 DS1	HPS4272 HPS4270	• Trisomy 21 individual • Male • Aged <10 • Skin fibroblast	Non-integrating episomal vector	RIKEN BioResource Center, Japan
C2 DS2	WC-24-02-DS-A WC-24-02-DS-M	• Mosaic DS individual • Female • Aged 25 • Skin fibroblast	Non-integrating episomal vector	WiCell Research Institute, University of Wisconsin
C3	ATCC-DYS0100	• Healthy individual • Male • Neonate • Skin fibroblast	Sendai viral transfection system	American Type Culture Collection (ATCC)
DS3	UWWC1-2DS3	• Trisomy 21 individual • Male • Neonate • Skin fibroblast	Non-integrating episomal vector	WiCell Research Institute, University of Wisconsin

3.3 Materials and Methods

3.3.1 Maintenance and Expansion of iPSCs

Upon procurement of the iPSCs, the cryovials of each cell line were carefully revived, maintained, expanded and then cryopreserved. From the initial cryovial, the cells of each line were expanded into 12 new cryovials. This ensured a sufficient iPSC cryovial stock in the liquid nitrogen tank.

3.3.1.1 Media and Reagent Preparation

The iPSCs were maintained in a specialized culture medium called mTeSR plus media (StemCell Technologies, Canada). To prepare mTeSR plus full medium, 40 mL of mTeSR plus basal medium was added into a 50 mL falcon tube. Subsequently, 10 mL of thawed 5X mTeSR plus supplement was added, with the remaining thawed supplement aliquoted into 15 mL falcon tubes, 10 mL each, and stored at -20°C. The mixture was gently inverted and ready for use. Furthermore, it is necessary to culture the iPSCs on a coating solution for attachment. The coating solution for iPSCs is Geltrex (Gibco, USA). Upon arrival, Geltrex was thawed on ice and aliquoted into pre-cooled 1.5 mL tubes, 150 µL each, then stored at -20°C. To prepare the working solution, Geltrex was added to cold DMEM/F12 media (Gibco, USA) at a 1:100 ratio. For instance, 300 µL of Geltrex was added to 29.7 mL of cold DMEM/F12 media to prepare 30 mL of the working solution. The mixture was kept on ice before use. The volume needed to coat a 6-well plate varied: 2 mL for reviving cryopreserved cells and 1.5 mL for passaging cells.

Upon cell revival, the cells were nourished with Rho-associated protein kinase inhibitor Y-27632 (ROCKi) to enhance cell survival and maximize cell recovery. Upon arrival, the stock solution of ROCKi was prepared by adding 1560 µL of double distilled water to 5 mg of lyophilized ROCKi (StemCell Technologies, Canada) using a syringe, resulting in a 10 mM concentration. This stock solution was then aliquoted and stored at -20°C. The working concentration of 10 µM was achieved by diluting the stock 1:1000 with full media. Moreover, for

iPSCs cryopreservation, the cryopreservation media was prepared by mixing KnockOut™ Serum Replacement (Gibco, USA) with 10% dimethyl sulfoxide (DMSO) (Sigma, USA). The volume of cryopreservation media needed for one cryovial is 500 µL. Hence, to cryopreserve 10 cryovials of cells, 5 mL of cryopreservation media was prepared by adding 500 µL of DMSO to 4.5 mL of KnockOut™ serum. Lastly, to prepare Dulbecco's Phosphate Buffered Saline (DPBS) for cell washing, 500 mL of 1X DPBS was made by adding 50 mL of 10X DPBS (StemCell Technologies, Canada) to 450 mL of distilled water. The mixed 1X DPBS was then autoclaved. After sterilization, the 1X DPBS was aliquoted into 50 mL falcon tubes and stored at 4°C.

3.3.1.2 Cells Reviving

Full media of mTeSR plus was thawed in a 37°C water bath for 10 to 20 minutes, while the Geltrex working solution was prepared based on the number of wells to be used. ROCKi was thawed at room temperature. Then, 2 mL of cold Geltrex solution was added into each well of a 6-well plate for coating and kept in an incubator at 37°C and 5% CO_2 for one hour. After one hour, the Geltrex solution was discarded using 1000 µL blue tips connected to the hose of an aspiration vacuum pump system. After each use, the blue tip was discarded into the waste bin, and the hose opening was rinsed with 70% ethanol. Subsequently, 1 mL of mTeSR plus full media was added into each well and kept in the incubator before use. Meanwhile, 15 mL Falcon tubes were prepared and labelled according to the cell line to be revived. The dedicated cryovials were removed from the liquid nitrogen tank and thawed directly by

swirling and submerging half of the tube body in a 37°C water bath until only a small piece of ice remained. The thawed cryovial was wiped with tissue to remove excess water and sprayed with 70% ethanol before being placed into the biosafety cabinet.

Next, 4.5 mL of mTeSR plus full media was aspirated using a 5 mL serological pipette, with approximately 0.5 mL of the media released into a cryovial. The mixture of revived cells was then aspirated back into the serological pipette and transferred directly into the bottom of a labelled 15 mL Falcon tube. The tube was centrifuged at 400 x g for three minutes. After centrifugation, a cell pellet was visible at the bottom of the tube, and the supernatant was discarded by aspirating through a stack of three blue tips connected to the hose of an aspiration vacuum pump system. This was done gently to avoid disturbing the cell pellet. One mL of mTeSR plus full media was added to the cell pellet and resuspended gently to prevent dissociating the cells into single cells and to avoid shearing forces. The cells were best plated in small clumps as single cells were more prone to differentiation upon culturing. The 1 mL cell suspension was then transferred into a well pre-filled with 1 mL of full media. To enhance cell survival and maximize cell recovery, 2 µL of ROCKi was added to the well. The plate was moved in a cross-like pattern several times to ensure homogenous cell distribution. Finally, the cells were observed under an inverted phase contrast microscope and incubated at 37°C and 5% CO_2.

3.3.1.3 Media Changing and Cells Expansion

On the second day, if the cells could attach onto the coated Geltrex, media changing was performed to eliminate the ROCKi treatment. Full media of mTeSR plus was thawed in a 37°C water bath for 10 to 20 minutes. The plate with cells was removed from the incubator, and the media was discarded using the vacuum pump system. The blue tip on the vacuum pump system was constantly replaced when removing media from different types of cells to avoid cross-contamination. Removal of media was done by placing the blue tip close to the bottom of the well while the plate was slanted at approximately 35 degrees, ensuring that the tip do not touch the base of the culture well. Occasionally, a significant number of dead cells were seen in the culture media on the second day of cell reviving or the day after the removal of ROCKi. In such cases, the cells were rinsed with 2 mL of 1X DPBS to wash off the dead cells before adding fresh media. Then, 2 mL of fresh mTeSR plus full media was added slowly into each well using a serological pipette. Media changing was performed once every two days. On Fridays, 3 mL of full media was added, usually in the late afternoon. While on Mondays, the media was changed in the early morning.

When the cells reached 70-80% confluency, they were either passaged for expansion or cryopreserved. Accutase solution (StemCell Technologies, Canada) was used for cell detachment purpose. Before detaching the cells, mTeSR plus full media was thawed in a 37°C water bath for 10 to 20 minutes, while Accutase was thawed at room temperature to prevent inactivation from

prolonged warming. For cell expansion purpose, the Geltrex working solution was prepared according to the number of wells to be used for cell passaging, requiring 1.5 mL of Geltrex solution for each well of a 6-well plate. The plate was incubated for one hour in a 37°C and 5% CO_2 incubator. Prior to Accutase treatment, ROCKi was also added to the well containing cells that had reached 70-80% confluency, and incubated for at least 30 minutes in the 37°C and 5% CO_2 incubator.

After one hour, Geltrex was discarded from the coated plate, and 1 mL of mTeSR plus full media was added to the well and kept in the incubator for further use. After at least 30 minutes of ROCKi incubation, the plate with cells was removed, and the media was discarded. One mL of Accutase was added to each well and incubated in the 37°C and 5% CO2 incubator for 5 to 10 minutes. After 5 minutes, the plate was observed under the microscope. If a large portion of cells were still attached, the plate was incubated further until it reached 10 minutes of incubation time. After 10 minutes, 2 mL of mTeSR plus full media was added to each well containing Accutase. If many cells remained attached, a serological pipette was used to scrape off the cells. Everything from the well was then transferred into a 15 mL Falcon tube. The tube was centrifuged at 400 x g for 3 minutes. After centrifugation, the tube was removed and placed into the biosafety cabinet. A visible cell pellet was expected at the bottom of the tube. Using three stacks of blue tips connected to the aspiration vacuum pump, the supernatant was aspirated slowly without disturbing the cell pellet.

mTeSR plus full media was added to the tube to resuspend the cell pellet, with the volume depending on the number of wells to be seeded, which required 1 mL of media for each well. Then, 1 mL of the cell suspension was transferred into each new well pre-filled with 1 mL of full media. The plate was moved in a cross-like pattern several times to ensure homogeneous cell distribution. The cells were observed under an inverted phase contrast microscope and incubated in a 37°C and 5% CO_2 incubator. As for cryopreservation, the cell pellet was resuspended with cryopreservation media instead. The volume of cryopreservation media needed depended on the number of cryovials to be cryopreserved, which is 0.5 mL of media per cryovial. The cell suspension was transferred into pre-labeled cryovials, 0.5 mL each. Finally, the cryovials were placed in a Mr. Frosty cell freezing container (Biosharp, China) and kept at -80°C for 24 to 48 hours before being transferred into liquid nitrogen tank.

3.3.2 Generation of iPSC-Derived Neurons

After establishing the iPSC lines, the next step was to perform neural induction and expansion to obtain neural stem cells (NSCs), and neuron differentiation to generate neurons. Overall, the neural induction process takes 7 days, and the induced NSCs will be expanded for another 3 to 4 days, and finally another 14 days for the neural differentiation process. The overall workflow for the generation of iPSC-derived neurons is illustrated by **Figure 4** below.

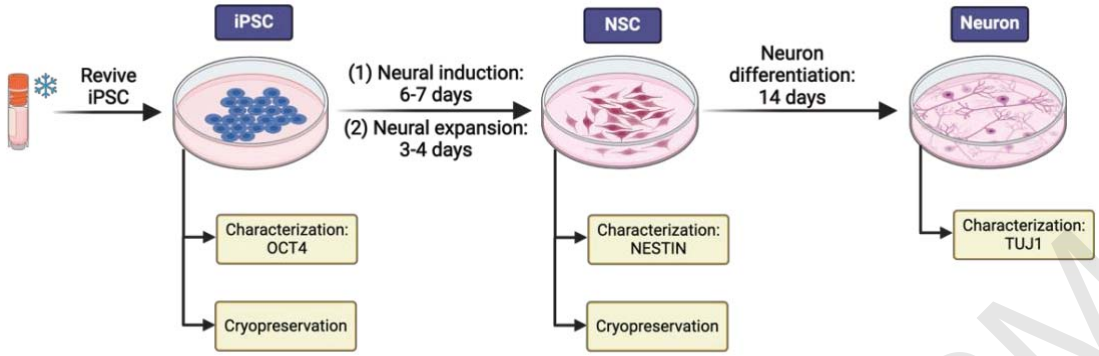

Figure 4: Overall workflow for the generation of iPSC-derived neurons.

3.3.2.1 Media and Reagent Preparation

The iPSCs were neural induced with a specialized culture media kit known as the PSC Neural Induction Medium (Gibco, USA). To prepare the neural induction full medium, 49 mL of Neurobasal medium (Gibco, USA) was mixed with 1 mL of thawed 50X neural induction supplement (Gibco, USA) in a 50 mL Falcon tube. The remaining supplement was aliquoted into 1.5 mL microcentrifuge tubes, each containing 1 mL, and kept at -20°C. As for the neural expansion full medium, 24.5 mL of Neurobasal medium, 24.5 mL of Advanced™ DMEM/F12 (Gibco, USA), and 1 mL of 50X neural induction supplement were added to a 50 mL falcon tube. To prepare the neuron differentiation full medium, 48 mL of Neurobasal medium, 1 mL of 50X B-27 Supplement (Gibco, USA), 0.5 mL of GlutaMAX supplement (Gibco, USA), 0.5 mL of 100X CultureONE supplement (Gibco, USA), and 50 µL of 200 mM L-ascorbic acid (Sigma, USA) were added to a 50 mL falcon tube. The neuron differentiation full medium was gently inverted to mix and was ready for use.

After the neural expansion process, the NSCs were usually either expanded, cryopreserved or differentiated into neurons. The cryopreservation media for NSCs was prepared by mixing 20% DMSO (Sigma, USA) in neural expansion full media. The volume needed for one cryovial was 500 µL. For instance, to cryopreserve 8 cryovials of cells, 4 mL of cryopreservation media was prepared by adding 800 µL of DMSO to 3.2 mL of neural expansion full media.

Cultivating neurons requires specialized coating solution to enhance the differentiation process. The coating solution used here was a combination of poly-D-lysine and laminin (PDL/laminin). To prepare a 500 µg/mL of poly-D-lysine (PDL) stock solution, a sterile syringe and needle were used to aspirate 10 mL of sterile distilled water to reconstitute 5 mg of lyophilized PDL powder (Sigma, USA). The dissolved PDL stock solution was transferred to a wrapped 15 mL Falcon tube and stored at 4°C. To prepare a working concentration of 50 µg/mL, a 1 in 10 dilution using 1X sterile DPBS was performed. Furthermore, Natural Mouse Laminin (Gibco, USA) originally stored at -80°C, was thawed at 4°C. Before aliquoting the laminin, yellow tips and labeled PCR tubes were pre-cooled at -20°C overnight. The stock laminin (1.2 mg/mL) was aliquoted into PCR tubes, 30 µL each, and stored at -80°C. To prepare a working concentration of 3 µg/mL, a 1 in 400 dilution using sterile distilled water was performed.

3.3.2.2 Neural Induction and Expansion

The starting material for the neural induction process is iPSCs. Upon 70 – 80% confluency, the iPSCs were harvested following the steps mentioned in section 3.3.1.3. Cell count was performed on the harvested iPSCs by using the formula $\frac{total\ no.of\ living\ cells}{4} \times dilution\ factor \times 10{,}000$ where the dilution factor is 2. The optimal starting iPSC seeding density for neural induction was 5 x 10^4 cells per well of a 6-well plate, or equivalent to around 20% cell confluency. The iPSCs were seeded in 1.5 mL of mTeSR plus full media. The plate was moved in a cross-like pattern a few times to ensure homogenous cell distribution. The cells were incubated with 37ºC and 5% CO_2. On the next day, when the iPSCs had attached to the Geltrex-coated surface, the mTeSR plus full media was replaced with neural induction full media. Neural induction full media was changed every 2 days until the cells became confluent on day 6 or 7. The formation of neural rosettes was observed as an indication of successful neural induction.

After 6 to 7 days of neural induction, the cell population in each well was examined for homogeneity. If most of the iPSCs had successfully differentiated into NSCs and had obvious neural rosettes formation, the entire well would be treated with Accutase solution for cell detachment and expansion. Alternatively, if there was a heterogenous cell population where only certain areas showed nice NSCs with obvious neural rosette formation, cells in those specific areas were picked for subsequent expansion. Meticulous preparation was undertaken prior to picking cells. The surfaces of the inverted microscope and

surrounding benches were disinfected with 70% ethanol. Cells were rinsed with 1X DPBS to minimize debris in the wells. Under the inverted microscope, cells that had formed neural rosettes were carefully picked using 10 µL fine-filtered tips. In contrast, if the majority of the cell population achieved the desired NSC morphology while only a minor cell population did not grow well as desired, those unwanted cells would be scraped off and washed away. The remaining attached cells were harvested and expanded. These harvested or picked NSCs to be expanded, were then filtered through a 100 µm cell strainer, and then centrifuged at 400 x g for 3 minutes. After centrifugation, the supernatant was aspirated slowly without disturbing the cell pellet. The cell pellet was then resuspended with neural expansion full media and seeded onto a Geltrex-coated well plate. Media changing was performed every 2 days depending on the cell confluency. The expanded NSCs currently in the first passage (P1), were either further passaged, cryopreserved, or proceeded for neuron differentiation.

3.3.2.3 Neuron Differentiation

On the day before neuron differentiation, the culture surface was first incubated with 50µg/mL of PDL solution overnight at 37^{o}C and 5% CO_2. The next day early morning, the PDL solution was removed and the wells were rinsed twice with warm sterile distilled water. The plate was left inside the biosafety cabinet with lid uncovered to let it air dry for around 2 hours. Each well was ensured to be totally dried up as remnant of PDL may be toxic to the cells. Meanwhile, the 1.2 mg/mL of laminin stock solution from -80^{o}C was

thawed on ice. The desired volume of laminin working solution (3 µg/mL) was prepared by performing 1 in 400 dilutions in sterile distilled water. The prepared laminin was always kept on ice. After the PDL-coated plate had fully dried up, each well was then filled with the appropriate volume of 3 µg/mL laminin and the plate was kept in an incubator with 37ºC and 5% CO_2 for 2 hours. The volume of the coating solution depends on the size of the culture well. It is crucial that the volume of the coating solution is sufficient to cover the culture surface fully and is able to withstand a few hours of 37ºC incubation as evaporation might occur.

After approximately 1.5 hours of laminin incubation, the NSCs pre-treated with ROCKi, were harvested and counted. After centrifugation, the cell pellet was resuspended with 1 mL of full B-27 neuron differentiation media and cell counting was performed. The optimal cell seeding density for neuron differentiation was 5×10^4 cells/cm^2. For instance, to seed NSCs into a 24-well with the surface area of 1.9 cm^2, the total number of NSCs to be seeded will be $5 \times 10^4 \times 1.9 = 9.5 \times 10^4$ cells. The desired number of cells were then seeded onto the PDL/laminin-coated wells, with the addition of 10 µM ROCKi. Every 2 to 3 days, a half-medium-change was performed as the differentiating neuron cells can detach easily. After 5 days of differentiation, the cells should have shown neuronal morphology by developing neurite formation. After 2 weeks of differentiation, the neurons were ready to be treated or harvested.

Table 2: Medium and reagents used throughout the generation of iPSC-derived neurons

Cell type	Procedure	Media/Reagent	Component
iPSC	Coating	Geltrex	100X Geltrex solution
			DMEM/F12 media
	Culture maintenance	mTeSR+ full media	mTeSR+ basal media
			5X mTeSR+ supplement
	Cryopreserva-tion	Cryopreserva-tion media	Knockout serum
			10% DMSO
NSC	Coating	Geltrex	100X Geltrex solution
			DMEM/F12 media
	Neural induction	Neural induction full media	Neurobasal media
			50X Neural induction supplement
	Neural expansion	Neural expansion full media	Neurobasal media
			Advanced DMEM/F12 media
			50X Neural induction supplement
	Cryopreserva-tion	Cryopreserva-tion media	Neural expansion full media
			20% DMSO
Neuron	Coating	PDL/Laminin	50 µg/mL Poly-D-lysine
			3 µg/mL Laminin
	Differentiation	B-27 Neuron differentiation full media	Neurobasal media
			50X B-27 supplement
			100X Glutamax supplement
			100X CultureONE supplement
			200 mM L-ascorbic acid

3.3.3 Morphological and immunocytochemical characterization of cells

Throughout the process of generating neurons from iPSCs, it is crucial to perform characterization on the cells in each development stage. This is to verify that the cells obtained were of the correct type and hence ensuring the validity, reliability and reproducibility of the experiment results.

3.3.3.1 Daily Morphological Observations of Cells in Each Developmental Stage

Throughout the cell culturing process, the morphology of cells was constantly monitored through an inverted phase contrast microscope (Olympus, Japan). The morphology of cultured cells is an important indicator to verify the culture status, such as the growth rate and the homogeneity of their undifferentiated or differentiated states (Nagasaka et al., 2017). The typical morphological criteria of undifferentiated iPSCs includes: compact colonies with distinct and well-defined edges, the cells are multi-nucleated and generally have large nuclei with less cytoplasm (Robinton & Daley, 2012; Wakao et al., 2012).

Upon neural induction and expansion, the iPSCs form NSCs that also possess high proliferative capacity and high nucleus-to-cytoplasmic ratio. When cultured on adhered monolayer, NSCs commonly form rosette-like structures that resemble a group of cells radially arranged surrounding a central lumen (Miotto et al., 2023; Townshend et al., 2020). Furthermore, when the neuron differentiation process is initiated, NSCs commonly exhibit a triangular cell body morphology with short processes. As the differentiation protocol

progresses, cells exhibit a smaller cell body with long extended processes or also known as neurites formation, which is a typical characteristic of neurons (Gordon et al., 2013; Peng et al., 2021).

3.3.3.2 Immunocytochemical (ICC) Characterization of Cells in each Developmental Stage

Apart from verifying the cells through morphological observations, immunocytochemistry (ICC) is also a promising method to characterize the cells through the detection and visualization of markers or proteins that are specific to certain cell types.

For instance, OCT4 is a well-known marker that regulates the pluripotency of stem cells and its expression disappears upon differentiation (Shi & Jin, 2010; Zeineddine et al., 2014). Nestin is an intermediate filament protein responsible for maintaining the undifferentiated multipotent neural stem cells (Park et al., 2010; Suzuki et al., 2010). Moreover, upon differentiation, class III beta tubulin (TUJ1) acts as a marker for the early differentiated neurons (Jouhilahti et al., 2008). Therefore, in this study, the expression of OCT4 was measured as an indicator for the pluripotent iPSCs, Nestin as a neural stem cell marker, while TUJ1 as the neuronal marker.

3.3.3.3 Fixation, Staining and Imaging of Cells for ICC Characterization

Throughout the process of generating neurons from iPSCs and NSCs, ICC was performed at each stage of cell development to characterize the iPSCs,

NSCs and neurons respectively. To start the ICC characterization experiment, the cells were first cultured on rounded grade 1 glass coverslips with a diameter of 13 mm (Paul Marienfeld, Germany) placed in 24-well plates. Prior to use, the glass coverslips were wrapped in aluminium foil and autoclaved. One side of each autoclaved coverslip was labelled with a small “p” at the edge to accurately identify which side faced upwards or downwards, preventing ICC from being performed on the wrong side where no cells could be found. Using a pair of curved fine forceps, the labelled coverslips were flipped and placed in each indicated well of a 24-well plate, so the letter “p” on the coverslip appeared as “q”. Each well was then coated with 0.5 mL of coating solution depending on the cell types: Geltrex solution for iPSCs and NSCs, while PDL/laminin for neurons. The respective cells were then seeded onto the coated coverslips.

Once the iPSCs and NSCs had reached the desired confluency (around 50-70%) and the neurons had completed 14 days of differentiation, the media was discarded and the cells were rinsed with 1X DPBS. The cells were then fixed with 4% PFA solution for 15 minutes at room temperature. The 4% PFA solution was prepared by dissolving 4 g of paraformaldehyde powder (VWR, USA) in 100 mL of 65^{o}C 1X PBS and then filtered through a 0.22 µm filter. After 15 minutes, the fixative solution was removed, and the cells were washed with 1X PBS three times for 5 minutes each. The fixed cells on coverslips were either directly proceeded with ICC staining or stored in cold 1X PBS for future use.

The ICC staining process began with preparing a humidified chamber, by placing a thin layer of wet tissue paper in a dark or opaque container and overlaying small pieces of parafilm on the wet tissue paper. The parafilm serves as a hydrophobic layer to prevent overflow of the incubation solution o coverslips. Using a pair of curved fine forceps, the fixed coverslips were carefully removed from each well and placed on the piece of parafilm, ensuring the cells were facing upwards. The coverslips were incubated with 100 µL of blocking solution for 30 minutes at room temperature, with the solution being added drop by drop directly onto the coverslip, forming a smooth water droplet due to the hydrophobic property of the parafilm underneath. The blocking solution was prepared by mixing 10% donkey serum (Sigma, USA) and 0.3% Triton X-100 (Sigma, USA) in 1X PBS.

Meanwhile, primary antibody solutions were prepared in 1:200 dilution with the blocking solution prepared earlier, and the volume depended on the number of coverslips to be stained (100 µL per coverslip). The primary antibodies used were anti-rabbit OCT4 (Sigma, USA) anti-mouse Nestin (Invitrogen, USA) and anti-rabbit TUJ1 (Sigma, USA). Each coverslip was incubated with 100 µL of primary antibody solution overnight at 4°C. The next day, the coverslips were washed with 1X PBS three times for 10 minutes each. They were then incubated with secondary antibodies (1:1000) for 2 hours in the dark at room temperature. The secondary antibodies used were donkey anti-rabbit IgG conjugated with Alexa Fluor 488 (Invitrogen, USA), donkey anti-rabbit IgG conjugated with Alexa Fluor 555 (Invitrogen, USA) and donkey anti-mouse IgG conjugated with Alexa Fluor 555 (Invitrogen, USA).

The types and dilution for each antibody were tabulated in **Table 3**. After 2 hours, the coverslips were washed with 1X PBS three times for 10 minutes each. Following the washing steps, a small drop of DAPI mounting media (Abcam, England) was placed on a microscopic slide. Using a pair of curved forceps, one edge of the stained coverslip was carefully held, flipped, and placed onto the DAPI droplet, ensuring the surface containing cells faced downwards. The top surface of the coverslip was gently tapped with the forceps to remove any air bubbles. The stained coverslip was immobilized by applying nail polish at its border and left overnight in the dark at room temperature. The next day, the slides were observed under a fluorescence microscope (Olympus, Japan).

Table 3: Primary and secondary antibodies used for cell characterization

	Antibody	Brand	Dilution
Primary antibody	anti-rabbit OCT4	Sigma	1:200
	anti-mouse NESTIN	Invitrogen	
	anti-rabbit TUJ1	Sigma	
Secondary antibody	Donkey anti-rabbit IgG conjugated with Alexa Fluor 488	Invitrogen	1:1000
	Donkey anti-mouse IgG conjugated with Alexa Fluor 555	Invitrogen	
	Donkey anti-rabbit IgG conjugated with Alexa Fluor 555	Invitrogen	

3.4 Results and Discussion

3.4.1 Morphological Characterization of Cells

Throughout the maintenance and expansion of iPSCs, the morphological appearance and culture condition of both disomic control and trisomic DS iPSCs was monitored daily. Commonly, the cell seeding day is known as DIV 0 (day *in vitro* = 0). On the day after cell seeding (DIV 1), most of the iPSCs had attached onto the Geltrex-coated surface, leaving a sparse number of dead cells wandering around in the culture medium. The attached cells appeared dense, spindle-shaped, and had tiny processes. These morphological changes were hypothesized due to the treatment effect of ROCKi, as it had been reported that ROCKi can alter the cytoskeleton by inhibiting actomyosin, thereby enhancing the migration and proliferation of cells (Matsumoto et al., 2022; Wang et al., 2017). Nevertheless, the role of ROCKi in cell revival and cell passaging is pivotal as ROCKi has been proven to exert a significant effect in enhancing cell survival and maximize the cell recovery in cryopreserved embryonic and pluripotent stem cells (Claassen et al., 2009; Pakzad et al., 2010).

On DIV 1, the culture media containing ROCKi was usually replaced with fresh full mTeSR plus media to eliminate the ROCKi treatment. On DIV 3, when the iPSCs had been maintained in full media without ROCKi for 2 days, the cells continued to increase in number, forming compacted cell clumps. When observed under 40X magnification, the cell clumps appeared homogenous,

and distinct edges bordered each cell clump. When observed under higher magnification (100X and 200X), individual iPSC could be seen clearly and the cells exhibited typical characteristics of pluripotent stem cells: multi-nucleated, high nuclear-to-cytoplasmic ratio, and each cell had distinct edges and well-defined borders **(Figure 5)**.

Upon neural induction, the iPSCs transformed into NSCs and exhibited slight changes in cell morphology compared to iPSCs **(Figure 6)**. As the 7 days of neural induction progressed, the cells remained in cell clumps. However, differences were noticed when individual cells increased in size and the cell shapes were irregular as well. On the edges of the cell clumps, spiny projections could be seen indicating possible NSC formation **(Figure 6b)**. Intriguingly, at the end stage of neural induction, usually on DIV 6 or 7, obvious lumen-like structures could be observed in the culture where cells were arranged in a circular manner **(Figure 6c)**. These are known as neural rosettes where cells were radially arranged surrounding a central lumen (Miotto et al., 2023; Townshend et al., 2020).

According to a previous study by Fedorova et al. (2019), they discovered that the iPSC-derived neural rosettes had progressively downregulated expression of pluripotency markers (OCT4, NANOG, c-MYC) in the iPSC-derived neural rosettes. Inversely, the expression of a potent neural stem cell marker, SOX2 (Ellis et al., 2004) and some of the neurodifferentiation-associated markers, BRN2/POU3F2, and NR2F2, were upregulated. This study had suggested that, upon neural rosettes formation in iPSC neural induction, the pluripotency

program has been terminated and neural differentiation has been initiated. Hence, iPSC-derived NSCs are likely to develop at this time point of neural induction (Fedorova et al., 2019).

Once neural rosettes formed in the culture, the NCSs were picked and expanded. The expanded NSCs that were initially seeded in isolated single cells **(Figure 6d)**, eventually formed clumps as well **(Figure 6e)**. However, the tendency of cells to clump together was reduced as compared to iPSCs, evident through the presence of single isolated NSCs surrounding the irregularly shaped NSC clumps **(Figure 6f)**. Interestingly, when NSCs were revived from cryopreservation, the cells clumped less, and each cell exhibited obvious spiny projections resembling typical morphology of a neural stem cell **(Figure 6g & h)**.

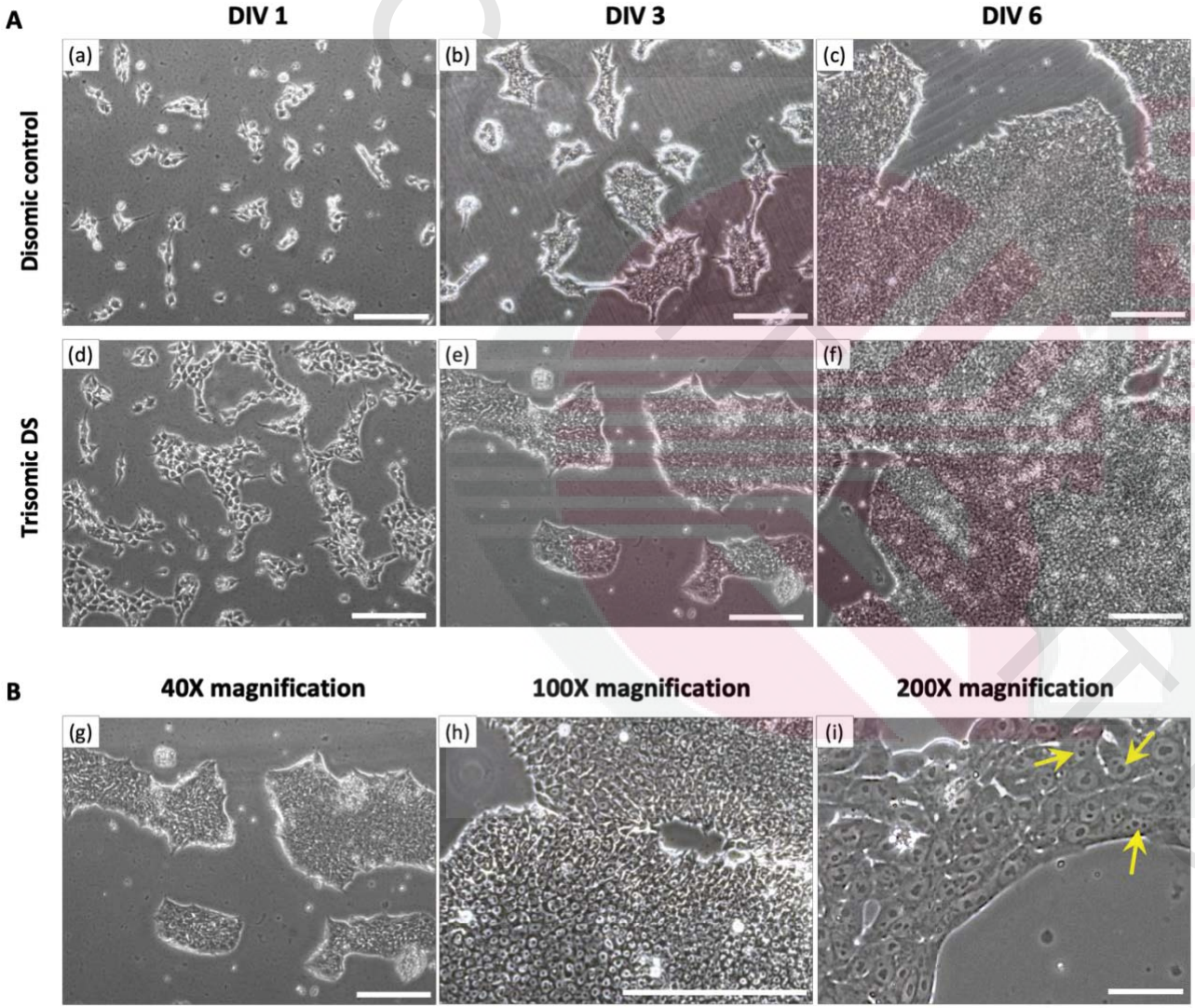

Figure 5: Morphological observations of hiPSC culture (representative micrographs).

(A) Phase contrast microscopy of the disomic control (a – c) and trisomic DS hiPSC cell lines (d – f) at day 1, day 3 and day 6. Upon cell seeding (day 0), the cells were treated with ROCK inhibitor (ROCKi) Y27632 to minimize cell death and maximize cell recovery from cryopreservation. Hence, the cells on day 1 appeared slightly denser, with spiny projections at both ends most probably due to the ROCKi effect. A few days later, the cells grew into densely-packed cell patches and the cell patches slowly expanded and closed up after almost one week of culturing.
(B) A closer look-up on the morphology of hiPSCs in different magnifications. The actively proliferating cells had large nucleus. Yellow arrows indicating examples of multinucleated cells. The cells generally had high nuclear-to-cytoplasmic ratio, showing hallmark of pluripotent stem cells. DIV = day *in vitro*. Scale bar: (a – h) 250 µm; (i) 50 µm.

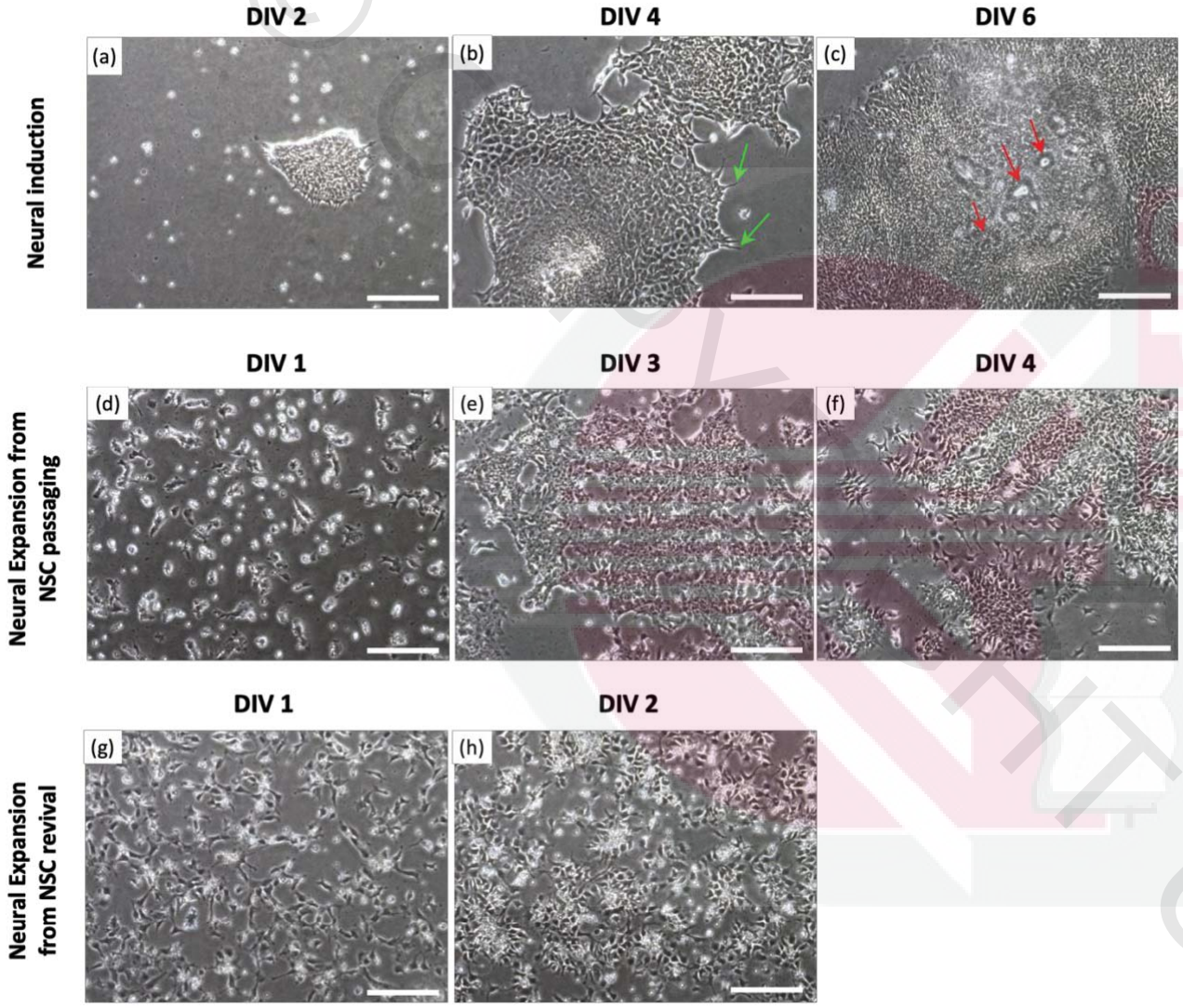

Figure 6: Phase contrast microscopy of neural induction and expansion (representative micrographs).

(a) Day 2 of neural induction: cells remained as iPSCs in a small clump, with some dead cells in the surrounding due to stress caused by media changing from mTeSR+ to neural induction media.
(b) Day 4 of neural induction: iPSCs started to differentiate into NSCs. The cells appeared denser, expanded in size and some spiny processes could be seen at the edge of the cell clump (green arrow).
(c) Day 6 of neural induction: NSCs formed neural rosettes (red arrow) and the cells were picked for expansion.
(d – f) After one week of neural induction, the newly differentiated NSCs was passaged for expansion. On day 1 of neural expansion, the single NSCs looked stressed but eventually expanded and formed clumps. On day 4, the cells were harvested for cryopreservation.
(g – h) The revived NSCs showed spiny processes and all cells were generally denser. The cells had lesser tendency to form clumps. DIV = day *in vitro.* Scale bar, 250 µm.

Even though iPSCs and NSCs are both stem cells, they do exhibit distinct morphological features. As shown in **Figures 7a** and **7b**, NSCs resembled iPSCs as they were multi-nucleated, however, due to the fact they had smaller nucleolus and larger cytoplasmic area, their nuclear-to-cytoplasmic ratio was relatively lower as compared to iPSCs. Furthermore, expanded iPSCs usually formed compacted clumps as they grew, and single-isolated iPSCs tend to differentiate easily **(Figure 7c)**. In contrast, expanded NSCs usually appeared in single isolated cells, and all the cells generally had spiny processes resembling a typical morphology of NSCs **(Figure 7d)**. When both types of cells were observed under the same magnification, it was obvious that the size of a single NSC **(Figure 7d)** was larger than that of a single iPSC **(Figure 7c)**. Moreover, when in clumps, iPSCs in overall exhibited a flat two-dimensional appearance **(Figure 7e)**, while the NSCs overall had a bumpy appearance or are also described as having a mountain-like structure **(Figure 7f)**.

Subsequently, when the NSCs were cultured in B27-supplemented neuron differentiation full media, the cells differentiated into neurons and obtained neuronal morphology: a cell body with extended long projections known as neurites. From the captured phase contrast micrographs **(Figure 8)**, a variety of unipolar, bipolar, and multipolar neurons could be seen. Throughout the 14 days of *in vitro* differentiation, the neuronal morphology became observable at DIV 5 **(Figure 8c)**. Before DIV 5, the cells were sparse and relatively smaller with short extensions **(Figure 8a & b)**. On DIV 7 onwards, the cells had stopped proliferating as there was no visible increment in the cell confluency upon that stage of differentiation. Meanwhile, the cells gained length in the

projections, indicating active neurites formation **(Figure 8d & e)**. On DIV 14, the neuronal cell bodies clump together forming a mass body, with extensive neurites outgrowth **(Figure 8f)**.

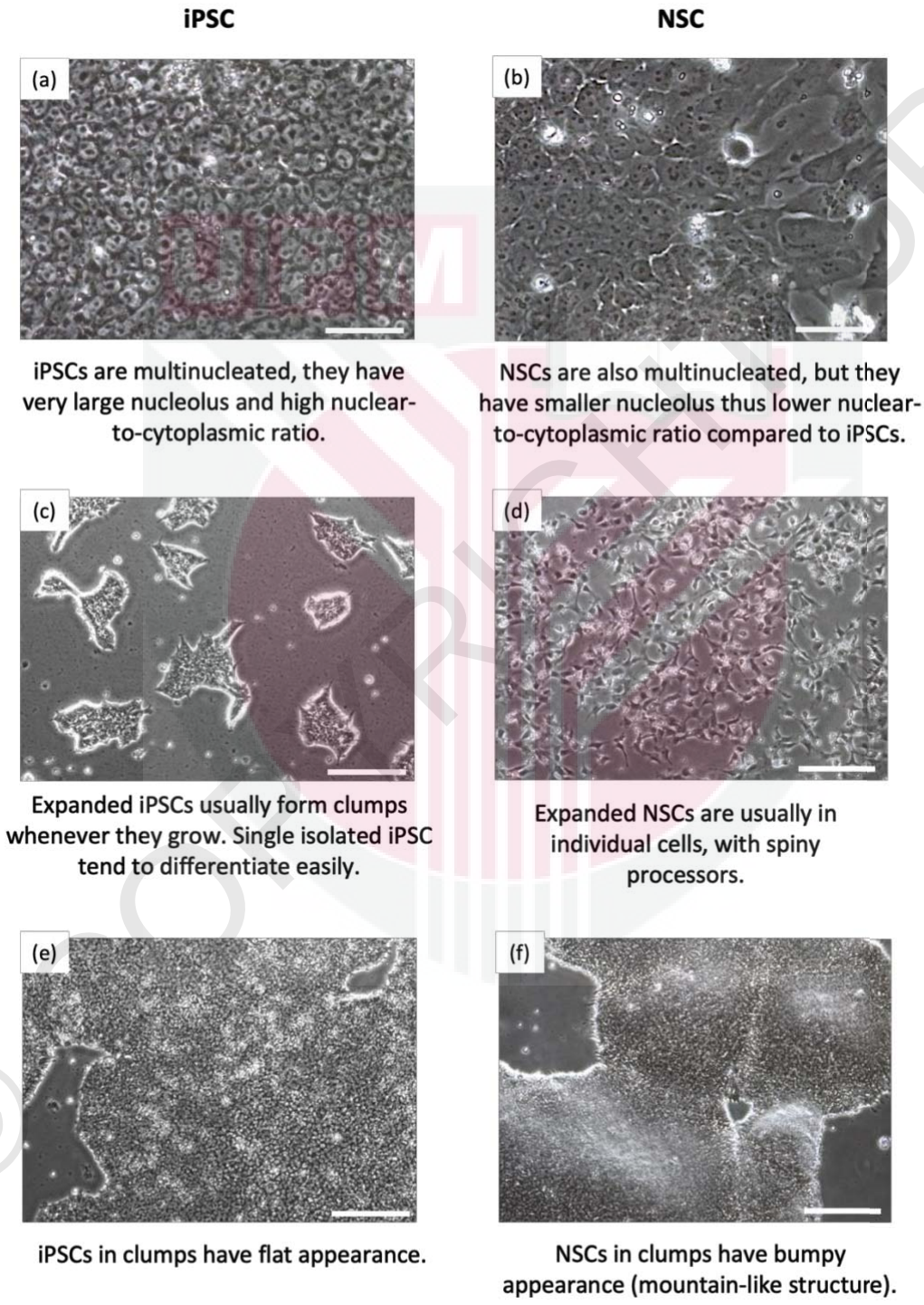

Figure 7: Morphological differences between iPSC and NSC.
Scale bar, (a – b): 50 µm; (c – f): 250 µm.

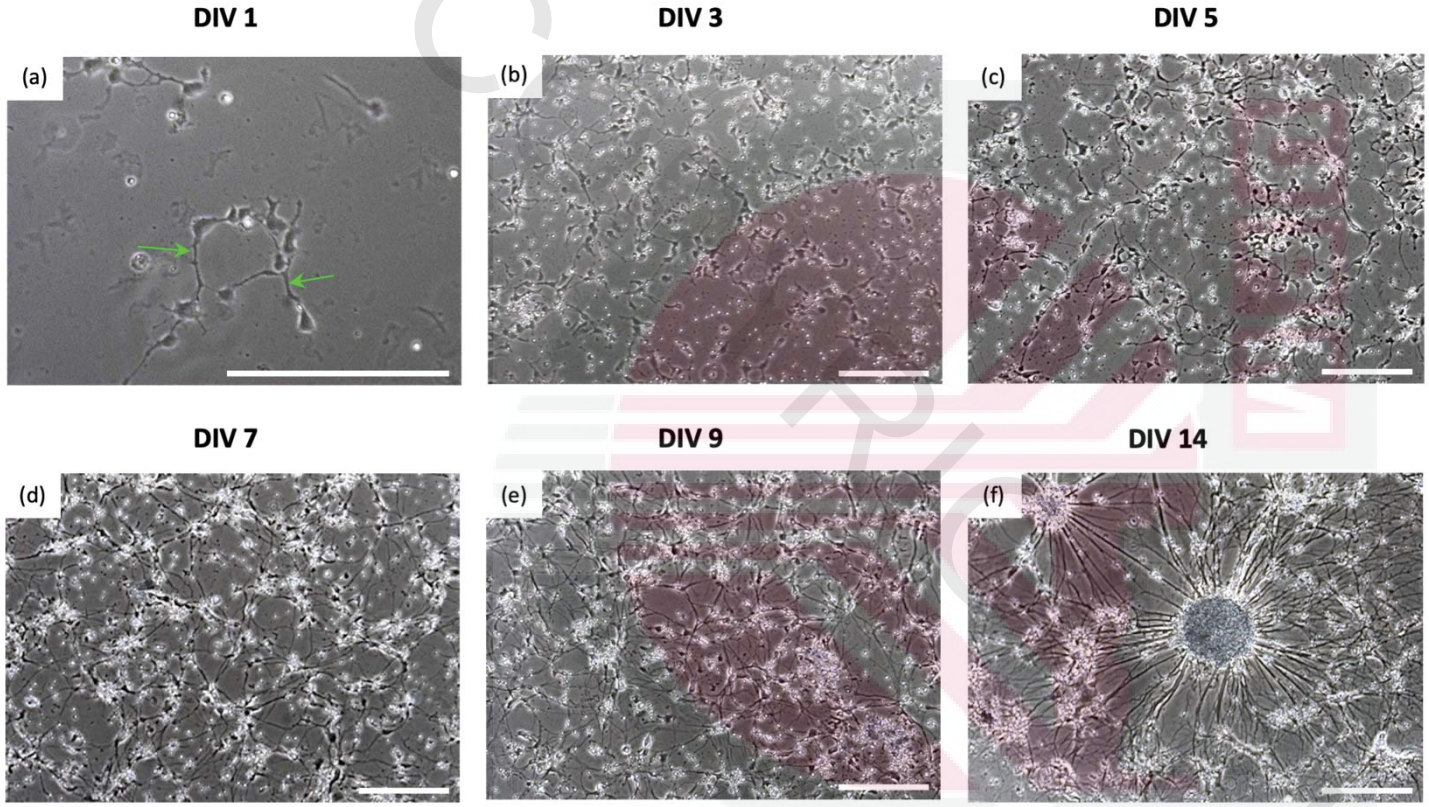

Figure 8: Phase contrast microscopy of the neural differentiation process (representative micrographs). (a) After one day of seeding the NSCs, the cells attach to the PDL/laminin-coated surface and start to develop processes (green arrow). **(b – c)** On Day 3, the processes further develop into neurites, and the cells show neuronal morphology on Day 5. **(d – e)** After one week of differentiation, the neurites continue to outgrow and form a neuronal web. **(f)** On Day 14, some areas of the neuronal culture show the formation of a mass of the cell body with abundant neurites branching out. DIV = day *in vitro.* Scale bar, 250 µm.

3.4.2 Immunocytochemical Characterization of Cells

Apart from verifying the cells through morphological observations, ICC characterization was also performed to visualize the expression of markers specific to the cell type. In this study, OCT4, Nestin and TUJ1 expression was visualized through ICC to characterize iPSCs, NSCs, and neurons respectively. As shown in **Figure 9A**, the iPSCs showed strong positive staining for the key pluripotency marker OCT4 (green), with the protein localized in the nuclei as confirmed by DAPI (blue) co-staining. **Figure 9B** reveals NSCs positively expressing Nestin (red), a neural progenitor marker, with DAPI highlighting the nuclei. In **Figure 9C**, neurons exhibited robust expression of early neuron marker TUJ1 (red), clearly delineating the extensive neuronal processes. DAPI staining was present in all cell types, allowing visualization of cell nuclei. The merged images in the bottom row confirmed the co-localization of each specific marker with DAPI. These results positively characterized the distinct stages of neural differentiation from iPSCs to neurons, giving the green light for their continued use in the downstream analysis in this study.

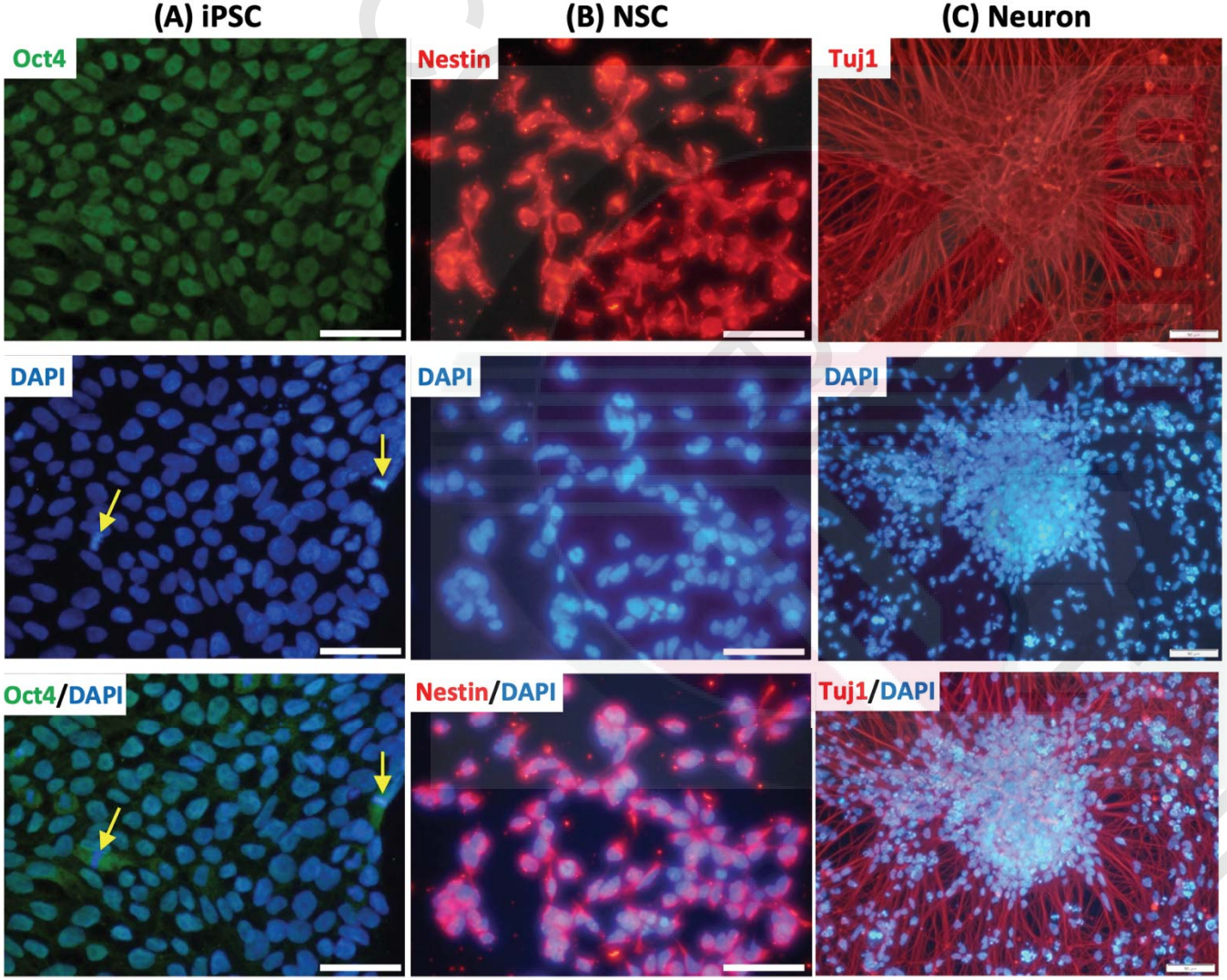

Figure 9: Representative fluorescent micrographs for immunocytochemical (ICC) characterization of iPSC, NSC and neurons.

(A) Positive nuclear OCT4 staining indicated strong expression of OCT4 as a pluripotent marker in the iPSCs. Some cells that were potentially undergoing mitosis could be detected (yellow arrow) which indicated the actively proliferative characteristic of iPSCs.
(B) True positive cytoplasmic Nestin staining indicated positive expression of a neural stem/progenitor marker in the NSCs.
(C) True positive TUJ1 staining indicated positive expression of an early differentiated neuron marker in the neurons.

Nuclei were counterstained with DAPI. Scale bar: 50 µm.

3.5 Conclusions

In conclusion, both morphological and ICC characterization experiments on the iPSCs, NSCs, and neurons have added value to the effort of validating their suitability and reliability as cell models for this study. Indeed, both disomic control and trisomic DS iPSC-derived neurons have been proven to be true iPSCs, NSCs and neurons, thereby ensuring the reliability and validity of the results obtained in the subsequent analysis in this study.

CHAPTER 4

INVESTIGATING THE RESTORATION OF REST IN LITHIUM-TREATED DISOMIC AND TRISOMIC iPSC-DERIVED NEURONS

4.1 INTRODUCTION

The repressor element-1 silencing transcription factor (REST) is a vital transcription repressor in neurodevelopment. Proper functioning and localization of REST are essential, as its dysregulation can negatively impact brain development (Lam et al., 2023). In fact, REST dysregulation had been reported in several DS studies (Bahn et al., 2002; Canzonetta et al., 2008; Lepagnol-Bestel et al., 2009; Lim et al., 2024). To date, effort has been made to improve the DS neuropathologies and cognitive deficits (Hendrix et al., 2021; Sterling et al., 2023; Torres-Carrión et al., 2019). Agreeing that REST is dysregulated in DS brains, corrective actions to restore REST levels would be beneficial to combat DS neuropathologies.

Several strategies targeting REST have been suggested to counteract the pathological effects of REST dysregulation, indicating its potential as a pharmacotherapeutic target. One significant aspect is that REST is regulated by the Wnt signaling pathway (Nishihara et al., 2003), which positions lithium as a promising drug since it can activate this pathway (Lu et al., 2014; Zhang et al., 2019). Moreover, it is noteworthy that there have been successful cases of lithium being able to enhance neurogenesis, synaptic plasticity, and memory in DS mouse models (Bianchi et al., 2010; Contestabile et al., 2013). However,

these studies did not implicate REST. Therefore, in this chapter, the association between lithium and REST would be investigated in DS iPSC-derived neuronal models.

4.2 Experimental Design

The 6 cell lines in this study were assigned to 2 groups: untreated and lithium treated. In the untreated group, the neurons were maintained as usual in the B27 neuron differentiation full media, without the addition of lithium. Whereas in the lithium treated group, after 14 days of *in vitro* differentiation, an optimized lithium dosage was added into the neuron differentiation full media for 24 hours. Prior to this, the safety dosage of lithium in an isogenic pair of iPSC-derived neurons (1 control line & 1 DS line) was first determined through the MTT cell viability assay. After that, the untreated and lithium-treated neurons cultured on coverslips, would be fixed with 4% paraformaldehyde and stained with REST antibody. The acquired fluorescence micrographs were then analysed via the ImageJ software to quantify REST expression in the neurons.

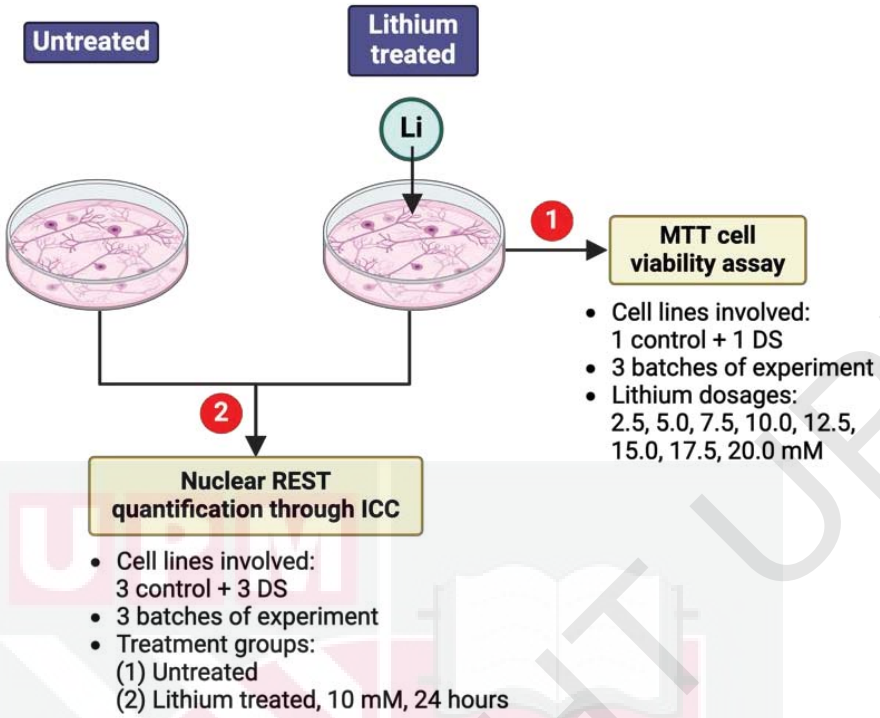

Figure 10: Experimental design to investigate the lithium-mediated nuclear REST restoration in disomic and trisomic iPSC-derived neurons.

4.3 Materials and Methods

4.3.1 Lithium Preparation

The molar mass of lithium carbonate, Li_2CO_3 (Sigma, USA), is 73.891 g/mol. To prepare a 10 mL stock solution of 100 mM concentration, 0.0739 g of Li_2CO_3 powder was carefully weighed and dissolved in 10 mL of sterile deionized water (1st Base, Singapore). This stock solution was always freshly prepared before each experiment. It was noted that each Li_2CO_3 molecule contains 2 lithium cations (Li^+), meaning that the effective dosage of Li^+ is half that of Li_2CO_3. For instance, a 10 mM concentration of Li^+ corresponds to a 5 mM concentration of Li_2CO_3.

4.3.2 MTT Cell Viability Assay to Establish the Safety Dosage of Lithium Treatment in Neurons

The MTT assay is a widely used colorimetric microplate assay in cell toxicity studies. MTT (3-(4,5-dimethylthiazol-2-yl)-2,5-diphenyl-2H-tetrazolium bromide) is a monotetrazolium salt that can penetrate the cell membrane and reduced by metabolically active cells. This redox chemical reaction produces an intracellular by-product called formazan that can later be solubilized, visualized and quantified through a colorimetric microplate reader. This assay is usually utilized to assess treatment toxicity, cell viability and metabolic activity in research studies (Ghasemi et al., 2021; Mosmann, 1983).

In this study, the treatment dosages of lithium to be tested were 2.5, 5.0, 7.5, 10.0, 12.5, 15.0, 17.5 and 20.0 mM of Li^+. The dosage range (2.5 – 20.0 mM) and treatment duration (24 hours) were selected based on previous publications in the field (Alural et al., 2015; Hou et al., 2015; Qu et al., 2011) that also tested similar dosages of lithium on neural cells and obtained significant results. The higher doses (>12.5 mM) were included to clearly establish the toxicity threshold and identify the safety margin between therapeutic and toxic concentrations. For sample preparation, the neurons were cultured in a 96-well clear plate and underwent 14 days of *in vitro* neuron differentiation. Prior to cell seeding, cell counting was carefully performed on the harvested NSCs so that only 1.6×10^4 cells were seeded into each well. It is crucial to ensure a consistent number of starting materials for all the treatment wells in the MTT assay to prevent misleading results. In addition, since different cell line has different cell growth rate, to prevent variations

between the cell lines which possibly might ended up getting misleading results, the MTT assay was only conducted and compared within the same cell line.

On DIV 13, lithium treatment was initiated. The different dosages of lithium treatment (2.5, 5.0, 7.5, 10.0, 12.5, 15.0, 17.5, 20.0 mM) was prepared by diluting the 100 mM lithium stock solution with B27 neuron differentiation full media. The total volume of media in each well was 100 µL. For example, to prepare 100 µL of 20 mM lithium treatment, 20 µL of the 100 mM lithium stock solution was mixed with 80 µL of full media. A total of 3 wells were assigned for each treatment group, making it a triplicated set of data for each group. Apart from the eight groups of lithium dosages, additional groups of neurons were also prepared as negative control (untreated), positive control and blank wells. The positive control group consisted of 3 different treatments: 400 µM of hydrogen peroxide for 24 hours, 1 M of hydrogen peroxide for 2 hours, and 20% DMSO for 24 hours. The blank wells were made up of only media without cells.

After the completion of dedicated treatment groups, media in all wells were removed and replaced with 90 µL of fresh full media plus 10 µL of MTT solution provided by the kit (Solarbio, China). The total volume of fresh full media and MTT solution were added into a sterile reservoir and mixed. A multichannel pipette was used to load 100 µL of mixture into each well. The plate added with MTT solution was incubated at 37^{o}C and 5% CO_2 for 4 hours. After 4 hours, all media was aspirated and 110 µL of MTT solubilization solution

(provided by kit) was added into each well, by using a multichannel pipette. The 96-well plate was placed on a shaker inside an incubator for 10 minutes to fully dissolve the formazan crystals formed. The plate absorbance was read with a microplate reader under the 490 nm wavelength. Once obtained the absorbance readings, the raw data was recorded in an Excel datasheet. Each reading was subtracted from the mean blank. An average of absorbance reading was obtained from the triplicates of each treatment group. Readings form the untreated neurons were taken as control. The percentage of cell viability for each treatment group was calculated by using the formula $\frac{Average\ OD_{treatment}}{Average\ OD_{control}} \times 100\%$, where OD refers to the raw absorbance or also known as optical density obtained from the microplate reader.

4.3.3 Comparing Nuclear REST Expression between Untreated and Lithium-treated Control and DS Neurons

4.3.3.1 Immunocytochemical (ICC) Staining

ICC was performed on the untreated and lithium-treated neurons to quantitate and compare the level of nuclear REST expression between the treatment groups in both genotypes. The ICC fixation and staining methods were as mentioned in section 3.3.3.3 above. The primary antibodies used in this experiment were anti-mouse REST (Invitrogen, USA) and anti-rabbit TUJ1 (Sigma, USA), while the secondary antibodies were donkey anti-rabbit IgG conjugated with Alexa Fluor 488 (Invitrogen, USA) and donkey anti-mouse Texas Red (Abcam, England). The dilution factors were 1:200 and 1:1000 for

primary and secondary antibodies respectively. All coverslips were counterstained with DAPI.

Table 4: Primary and secondary antibodies used for nuclear REST quantification in iPSC-derived neurons

	Antibody	Brand	Dilution
Primary antibody	anti-mouse REST	Invitrogen	1:200
	anti-rabbit TUJ1	Sigma	
Secondary antibody	Donkey anti-rabbit IgG conjugated with Alexa Fluor 488	Invitrogen	1:1000
	Donkey anti-mouse IgG conjugated Texas red	Abcam	

4.3.3.2 Nuclear REST quantification using ImageJ

After acquiring images from the fluorescence microscope, the fluorescent micrographs were analyzed by using the ImageJ software. In the ImageJ software, the measurement parameters were first defined as “area”, “mean grey density” and “integrated density”. The scale in ImageJ software was set by opening a JPEG image with a scale bar from the same microscope as the TIFF images to be analyzed, enlarging it to clearly see the scale bar, then using the Set Scale function to calibrate the measurement using the known scale bar length in µm. A composite image was created by merging nuclear-stained DAPI and neuron-stained Tuj1 images in ImageJ. The region of interest (ROI) was then manually selected using the ROI manager. Thirty DAPI-stained and Tuj1-positive neuronal nuclei of similar size were outlined as ROIs using the freehand drawing function, and these ROIs were saved for

further analysis. These ROIs would be used to quantify the nuclear REST expression in the REST-stained images later on. The manual selection process is crucial to ensure that only prominent neurons were selected for the nuclear REST quantification. The composite image was closed while keeping the ROI manager window open.

To prepare for nuclear REST quantification, background signal correction was performed on the REST-stained (Texas red dye) image. This process involved using a technical negative control image that had been incubated with only the secondary Texas red antibody, without the primary anti-REST antibody. The brightness and contrast of this control image (in TIFF format) were adjusted in ImageJ to determine the appropriate exposure range where no signal was visible. This exposure range was then applied to the actual REST TIFF image to standardize the signal intensity. With the adjusted REST image open alongside the ROI manager, the previously saved ROIs (representing 30 neuronal nuclei) were applied to the image. Measurements were taken for all selected ROIs simultaneously, generating a results window with quantitative data. This data was then transferred to an Excel sheet for further analysis, providing a standardized method to quantify nuclear REST levels across the selected neurons.

4.3.3.3 Statistical Analysis

The nuclear REST quantification process involved a comprehensive analysis of 90 neurons per treatment group for each cell line, spanning three

experimental batches. To ensure accuracy and reliability, a meticulous batch-to-batch and line-to-line normalization was performed using GraphPad Prism software (version 9.0). Raw integrated density data was carefully organized into grouped formats, cleaned of outliers using the ROUT method (Q=5%), and transformed to normalize values across isogenic cell line pairs and experimental batches. This transformation step involved dividing all data by the mean of the untreated control for each isogenic line pair. Descriptive statistical analyses, including calculations of mean, standard deviation, and standard error, were conducted at various stages of data processing to monitor the normalization process and prepare for further statistical evaluation.

Following data normalization, multiple data tables were created to compile and organize the results according to different grouping criteria, such as genotype, cell line, and treatment conditions. These tables facilitated a multi-layered analysis approach, allowing for comparisons between individual cell lines, genotypes, and treatment groups. Statistical analyses began with normality tests, which revealed non-parametric distributions, leading to the use of appropriate non-parametric tests such as one-way ANOVA, Mann-Whitney, and Kruskal-Wallis tests. These analyses were performed on combined data sets to identify significant differences in REST expression between treatment groups and genotypes. The results were visualized using a violin plot to summarize individual data points for each neuron across treatment groups and genotypes. These rigorous statistical analyses and visualizations aimed to robustly characterize REST expression patterns while accounting for experimental variability across batches and cell lines.

4.4 Results and Discussion

4.4.1 Optimization of Safety Dosage of Lithium Treatment in iPSC-Derived Neurons

The MTT cell viability assay was performed to optimize the safety dosage of lithium treatment in the iPSC-derived neurons. The effects of different concentrations of Li_2CO_3 on neuron cell viability over 24 hours **(Figure 11A)**. The x-axis represents the dosage of Li_2CO_3 in mM, ranging from 0 to 20 mM, with additional conditions for apoptosis inducers. The y-axis shows cell viability as a percentage, with 100% (marked by a dotted line) representing normal viability. Lower concentrations of Li_2CO_3 (up to 12.5 mM) appear to maintain or slightly increase cell viability above 100%. However, at higher concentrations (15 mM and above), cell viability decreases. The graph also includes positive control conditions using H_2O_2 and DMSO as apoptosis inducers, which show dramatically reduced cell viability **(Figure 11A)**. Overall, this data suggests that Li_2CO_3 has a dose-dependent effect on neuron survival, with potential protective effects at lower doses but becoming harmful at higher concentrations.

While the safety threshold for lithium treatment in iPSC-derived neurons was determined to be 12.5 mM and below, the 10 mM dosage was eventually chosen due to its demonstrated efficacy in producing significant results, as evidenced by previous studies. According to Qu et al. (2011), 10 mM of lithium treatment was shown to effectively promote neural precursor cell proliferation and activate key signalling pathways, including GSK-3β inhibition and NF-AT

activation. On the other hand, another study reported that 10 mM of lithium provided the most significant cytoprotection against rotenone-induced toxicity in SH-SY5Y cells (Hou et al., 2015). Collectively, the selected dosage of 10 mM provides an adequate safety margin below the maximum tolerated dose while ensuring sufficient potency to induce the cellular and molecular changes of interest. Furthermore, this concentration aligns with those commonly employed in the field, facilitating comparisons with existing literature. Therefore, 10 mM lithium represents an optimal dosage that balances safety considerations with the potential to observe robust effects on neuron cells, making it suitable for the objectives of this thesis research.

4.4.2 Comparing Nuclear REST Expression between Untreated and Lithium-treated Control and DS Neurons

The optimized 10 mM of lithium dosage was used to treat both disomic control and trisomic DS neurons for 24 hours. The effect of post-lithium treatment was evaluated through ICC nuclear REST quantification in the 6 cell lines of neurons **(Figure 11C)**. **Figure 11B** demonstrates the nuclear REST expression in both control and DS neurons under two conditions: untreated and treated with lithium (Li). The y-axis represents the normalized fold change of nuclear REST expression, while the x-axis categorizes the four experimental groups. The data is presented as violin plots, showing the distribution of data points.

The graph reveals several key findings **(Figure 11B)**. First, there is a significant difference in the baseline nuclear REST levels between the

untreated control and DS neurons, with DS neurons showing significantly lower nuclear REST expression. The current finding supports existing literature where REST expression was found to be downregulated in DS patient-derived neural progenitor cells (Bahn et al., 2002) and several DS mouse models (Canzonetta et al., 2008; Lepagnol-Bestel et al., 2009; Lim et al., 2024). In this study, REST quantification was focused on the nuclear level because the nuclear translocation of this protein is a prerequisite for it to exert proper function. When REST has impaired nuclear localisation, there will be several pathological consequences in the central nervous system (Lam et al., 2023).

Next, lithium treatment appears to have different effects on disomic control and trisomic DS neurons. In the control group, lithium treatment did not seem to exert significant changes in the nuclear REST expression (marked as 'ns'). On the other hand, lithium treatment significantly increased nuclear REST expression in the DS neurons (indicated by ****), bringing it to levels comparable to or even higher than the untreated control neurons. These significant changes highlight the differential response to lithium treatment between disomic and trisomic neurons, with trisomic neurons showing a much more pronounced upregulation of REST expression in response to lithium. This suggests that lithium may restore nuclear REST expression in DS neurons, potentially counteracting some of the molecular differences associated with trisomy 21.

4.5 Conclusions

In a nutshell, the downregulation of nuclear REST expression in DS neurons has been confirmed, and REST dysregulation can be restored when the neurons were pre-treated with 10 mM of lithium for 24 hours. This is considered a novel discovery about the restoration effect of lithium in DS. Collectively, these findings not only corroborate previous research on REST dysregulation in DS but also open new avenues for targeted therapeutic interventions.

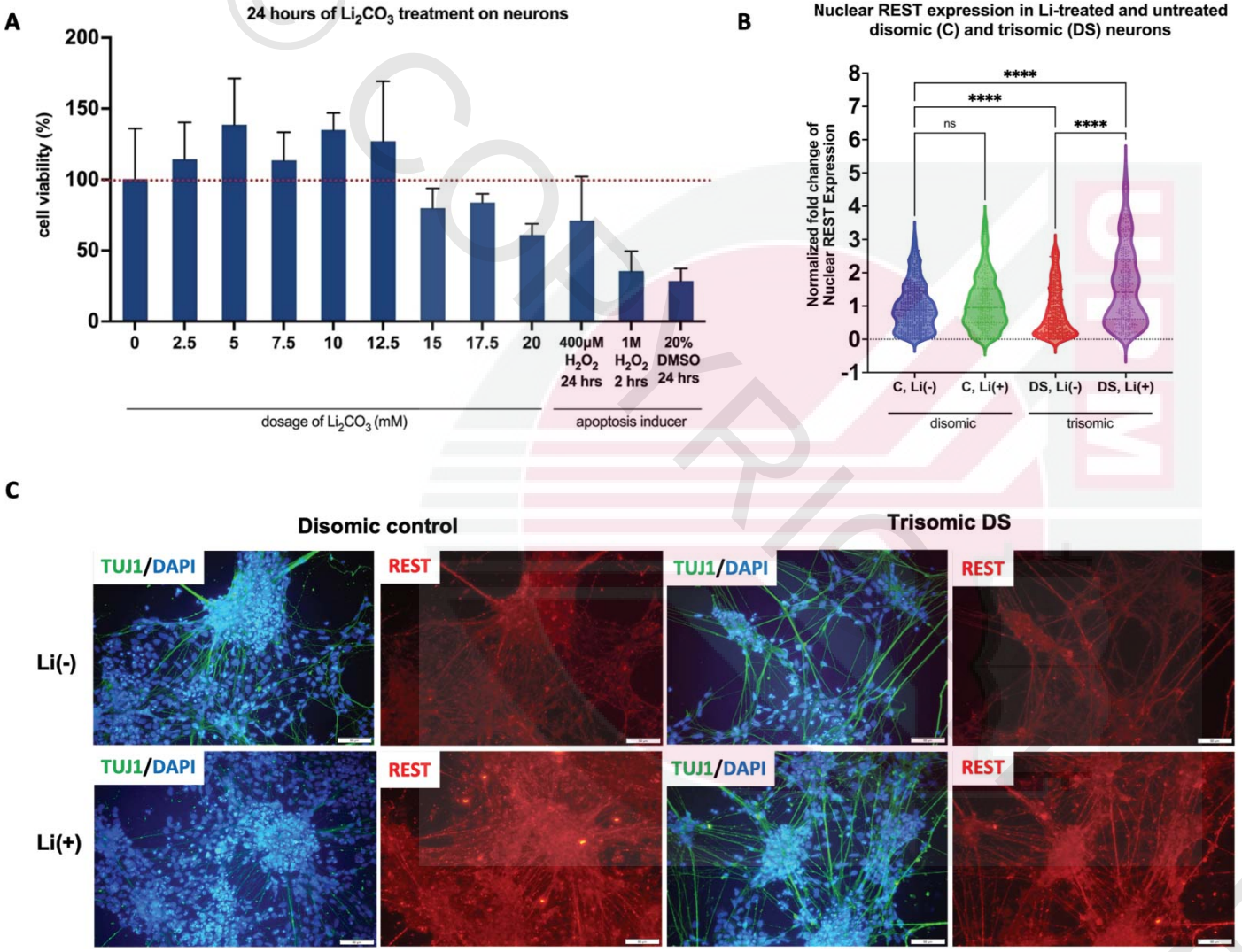

Figure 11: Investigation of REST restoration in disomic and trisomic iPSC-derived neurons.

(A) Optimization of safety dosage of lithium treatment in iPSC-derived neurons through MTT cell viability assay. Experiment was conducted on one control line and one DS line, triplicated wells in each of three experiment batches. Treatment with lithium up to 12.5 mM for 24 hours was considered safe for the neurons in which the cell viability did not drop below 100%.
(B) Nuclear REST expression in lithium treated and untreated control and DS neurons. Experiment was conducted on all 6 cell lines, for 3 experimental batches. Nuclear REST level was significantly reduced in the untreated DS neurons compared to control neurons. After treated with lithium, there was a significant increment in the nuclear REST level in the DS neurons. Kruskal-wallis test, ****p<0.0001.
(C) Representative fluorescent micrographs showing REST staining in untreated (Li-) and lithium treated (Li+) control and DS neurons. Scale bar: 50 μm.

CHAPTER 5

INVESTIGATING OXIDATIVE STRESS IN LITHIUM-TREATED DS iPSC-DERIVED NEURONS

5.1 INTRODUCTION

Having confirmed that lithium treatment positively rescues REST dysregulation in DS iPSC-derived neurons, our next step is to investigate the effects of this lithium-mediated REST restoration. Given that individuals with DS commonly experience chronic oxidative stress in the brain (Buczyńska et al., 2023), it is particularly intriguing to explore how restoring REST through lithium treatment might alleviate oxidative stress in DS neurons.

To assess this, the DCFDA intracellular ROS assay kit was employed to evaluate the post-lithium effects on DS neurons, specifically focusing on oxidative stress levels. The DCFDA (2',7'-dichlorofluorescin diacetate) ROS assay is a widely used method to measure intracellular ROS (Ng & Ooi, 2021). In this assay, the cell-permeable DCFDA compound is oxidized by ROS within the cell, resulting in a fluorescent molecule that can be quantified using fluorescence spectroscopy or microscopy. The intensity of the fluorescence signal correlates with the level of intracellular ROS, providing a reliable indicator of oxidative stress (Ng & Ooi, 2021).

By utilizing this assay, it is possible to quantitatively assess whether the lithium-mediated restoration of REST in DS neurons reduces oxidative stress,

potentially offering insights into a novel therapeutic approach for managing this aspect of DS.

5.2 Experimental Design

In this study, the six cell lines (3 control lines + 3 DS lines) were divided into four experimental groups:

- Untreated: Neurons maintained in standard B27 neuron differentiation full media without additional treatments.
- Lithium-treated [H_2O_2(-), Li(+)]: After 14 days of *in vitro* differentiation, neurons were exposed to 10 mM lithium for 24 hours.
- Stress-induced [H_2O_2(+), Li(-)]: Neurons were treated with 100 µM hydrogen peroxide (H_2O_2) for 4 hours to induce oxidative stress.
- Lithium-treated and stress-induced [H_2O_2(+), Li(+)]: Neurons were pre-treated with 10 mM lithium for 24 hours, followed by 4 hours of exposure to 100 µM hydrogen peroxide.

Following these treatments, we assessed intracellular ROS levels in the neurons using the DCFDA intracellular ROS assay kit. Fluorescence micrographs were captured using a fluorescence microscope and the images were subsequently analyzed with ImageJ software to quantify DCF signals in the neurons. This approach allowed the comparison of the effects of lithium treatment and oxidative stress induction on ROS levels across the different experimental groups.

5.3 Materials and Methods

5.3.1 Reagent Preparation

The 100 mM lithium carbonate stock solution and 10 mM lithium working solution were prepared following the protocol outlined in section 4.3.1. For the H_2O_2 preparation, a 30% (9.8 M) stock solution (Sigma, USA) was used as the starting point. To achieve the desired 100 µM working concentration, the stock solution was first diluted to 1 M by combining 0.102 mL of H_2O_2 stock with 0.898 mL of sterile distilled water. A 1:100 dilution was then performed to create a 10 mM H_2O_2 solution. Finally, the 100 µM H_2O_2 working solution was prepared by carrying out another 1:100 dilution in B27 neuron differentiation full media. For treatment purposes in a 96-well plate, 100 µL of this final working solution was prepared per well.

Furthermore, in preparation for the ROS assay, the DCFDA intracellular ROS assay kit (Abcam, England) was employed, comprising a 10X dilution buffer solution, DCFDA reagent, and tert-butyl hydroperoxide (TBHP) as a positive control. A series of dilutions were meticulously performed to prepare the working solutions. Initially, the 10X dilution buffer solution was diluted with double distilled water to create a 1X dilution buffer. This 1X buffer then served as the diluent for the DCFDA reagent, which was reduced from its stock concentration of 20 mM to a working solution of 20 µM through a 1:1000 dilution. Finally, the positive control, TBHP, transformed its original 50 mM

stock to a 400 µM working concentration, achieved by diluting it in B27 neuron differentiation full media.

5.3.2 DCFDA Intracellular ROS Assay

The ROS assay began with seeding NSCs onto a dark, clear-bottomed 96-well plate (Corning, USA) at 5 x 10^4 cells/cm^2 density. Both disomic control and trisomic DS cells were divided into four treatment groups as described in section 5.2, with an additional group designated for positive control (TBHP treatment). Each group was allocated two wells. After 14 days of *in vitro* neuron differentiation, the respective treatments were applied to each group. The existing media was removed upon completion, and wells were gently rinsed with 100 µL of 1X buffer solution. The cells were then incubated with 100 µL of 20 µM DCFDA solution for 45 minutes in a 37°C incubator with 5% CO_2. Due to DCFDA's light sensitivity, solution handling was performed carefully to minimize light exposure.

Following incubation, the DCFDA solution was removed, and cells were gently rinsed with 1X buffer solution once more. Subsequently, 50 µL of B27 neuron differentiation full media was added to each well. Additional wells with only media without cells, were assigned as blank wells. Live cell microscopy was conducted using a fluorescence microscope, with at least two fluorescence micrographs captured for each treatment group. The images were acquired using the filter set appropriate for fluorescein isothiocyanate (FITC).

5.3.3 Quantification of ROS Signals using ImageJ

The fluorescent micrographs acquired from the microscope were analysed using ImageJ software. The initial setup involved defining measurement parameters as "area", "mean grey density", and "integrated density". The software's scale was calibrated using a JPEG image with a known scale bar from the same microscope to ensure accurate measurements. This calibration process involved enlarging the image to view the scale bar, then utilizing the Set Scale function to input the known length in μm. Prior to quantifying ROS signals, a crucial background correction step was performed using a technical negative control image containing only media without cells. The brightness and contrast of this control image were adjusted in ImageJ to establish an exposure range where no signal was visible. This standardized exposure range was applied to all ROS images to ensure consistent signal intensity across samples.

The quantification process began with manually selecting regions of interest (ROIs) using the ROI manager in ImageJ. For each treatment group, fifty neuronal ROS signals were carefully outlined using the freehand drawing function, and these ROIs were saved. Measurements for all selected ROIs were taken simultaneously, generating a comprehensive results window with quantitative data. This data was then transferred to an Excel sheet for further analysis.

5.3.4 Statistical Analysis

A comprehensive analysis of intracellular ROS levels was conducted, examining 50 neurons per treatment group for each cell line. The analysis began with organizing raw integrated density data into grouped formats. The ROUT method, with a Q value of 5%, was applied to remove statistical outliers, enhancing the reliability of the dataset. To ensure data accuracy and comparability, a line-to-line normalization process was implemented using the GraphPad Prism software (version 9.0). This involved transforming the values by dividing all data points by the mean of the untreated control for each isogenic line pair. Following normalization, multiple data tables were created to organize and compile the results. These tables were structured according to various grouping criteria, including genotype, cell line, and treatment conditions. This organizational approach facilitated a multi-layered analysis, enabling comparisons at different levels - between individual cell lines, across genotypes, and among various treatment groups.

The statistical analysis began with normality tests to determine the distribution of the data. These tests revealed non-parametric distributions, which informed the choice of Mann-Whitney and Kruskal-Wallis tests to be selected as the appropriate methods for analysis. This test was applied to combined data sets to identify statistically significant ROS signal differences between different treatment groups and genotypes. To visually represent the findings, a box plot was created to summarize individual data points for each neuron across the various treatment groups and genotypes. The box plot provided a

comprehensive view of the data distribution, allowing for easy identification of trends, outliers, and differences between groups.

5.4 Results and Discussion

To validate the effectiveness of the DCFDA intracellular ROS assay kit, a preliminary test was conducted using a set of control neurons. These neurons were treated with 400 µM of TBHP, which the kit manufacturer provided as a positive control reagent. This step was performed before measuring intracellular ROS levels in all the six lines of iPSC-derived neurons subjected to lithium treatment and stress induction. It ensures the reliability of the subsequent ROS measurements in the experimental groups. **Figure 12A** demonstrates that treatment with 400 µM TBHP significantly increases ROS levels in iPSC-derived neurons, confirming the efficacy of the kit.

Furthermore, from the second graph **(Figure 12B)**, it illustrates the effects of lithium treatment and hydrogen peroxide-induced stress on ROS levels in disomic control and trisomic DS neurons. There are several key findings. Firstly, the untreated DS neurons exhibit significantly higher baseline ROS levels than their disomic counterparts, indicating an inherently higher level of oxidative stress in DS neurons. Notably, lithium treatment (Li+) demonstrates a significant rescue effect in DS neurons, substantially reducing ROS levels to near-disomic baselines. Interestingly, lithium's effect appears specific to DS neurons, as it shows minimal or insignificant impact on ROS levels in the

control neurons. This observation is exciting as lithium has a selective rescue effect on trisomic neurons.

When exposed to H_2O_2, both control and DS neurons show significantly increased ROS levels, but the effect is more pronounced in DS neurons, suggesting their heightened sensitivity to oxidative stress. However, when the stress-induced DS neurons were pre-treated with lithium [DS, H_2O_2(+) Li(+)], there seems to be no obvious rescue effect of the lithium treatment, as the ROS level remained significantly high compared to the untreated control neurons, indicating failure to bring down the ROS levels to near-baseline level.

Moreover, the graph in **Figure 12B** reveals an interesting pattern: the four box plots representing the trisomy DS group appear generally longer than those of the disomic control group. This indicates a wider spread of data points in the DS neurons, suggesting variability in their responses. In other words, the DS iPSC-derived neurons showed diverse reactions to stress and treatment, pointing to heterogeneity in DS cellular behaviour.

5.5 Conclusions

In conclusion, this chapter highlights the inherently higher level of baseline oxidative stress in DS neurons, and the effective rescue of lithium to bring down oxidative stress in DS neurons to near-disomic level.

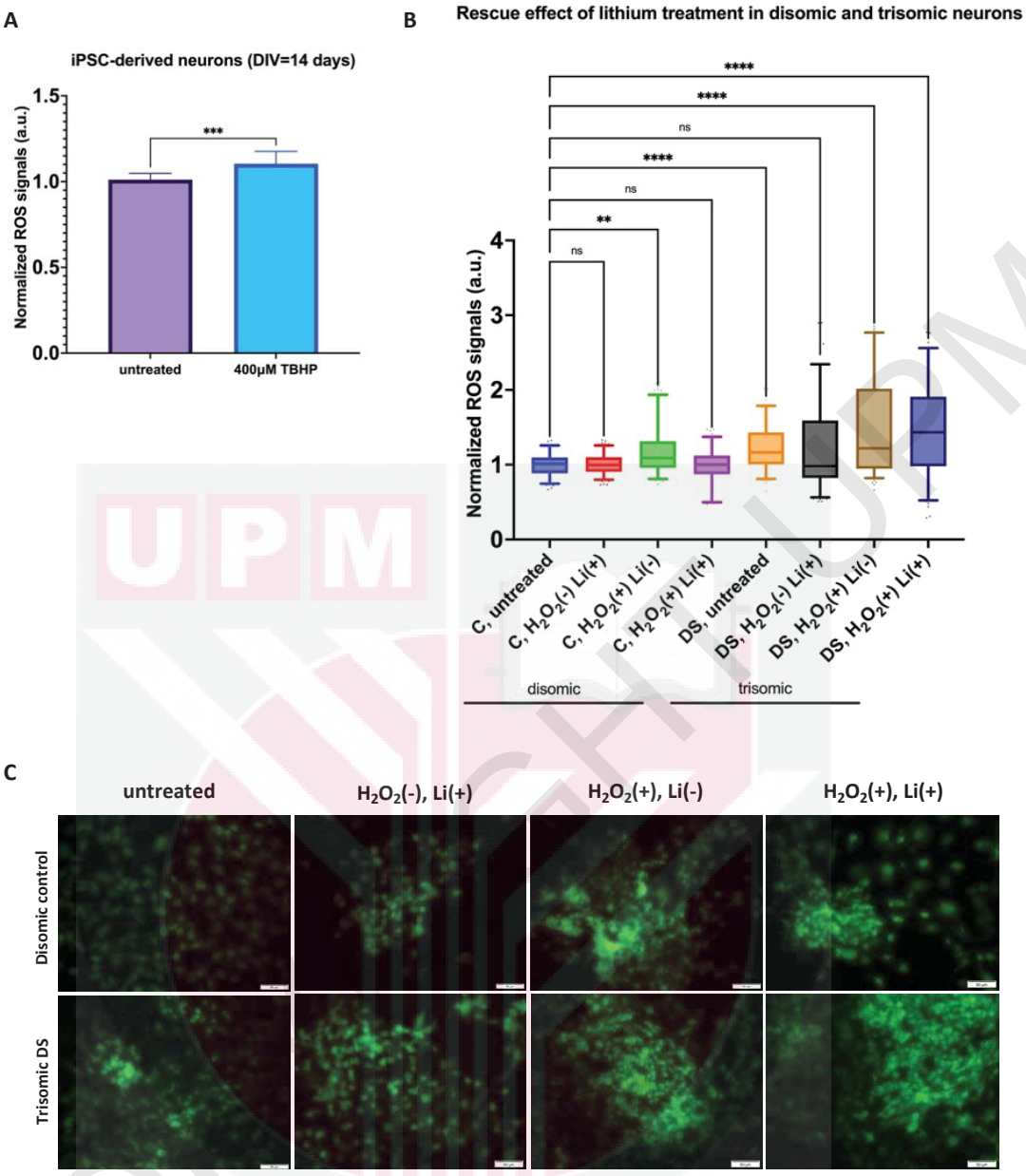

Figure 12: Rescue effect of lithium treatment against ROS in disomic and trisomic iPSC-derived neurons. (A) ROS level in iPSC-derived neurons is significantly elevated after being treated with 400 μM of TBHP (positive control), indicating proper functioning of the ROS assay kit. Mann-Whitney test: ***p=0.0001. **(B)** When compared to the untreated control group, DS neurons have significantly increased ROS levels. After being treated with lithium, the ROS level dropped to near-baseline level in both genotype groups. Upon hydrogen peroxide treatment (stress-induced), both control and DS neurons show significantly elevated ROS. When the stress-induced neurons were pre-treated with lithium, the disomic control neurons improved ROS reduction. However, this lithium-mediated ROS improvement is not seen in the DS group where the ROS level is still significantly high. Experiment was conducted on all six cell lines, for three batches of experiment. Kruskal-Wallis test: **p=0.0010; ****p<0.0001. **(C)** Representative fluorescent micrographs showing positive ROS staining in disomic control and trisomic DS neurons. Scale bar: 50 μm.

CHAPTER 6

GENERAL DISCUSSION

6.1 Downregulated Nuclear REST in DS iPSC-derived Neurons

This study confirms the downregulation of nuclear REST expression in DS iPSC-derived neurons compared to control neurons. Previous studies investigating the role of REST in DS neuropathologies have reported inconsistent REST expression levels (Bahn et al., 2002; Canzonetta et al., 2008; Lepagnol-Bestel et al., 2009; Lim et al., 2024). These discrepancies may be attributed to the diverse models used, including various cell and mouse models. It is important to note that mouse models, while valuable, have inherent limitations in mimicking human neurological conditions (Gupta et al., 2016; Herault et al., 2017). In contrast, this study utilized iPSC-derived neurons, believed to provide a more accurate representation of human neural cells. This approach likely yields more reliable results, offering a closer approximation of REST dynamics in human DS neurons. Using this advanced model, our findings contribute to a clearer understanding of REST's role in DS pathology.

In this study, the focus on nuclear REST is particularly relevant, given that its nuclear translocation is essential for proper function in the central nervous system (Lam et al., 2023). Studies have shown that AD and PD brains exhibit a deficiency in nuclear REST, in contrast to healthy aging brains. This absence

suggests a reduction in REST-mediated neuroprotection and stress resilience (Kawamura et al., 2019; Lu et al., 2014; Mampay et al., 2021; Meyer et al., 2019). Interestingly, the opposite trend is observed in Huntington's disease brains, where nuclear REST is abundant. This overexpression is attributed to mutant huntingtin proteins in the cytoplasm, which fail to sequester REST, allowing it to accumulate in the nucleus. The excessive nuclear REST leads to over-repression of crucial neuronal genes, including brain-derived neurotrophic factors (BDNF), ultimately hampering neuroprotective mechanisms (Zuccato et al., 2003, 2007). Therefore, the observed downregulation of nuclear REST in DS neurons in this study, is likely to contribute to the neurodevelopmental and cognitive impairments associated with DS individuals.

6.2 Lithium-mediated REST Restoration in DS iPSC-derived Neurons

It is engaging that the dysregulated nuclear REST in DS can be restored. In this study, while lithium had minimal effect on REST expression in control neurons, it significantly increased nuclear REST levels in DS iPSC-derived neurons, effectively restoring them to levels comparable to or even higher than untreated control neurons. This selective effect of lithium on DS neurons suggests a potential mechanism for countering the neurological abnormalities associated with trisomy 21. The differential response to lithium treatment between control and DS neurons provides a promising avenue for therapeutic intervention. These findings not only enhance our understanding of DS

pathology but also highlight lithium as a potential therapeutic agent for addressing REST dysregulation in DS.

This study confirms that lithium can restore nuclear REST levels in DS neurons **(Figure 11B)**, prompting further investigation into the relationship between lithium and REST. Current literature suggests that the Wnt signaling pathway regulates REST (Nishihara et al., 2003), while lithium acts as a GSK-3β inhibitor, consequently activating this pathway (Junde et al., 2023; Liu et al., 2024). This connection implies a potential positive correlation between lithium and REST. In fact, several studies have demonstrated neuroprotective effects resulting from lithium-mediated REST upregulation in various disease models, including AD (Lu et al., 2014), prion disease (Song et al., 2017), and bipolar disorder (Meyer et al., 2023). However, conflicting evidence exists, with a previous study indicating that lithium treatment can suppress REST through increased miR-124 expression (Doeppner et al., 2017).

Understanding the precise mechanism linking lithium and REST is crucial for developing more targeted and effective treatments for neurological disorders. Elucidating this complex relationship could provide valuable insights into the therapeutic potential of lithium and inform the development of novel interventions for conditions such as DS and other neurodegenerative diseases.

6.3 Lithium Selectively Rescues Oxidative Stress in DS Neurons

Findings from this study provide compelling evidence for the intrinsic vulnerability of DS iPSC-derived neurons to oxidative stress and highlight the potential therapeutic benefits of lithium treatment. The significantly higher baseline levels of ROS observed in untreated DS neurons compared to disomic control neurons **(Figure 12B)**, underscore the inherent oxidative imbalance in DS neuronal populations. Importantly, the selective rescue effect of lithium on DS neurons, which reduced ROS levels to near-disomic baselines without significantly affecting control neurons, presents an exciting avenue for targeted therapeutic interventions. This specificity suggests that lithium may address a unique aspect of DS cellular physiology, potentially related to the overexpression of chromosome 21 genes or downstream effects of trisomy.

Furthermore, the heightened sensitivity of DS neurons to hydrogen peroxide-induced oxidative stress emphasizes their vulnerability to environmental insults. The more pronounced increase in ROS levels in DS neurons compared to controls upon H_2O_2 exposure indicates a compromised ability to manage additional oxidative challenges. This observation may explain, in part, the accelerated neurodegeneration and cognitive decline often seen in individuals with DS (Hasina et al., 2022; Lockrow et al., 2012).

This study demonstrated lithium's ability to reduce oxidative stress in DS iPSC-derived neurons. While the exact mechanism was not being investigated, existing literature provides potential insights into how lithium might work. In DS,

BACH1, a gene located on chromosome 21, is overexpressed and acts as a repressor of NRF2 - a key regulator of cellular antioxidant responses. This overexpression of BACH1 leads to excessive suppression of NRF2, weakening the antioxidant defenses in DS neurons (Pagnotta et al., 2022; Zamponi et al., 2018; Zhang et al., 2018). Encouragingly, lithium has been shown to activate NRF2 through GSK3 inhibition (Alural et al., 2015; Castillo-Quan et al., 2016), suggesting that this pathway might explain the antioxidant effects we observed in DS neurons.

However, the lack of a significant rescue effect by lithium pre-treatment in stress-induced DS neurons is noteworthy. The NRF2-mediated rescue mechanism might be compromised in stressed DS neurons. This limitation highlights the complexity of oxidative stress management in DS neurons and underscores the need for multi-faceted therapeutic approaches. Nevertheless, lithium being able to reduce ROS levels in stress-induced disomic control neurons significantly, have provided a proof-of-concept as to the working hypothesis that lithium can indeed combat oxidative stress. While these connections are promising, further mechanistic studies are needed to confirm the exact pathway through which lithium provides its protective effects and to understand why this protection fails under stress conditions.

6.4 Limitations and Recommendations for Future Research

iPSC-derived neurons, while valuable for many research applications, have limitations compared to 3D cerebral organoids. They lack the complex cellular

organization. The simplified culture conditions of iPSC-derived neurons limit the cell-type diversity and complex cell-cell interactions that occur in the brain. While they can be differentiated into specific neuronal subtypes, they often lack the full range of cell types in the brain, including glia and other supporting cells. Cerebral organoids on the other hand, allow for more natural interactions between different cell types, potentially leading to more physiologically relevant results. Additionally, iPSC-derived neurons do not undergo the same developmental processes as the human brain, however cerebral organoids can recapitulate some aspects of early brain development and develop multiple brain regions with a degree of spatial organization (Chiaradia & Lancaster, 2020; Rizzuti et al., 2024). Therefore, future studies should consider using cerebral organoids to enhance the validity and robustness of their findings.

Moreover, this study confirms that lithium restores REST levels in DS iPSC-derived neurons, focusing on how this restoration affects oxidative stress. However, given that REST is an epigenetic transcription factor governing a network of genes (Lam et al., 2023), exploring its broader downstream effects would be exciting. Based on a study by Huang et al. (2023), a high percentage (60-86%) of differentially expressed genes in DS brain tissues and neural cells are targeted by REST. The researchers found that REST-targeted genes are significantly enriched in the JAK-STAT and HIF-1 signaling pathways across multiple brain regions, developmental stages, and neural cell types in DS. These pathways, along with processes related to nervous system development, cell differentiation, inflammation, and metabolism, appear to be

key mechanisms through which REST dysregulation contributes to DS neuropathogenesis (Huang et al., 2023). Future research could investigate these wider impacts of REST restoration and determine whether they translate to functional improvements in DS neurons.

Furthermore, DS iPSC-derived neurons respond differently to stress and treatment. Such variability presents both challenges and opportunities in developing treatments for DS. On one hand, such differences make it hard to find one treatment for all DS patients. On the other hand, it also means we could create treatments tailored to each person. Future research can focus on understanding the molecular mechanisms underlying this variability and exploring combination therapies that may provide more comprehensive protection against oxidative stress in DS neurons.

CHAPTER 7

CONCLUSIONS

This study has made significant strides in understanding the role of REST in DS iPSC-derived neurons and the potential therapeutic applications of lithium. It confirms the downregulation of nuclear REST in DS iPSC-derived neurons and demonstrates that lithium treatment can effectively restore nuclear REST levels. This restoration is particularly noteworthy as it selectively affects DS neurons, bringing their REST levels to or above those of untreated control neurons. The research also reveals the intrinsic vulnerability of DS neurons to oxidative stress and shows that lithium can reduce baseline ROS levels in these cells to near-disomic levels. Additionally, while the focus on oxidative stress provides crucial insights, exploring other downstream effects of REST restoration could offer a more comprehensive understanding of DS neuropathology. Moving forward, research should aim to elucidate the precise mechanisms linking lithium and REST, at the same time explore broader impacts of REST restoration.

REFERENCES

Aguirre, M., Escobar, M., Forero Amézquita, S., Cubillos, D., Rincón, C., Vanegas, P., Tarazona, M. P., Atuesta Escobar, S., Blanco, J. C., & Celis, L. G. (2023). Application of the Yamanaka transcription factors Oct4, Sox2, Klf4, and c-Myc from the Laboratory to the Clinic. *Genes*, *14*(9). https://doi.org/10.3390/GENES14091697

Akhtar, F., & Bokhari, S. R. A. (2023). Down Syndrome. *The 5-Minute Pediatric Consult, 8th Edition*, 306–307. https://doi.org/10.1017/9781316671863.043

Alberts, B., Johnson, A., Lewis, J., Raff, M., Roberts, K., & Walter, P. (2002). *Neural Development*. https://www.ncbi.nlm.nih.gov/books/NBK26814/

Alural, B., Ozerdem, A., Allmer, J., Genc, K., & Genc, S. (2015). Lithium protects against paraquat neurotoxicity by NRF2 activation and miR-34a inhibition in SH-SY5Y cells. *Frontiers in Cellular Neuroscience*, *9*(MAY). https://doi.org/10.3389/FNCEL.2015.00209

Anderson, N. C., Chen, P. F., Meganathan, K., Afshar Saber, W., Petersen, A. J., Bhattacharyya, A., Kroll, K. L., & Sahin, M. (2021). Balancing serendipity and reproducibility: Pluripotent stem cells as experimental systems for intellectual and developmental disorders. *Stem Cell Reports*, *16*(6), 1446–1457. https://doi.org/10.1016/j.stemcr.2021.03.025

Andrade Nunes, M., Araujo Viel, T., & Sousa Buck, H. (2013). Microdose lithium treatment stabilized cognitive impairment in patients with Alzheimer's disease. *Current Alzheimer Research*, *10*(1), 104–107. https://doi.org/10.2174/1567205011310010014

Aranha, M. R., Fortea, J., & Carmona-Iragui, M. (2022). Cerebral Amyloid Angiopathy-Related Inflammation in Down Syndrome-related Alzheimer disease. *Neurology*, *98*(24), 1021–1022. https://doi.org/10.1212/WNL.0000000000200704

Araujo, B. H. S., Kaid, C., De Souza, J. S., Gomes da Silva, S., Goulart, E., Caires, L. C. J., Musso, C. M., Torres, L. B., Ferrasa, A., Herai, R., Zatz, M., Okamoto, O. K., & Cavalheiro, E. A. (2018). Down Syndrome iPSC-Derived Astrocytes Impair Neuronal Synaptogenesis and the mTOR pathway in vitro. *Molecular Neurobiology*, *55*(7), 5962–5975. https://doi.org/10.1007/S12035-017-0818-6

Bahn, S., Mimmack, M., Ryan, M., Caldwell, M. A., Jauniaux, E., Starkey, M., Svendsen, C. N., & Emson, P. (2002). Neuronal target genes of the neuron-restrictive silencer factor in neurospheres derived from fetuses with Down's syndrome: a gene expression study. *Lancet (London, England)*, *359*(9303), 310–315. https://doi.org/10.1016/S0140-6736(02)07497-4

Baldessarini, R. J., Tondo, L., & Vázquez, G. H. (2019). Pharmacological treatment of adult bipolar disorder. *Molecular Psychiatry*, *24*(2), 198–217. https://doi.org/10.1038/S41380-018-0044-2

Ballas, N., Battaglioli, E., Atouf, F., Andres, M. E., Chenoweth, J., Anderson, M. E., Burger, C., Moniwa, M., Davie, J. R., Bowers, W. J., Federoff, H. J., Rose, D. W., Rosenfeld, M. G., Brehm, P., & Mandel, G. (2001). Regulation of neuronal traits by a novel transcriptional complex. *Neuron*, *31*(3), 353–365. https://doi.org/10.1016/S0896-6273(01)00371-3

Ballas, N., Grunseich, C., Lu, D. D., Speh, J. C., & Mandel, G. (2005). REST and its corepressors mediate plasticity of neuronal gene chromatin throughout neurogenesis. *Cell, 121*(4), 645–657. https://doi.org/10.1016/j.cell.2005.03.013

Bambrick, L. L., & Fiskum, G. (2008). Mitochondrial dysfunction in mouse trisomy 16 brain. *Brain Research*, *1188*(1), 9–16. https://doi.org/10.1016/J.BRAINRES.2007.10.045

Bedini, A., Baiula, M., & Spampinato, S. (2008). Transcriptional activation of human mu-opioid receptor gene by insulin-like growth factor-I in neuronal cells is modulated by the transcription factor REST. *Journal of Neurochemistry, 105*(6), 2166–2178. https://doi.org/10.1111/j.1471-4159.2008.05303.x

Bedini, A., Baiula, M., Carbonari, G., & Spampinato, S. (2010). Transcription factor REST negatively influences the protein kinase C-dependent up-regulation of human mu-opioid receptor gene transcription. *Neurochemistry International, 56*(2), 308–317. https://doi.org/10.1016/j.neuint.2009.10.014

Benhaourech, S., Drighil, A., & El Hammiri, A. (2016). Congenital heart disease and Down syndrome: various aspects of a confirmed association. *Cardiovascular Journal of Africa*, *27*(5), 287. https://doi.org/10.5830/CVJA-2016-019

Bhattacharyya, A., McMillan, E., Chen, S. I., Wallace, K., & Svendsen, C. N. (2009). A Critical Period in Cortical Interneuron Neurogenesis in Down Syndrome Revealed by Human Neural Progenitor Cells. *Developmental Neuroscience*, *31*(6), 497–510. https://doi.org/10.1159/000236899

Bianchi, P., Ciani, E., Contestabile, A., Guidi, S., & Bartesaghi, R. (2010). Lithium restores neurogenesis in the subventricular zone of the Ts65Dn mouse, a model for Down syndrome. *Brain Pathology (Zurich, Switzerland)*, *20*(1), 106–118. https://doi.org/10.1111/J.1750-3639.2008.00246.X

Birtele, M., Sharma, Y., Kidnapillai, S., Lau, S., Stoker, T. B., Barker, R. A., Rylander Ottosson, D., Drouin-Ouellet, J., & Parmar, M. (2019). Dual modulation of neuron-specific microRNAs and the REST complex promotes functional maturation of human adult induced neurons. *FEBS Letters, 593*(23), 3370–3380. https://doi.org/10.1002/1873-3468.13612

Bordon, Y. (2023). Immune dysregulation in Down syndrome. *Nature Reviews Immunology 2023 23:4*, *23*(4), 201–201. https://doi.org/10.1038/s41577-023-00855-z

Buczyńska, A., Sidorkiewicz, I., Krętowski, A. J., & Zbucka-Krętowska, M. (2023). The Role of Oxidative Stress in Trisomy 21 Phenotype. *Cellular and Molecular Neurobiology 2023 43:8*, *43*(8), 3943–3963. https://doi.org/10.1007/S10571-023-01417-6

Bull, M. J., Saal, H. M., Braddock, S. R., Enns, G. M., Gruen, J. R., Perrin, J. M., Saul, R. A., Tarini, B. A., Hersh, J. H., Mendelsohn, N. J., Hanson, J. W., Lloyd-Puryear, M. A., Musci, T. J., Rasmussen, S. A., Downs, S. M., & Spire, P. (2011). Health Supervision for Children with Down Syndrome. *Pediatrics*, *128*(2), 393–406. https://doi.org/10.1542/PEDS.2011-1605

Burkholder, N. T., Mayfield, J. E., Yu, X., Irani, S., Arce, D. K., Jiang, F., Matthews, W. L., Xue, Y., & Zhang, Y. J. (2018). Phosphatase activity of small C-terminal

domain phosphatase 1 (SCP1) controls the stability of the key neuronal regulator RE1-silencing transcription factor (REST). *The Journal of Biological Chemistry, 293*(43), 16851–16861. https://doi.org/10.1074/JBC.RA118.004722

Busciglio, J., & Yankner, B. A. (1995). Apoptosis and increased generation of reactive oxygen species in Down's syndrome neurons in vitro. *Nature 1995 378:6559*, *378*(6559), 776–779. https://doi.org/10.1038/378776a0

Canzonetta, C., Mulligan, C., Deutsch, S., Ruf, S., O'Doherty, A., Lyle, R., Borel, C., Lin-Marq, N., Delom, F., Groet, J., Schnappauf, F., De Vita, S., Averill, S., Priestley, J. V., Martin, J. E., Shipley, J., Denyer, G., Epstein, C. J., Fillat, C., … Nizetic, D. (2008). DYRK1A-dosage imbalance perturbs NRSF/REST levels, deregulating pluripotency and embryonic stem cell fate in Down syndrome. *American Journal of Human Genetics*, *83*(3), 388–400. https://doi.org/10.1016/J.AJHG.2008.08.012

Carducci, F., Onorati, P., Condoluci, C., Di Gennaro, G., Quarato, P. P., Pierallini, A., Sarà, M., Miano, S., Cornia, R., & Albertini, G. (2013). Whole-brain voxel-based morphometry study of children and adolescents with Down syndrome. *Functional Neurology*, *28*(1), 19. https://doi.org/10.11138/FNeur/2013.28.1.019

Castillo-Quan, J. I., Li, L., Kinghorn, K. J., Ivanov, D. K., Tain, L. S., Slack, C., Kerr, F., Nespital, T., Thornton, J., Hardy, J., Bjedov, I., & Partridge, L. (2016). Lithium Promotes Longevity through GSK3/NRF2-Dependent Hormesis. Cell Reports, 15(3), 638–650. https://doi.org/10.1016/J.CELREP.2016.03.041

Chen, C., Jiang, P., Xue, H., Peterson, S. E., Tran, H. T., McCann, A. E., Parast, M. M., Li, S., Pleasure, D. E., Laurent, L. C., Loring, J. F., Liu, Y., & Deng, W. (2014). Role of astroglia in Down's syndrome revealed by patient-derived human-induced pluripotent stem cells. *Nature Communications 2014 5:1*, *5*(1), 1–18. https://doi.org/10.1038/ncomms5430

Chen, X. Q., & Zuo, X. (2024). New insights into the effects of APP gene dose on synapse in Down syndrome. *Neural Regeneration Research*, *19*(5), 961–962. https://doi.org/10.4103/1673-5374.382245

Chiaradia, I., & Lancaster, M. A. (2020). Brain organoids for the study of human neurobiology at the interface of in vitro and in vivo. *Nature Neuroscience 2020 23:12*, *23*(12), 1496–1508. https://doi.org/10.1038/s41593-020-00730-3

Chong, J. A., Tapia-Ramirez, J., Kim, S., Toledo-Aral, J. J., Zheng, Y., Boutros, M. C., Altshuller, Y. M., Frohman, M. A., Kraner, S. D., & Mandel, G. (1995). REST: a mammalian silencer protein that restricts sodium channel gene expression to neurons. *Cell*, *80*(6), 949–957. https://doi.org/10.1016/0092-8674(95)90298-8

Claassen, D. A., Desler, M. M., & Rizzino, A. (2009). ROCK Inhibition Enhances the Recovery and Growth of Cryopreserved Human Embryonic Stem Cells and Human Induced Pluripotent Stem Cells. *Molecular Reproduction and Development*, *76*(8), 722. https://doi.org/10.1002/MRD.21021

Contestabile, A., Greco, B., Ghezzi, D., Tucci, V., Benfenati, F., & Gasparini, L. (2013). Lithium rescues synaptic plasticity and memory in Down syndrome mice. *The Journal of Clinical Investigation*, *123*(1), 348–361. https://doi.org/10.1172/JCI64650

Costa, A. C. S., Walsh, K., & Davisson, M. T. (1999). Motor dysfunction in a mouse model for Down syndrome. *Physiology & Behavior*, *68*(1–2), 211–220. https://doi.org/10.1016/S0031-9384(99)00178-X

Covey, M. V., Streb, J. W., Spektor, R., & Ballas, N. (2012). REST regulates the pool size of the different neural lineages by restricting the generation of neurons and oligodendrocytes from neural stem/progenitor cells. *Development (Cambridge)*, *139*(16), 2878–2890. https://doi.org/10.1242/DEV.074765/-/DC1

Czerminski, J. T., King, O. D., & Lawrence, J. B. (2023). Large-scale organoid study suggests effects of trisomy 21 on early fetal neurodevelopment are more subtle than variability between isogenic lines and experiments. *Frontiers in Neuroscience*, *16*, 972201. https://doi.org/10.3389/FNINS.2022.972201

Davisson, M., Akeson, E., Schmidt, C., Harris, B., Farley, J., & Handel, M. A. (2007). Impact of trisomy on fertility and meiosis in male mice. *Human Reproduction*, *22*(2), 468–476. https://doi.org/10.1093/HUMREP/DEL397

Davisson, M. T., Bechtel, L. J., Akeson, E. C., Fortna, A., Slavov, D., & Gardiner, K. (2001). Evolutionary breakpoints on human chromosome 21. *Genomics*, *78*(1–2), 99–106. https://doi.org/10.1006/GENO.2001.6639

DeWeirdt, P. C., Sangree, A. K., Hanna, R. E., Sanson, K. R., Hegde, M., Strand, C., Persky, N. S., & Doench, J. G. (2020). Genetic screens in isogenic mammalian cell lines without single cell cloning. *Nature Communications 2020 11:1*, *11*(1), 1–15. https://doi.org/10.1038/s41467-020-14620-6

Dierssen, M., Herault, Y., & Estivill, X. (2009). Aneuploidy: from a physiological mechanism of variance to Down syndrome. *Physiological Reviews*, *89*(3), 887–920. https://doi.org/10.1152/PHYSREV.00032.2007

Dimopoulos, K., Constantine, A., Clift, P., Condliffe, R., Moledina, S., Jansen, K., Inuzuka, R., Veldtman, G. R., Cua, C. L., Tay, E. L. W., Opotowsky, A. R., Giannakoulas, G., Alonso-Gonzalez, R., Cordina, R., Capone, G., Namuyonga, J., Scott, C. H., D'Alto, M., Gamero, F. J., … Broberg, C. S. (2023). Cardiovascular Complications of Down Syndrome: Scoping Review and Expert Consensus. *Circulation*, *147*(5), 425–441. https://doi.org/10.1161/CIRCULATIONAHA.122.059706

Diniz, B. S., Machado-Vieira, R., & Forlenza, O. V. (2013). Lithium and neuroprotection: Translational evidence and implications for the treatment of neuropsychiatric disorders. In *Neuropsychiatric Disease and Treatment* (Vol. 9, pp. 493–500). Dove Medical Press Ltd. https://doi.org/10.2147/NDT.S33086

Doeppner, T. R., Kaltwasser, B., Sanchez-Mendoza, E. H., Caglayan, A. B., Bähr, M., & Hermann, D. M. (2017). Lithium-induced neuroprotection in stroke involves increased miR-124 expression, reduced RE1-silencing transcription factor abundance and decreased protein deubiquitination by GSK3β inhibition-independent pathways. *Journal of Cerebral Blood Flow and Metabolism*, *37*(3), 914–926. http://dx.doi.org/10.1177/0271678X16647738

Ellis, P., Fagan, B. M., Magness, S. T., Hutton, S., Taranova, O., Hayashi, S., McMahon, A., Rao, M., & Pevny, L. (2004). SOX2, a persistent marker for multipotential neural stem cells derived from embryonic stem cells, the embryo

or the adult. *Developmental Neuroscience*, *26*(2–4), 148–165. https://doi.org/10.1159/000082134

Engel, T., Goñi-Oliver, P., Lucas, J. J., Avila, J., & Hernández, F. (2006). Chronic lithium administration to FTDP-17 tau and GSK-3beta overexpressing mice prevents tau hyperphosphorylation and neurofibrillary tangle formation, but pre-formed neurofibrillary tangles do not revert. *Journal of Neurochemistry*, *99*(6), 1445–1455. https://doi.org/10.1111/J.1471-4159.2006.04139.X

Fedorova, V., Vanova, T., Elrefae, L., Pospisil, J., Petrasova, M., Kolajova, V., Hudacova, Z., Baniariova, J., Barak, M., Peskova, L., Barta, T., Kaucka, M., Killinger, M., Vecera, J., Bernatik, O., Cajanek, L., Hribkova, H., & Bohaciakova, D. (2019). Differentiation of neural rosettes from human pluripotent stem cells in vitro is sequentially regulated on a molecular level and accomplished by the mechanism reminiscent of secondary neurulation. *Stem Cell Research*, *40*, 101563. https://doi.org/10.1016/J.SCR.2019.101563

Gardiner, K. (2004). Gene-dosage effects in Down syndrome and trisomic mouse models. *Genome Biology*, *5*(10), 1–4. https://doi.org/10.1186/GB-2004-5-10-244

Gensous, N., Bacalini, M. G., Franceschi, C., & Garagnani, P. (2020). Down syndrome, accelerated aging and immunosenescence. *Seminars in Immunopathology*, *42*(5), 635. https://doi.org/10.1007/S00281-020-00804-1

Ghasemi, M., Turnbull, T., Sebastian, S., & Kempson, I. (2021). The mtt assay: Utility, limitations, pitfalls, and interpretation in bulk and single-cell analysis. *International Journal of Molecular Sciences*, *22*(23). https://doi.org/10.3390/IJMS222312827/S1

Giacomini, A., Stagni, F., Emili, M., Guidi, S., Salvalai, M. E., Grilli, M., Vidal-Sanchez, V., Martinez-Cué, C., & Bartesaghi, R. (2018). Treatment with corn oil improves neurogenesis and cognitive performance in the Ts65Dn mouse model of Down syndrome. *Brain Research Bulletin*, *140*, 378–391. https://doi.org/10.1016/j.brainresbull.2018.06.009

Gomez, W., Morales, R., Maracaja-Coutinho, V., Parra, V., & Nassif, M. (2020). Down syndrome and Alzheimer's disease: common molecular traits beyond the amyloid precursor protein. *Aging*, *12*(1), 1011–1033. https://doi.org/10.18632/AGING.102677

Gordon, J., Amini, S., & White, M. K. (2013). General overview of neuronal cell culture. *Methods in Molecular Biology (Clifton, N.J.)*, *1078*, 1. https://doi.org/10.1007/978-1-62703-640-5_1

Gough, G., O'Brien, N. L., Alic, I., Goh, P. A., Yeap, Y. J., Groet, J., Nizetic, D., & Murray, A. (2020). Modeling Down syndrome in cells: From stem cells to organoids. *Progress in Brain Research*, *251*, 55–90. https://doi.org/10.1016/BS.PBR.2019.10.003

Grimes, J. A., Nielsen, S. J., Battaglioli, E., Miska, E. A., Speh, J. C., Berry, D. L., Atouf, F., Holdener, B. C., Mandel, G., & Kouzarides, T. (2000). The co-repressor mSin3A is a functional component of the REST-CoREST repressor complex. *The Journal of Biological Chemistry*, *275*(13), 9461–9467. https://doi.org/10.1074/JBC.275.13.9461

Gropp, A., Kolbus, U., & Giers, D. (1975). Systematic approach to the study of trisomy in the mouse. II. *Cytogenetics and Cell Genetics*, *14*(1), 42–62. https://doi.org/10.1159/000130318

Guidi, S., Bianchi, P., Stagni, F., Giacomini, A., Emili, M., Trazzi, S., Ciani, E., & Bartesaghi, R. (2017). Lithium Restores Age-related Olfactory Impairment in the Ts65Dn Mouse Model of Down Syndrome. *CNS & Neurological Disorders Drug Targets*, *16*(7). https://doi.org/10.2174/1871527315666160801143108

Guo, S., Arai, K., Stins, M. F., Chuang, D. M., & Lo, E. H. (2009). Lithium Upregulates Vascular Endothelial Growth Factor in Brain Endothelial Cells and Astrocytes. *Stroke; a Journal of Cerebral Circulation*, *40*(2), 652. https://doi.org/10.1161/STROKEAHA.108.524504

Gupta, M., Dhanasekaran, A. R., & Gardiner, K. J. (2016). Mouse models of Down syndrome: gene content and consequences. *Mammalian Genome : Official Journal of the International Mammalian Genome Society*, *27*(11–12), 538–555. https://doi.org/10.1007/S00335-016-9661-8

Haines, D. E., & Mihailoff, G. A. (2018). Fundamental Neuroscience for Basic and Clinical Applications. In *Fundamental Neuroscience for Basic and Clinical Applications: Fifth Edition* (5th ed.). Elsevier Inc. https://doi.org/10.1016/B978-0-323-39632-5.00016-5

Hamed, R. R., Maharem, T. M., Abdel-Meguid, N., Sabry, G. M., Abdalla, A. M., & Guneidy, R. A. (2011). Purification and biochemical characterization of glutathione S-transferase from Down syndrome and normal children erythrocytes: A comparative study. *Research in Developmental Disabilities*, *32*(5), 1470–1482. https://doi.org/10.1016/J.RIDD.2011.01.013

Hampton, T. G., Stasko, M. R., Kale, A., Amende, I., & Costa, A. C. S. (2004). Gait dynamics in trisomic mice: Quantitative neurological traits of Down syndrome. *Physiology and Behavior*, *82*(2–3), 381–389. https://doi.org/10.1016/j.physbeh.2004.04.006

Hasina, Z., Wang, N., & Wang, C. C. (2022). Developmental Neuropathology and Neurodegeneration of Down Syndrome: Current Knowledge in Humans. *Frontiers in Cell and Developmental Biology*, *10*. https://doi.org/10.3389/FCELL.2022.877711

Hattori, M., Fujiyama, A., Taylor, T. D., Watanabe, H., Yada, T., Park, H. S., Toyoda, A., Ishii, K., Totoki, Y., Choi, D. K., Soeda, E., Ohki, M., Takagi, T., Sakaki, Y., Taudien, S., Blechschmidt, K., Polley, A., Menzel, U., Delabar, J., … Yaspo, M. L. (2000). The DNA sequence of human chromosome 21. *Nature 2000 405:6784*, *405*(6784), 311–319. https://doi.org/10.1038/35012518

Head, E., Helman, A. M., Powell, D., & Schmitt, F. A. (2018). Down syndrome, beta-amyloid and neuroimaging. *Free Radical Biology & Medicine*, *114*, 102. https://doi.org/10.1016/J.FREERADBIOMED.2017.09.013

Hendrix, J. A., Amon, A., Abbeduto, L., Agiovlasitis, S., Alsaied, T., Anderson, H. A., Bain, L. J., Baumer, N., Bhattacharyya, A., Bogunovic, D., Botteron, K. N., Capone, G., Chandan, P., Chase, I., Chicoine, B., Cieuta-Walti, C., Deruisseau, L. R., Durand, S., Esbensen, A., … Yi, J. S. (2021). Opportunities, barriers, and

recommendations in down syndrome research. *Translational Science of Rare Diseases*, *5*(3–4), 99. https://doi.org/10.3233/TRD-200090

Herault, Y., Delabar, J. M., Fisher, E. M. C., Tybulewicz, V. L. J., Yu, E., & Brault, V. (2017). Rodent models in Down syndrome research: impact and future opportunities. *Disease Models & Mechanisms*, *10*(10), 1165. https://doi.org/10.1242/DMM.029728

Hetman, M., & Barg, E. (2022). Pediatric population with Down Syndrome: Obesity and the Risk of Cardiovascular Disease and Their Assessment Using Omics Techniques—Review. *Biomedicines*, *10*(12). https://doi.org/10.3390/BIOMEDICINES10123219

Hibaoui, Y., Grad, I., Letourneau, A., Sailani, M. R., Dahoun, S., Santoni, F. A., Gimelli, S., Guipponi, M., Pelte, M. F., Béna, F., Antonarakis, S. E., & Feki, A. (2014). Modelling and rescuing neurodevelopmental defect of Down syndrome using induced pluripotent stem cells from monozygotic twins discordant for trisomy 21. *EMBO Molecular Medicine*, *6*(2), 259–277. https://doi.org/10.1002/EMMM.201302848

Hithersay, R., Startin, C. M., Hamburg, S., Mok, K. Y., Hardy, J., Fisher, E. M. C., Tybulewicz, V. L. J., Nizetic, D., & Strydom, A. (2019). Association of Dementia With Mortality Among Adults With Down Syndrome Older Than 35 Years. *JAMA Neurology*, *76*(2), 152–160. https://doi.org/10.1001/JAMANEUROL.2018.3616

Holmes, G. (2014). Gastrointestinal disorders in Down syndrome. *Gastroenterology and Hepatology From Bed to Bench*, *7*(1), 6.

Hong, M., Chen, D. C. R., Klein, P. S., & Lee, V. M. Y. (1997). Lithium Reduces Tau Phosphorylation by Inhibition of Glycogen Synthase Kinase-3. *Journal of Biological Chemistry*, *272*(40), 25326–25332. https://doi.org/10.1074/JBC.272.40.25326

Hou, L., Xiong, N., Liu, L., Huang, J., Han, C., Zhang, G., Li, J., Xu, X., Lin, Z., & Wang, T. (2015). Lithium protects dopaminergic cells from rotenone toxicity via autophagy enhancement. *BMC Neuroscience*, *16*(1), 1–10. https://doi.org/10.1186/S12868-015-0222-Y

Hu, B. Y., Weick, J. P., Yu, J., Ma, L. X., Zhang, X. Q., Thomson, J. A., & Zhang, S. C. (2010). Neural differentiation of human induced pluripotent stem cells follows developmental principles but with variable potency. *Proceedings of the National Academy of Sciences of the United States of America*, *107*(9), 4335–4340. https://doi.org/10.1073/PNAS.0910012107

Huang, T., Fakurazi, S., Cheah, P. S., & Ling, K. H. (2023). REST Targets JAK–STAT and HIF-1 Signaling Pathways in Human Down Syndrome Brain and Neural Cells. *International Journal of Molecular Science, 24*(12), 9980. https://doi.org/10.3390/IJMS24129980/S1

Huang, W., Galdzicki, Z., Van Gelderen, P., Balbo, A., Chikhale, E. G., Schapiro, M. B., & Rapoport, S. I. (2000). Brain myo-inositol level is elevated in Ts65Dn mouse and reduced after lithium treatment. *Neuroreport*, *11*(3), 445–448. https://doi.org/10.1097/00001756-200002280-00004

Huggard, D., Doherty, D. G., & Molloy, E. J. (2020). Immune Dysregulation in Children With Down Syndrome. *Frontiers in Pediatrics*, *8*, 525223. https://doi.org/10.3389/FPED.2020.00073

Huo, H. Q., Qu, Z. Y., Yuan, F., Ma, L., Yao, L., Xu, M., Hu, Y., Ji, J., Bhattacharyya, A., Zhang, S. C., & Liu, Y. (2018). Modeling Down Syndrome with Patient iPSCs Reveals Cellular and Migration Deficits of GABAergic neurons. *Stem Cell Reports*, *10*(4), 1251–1266. https://doi.org/10.1016/j.stemcr.2018.02.001

Hyde, L. A., Frisone, D. F., & Crnic, L. S. (2001). Ts65Dn mice, a model for Down syndrome, have deficits in context discrimination learning suggesting impaired hippocampal function. *Behavioural Brain Research*, *118*(1), 53–60. https://doi.org/10.1016/S0166-4328(00)00313-2

Ishihara, K., Amano, K., Takaki, E., Shimohata, A., Sago, H., J. Epstein, C., & Yamakawa, K. (2010). Enlarged Brain Ventricles and Impaired Neurogenesis in the Ts1Cje and Ts2Cje Mouse Models of Down Syndrome. *Cerebral Cortex*, *20*(5), 1131–1143. https://doi.org/10.1093/CERCOR/BHP176

Izzo, A., Mollo, N., Nitti, M., Paladino, S., Calì, G., Genesio, R., Bonfiglio, F., Cicatiello, R., Barbato, M., Sarnataro, V., Conti, A., & Nitsch, L. (2018). Mitochondrial dysfunction in down syndrome: molecular mechanisms and therapeutic targets. *Molecular Medicine*, *24*(1). https://doi.org/10.1186/S10020-018-0004-Y

Jiang, J., Jing, Y., Cost, G. J., Chiang, J. C., Kolpa, H. J., Cotton, A. M., Carone, D. M., Carone, B. R., Shivak, D. A., Guschin, D. Y., Pearl, J. R., Rebar, E. J., Byron, M., Gregory, P. D., Brown, C. J., Urnov, F. D., Hall, L. L., & Lawrence, J. B. (2013). Translating dosage compensation to trisomy 21. *Nature 2013 500:7462*, *500*(7462), 296–300. https://doi.org/10.1038/nature12394

Jouhilahti, E. M., Peltonen, S., & Peltonen, J. (2008). Class III β-Tubulin Is a Component of the Mitotic Spindle in Multiple Cell Types. *Journal of Histochemistry and Cytochemistry*, *56*(12), 1113. https://doi.org/10.1369/JHC.2008.952002

Junde, Z., Tingting, L., Lu, Z., Shan, C., Dan, Y., & Yizhen, Z. (2023). Lithium chloride promotes neural functional recovery after local cerebral ischaemia injury in rats through Wnt signalling pathway activation. *Folia Morphologica (Poland)*, *82*(3), 519–532. https://doi.org/10.5603/FM.A2022.0068

Kanaumi, T., Milenkovic, I., Adle-Biassette, H., Aronica, E., & Kovacs, G. G. (2013). Non-neuronal cell responses differ between normal and Down syndrome developing brains. *International Journal of Developmental Neuroscience : The Official Journal of the International Society for Developmental Neuroscience*, *31*(8), 796–803. https://doi.org/10.1016/J.IJDEVNEU.2013.09.011

Kaneshiro, N. K. (2023). *Down syndrome*. Medline Medical Encyclopedia. https://medlineplus.gov/ency/article/000997.htm

Kawamura, M., Sato, S., Matsumoto, G., Fukuda, T., Shiba-Fukushima, K., Noda, S., Takanashi, M., Mori, N., & Hattori, N. (2019). Loss of nuclear REST/NRSF in aged-dopaminergic neurons in Parkinson's disease patients. *Neuroscience Letters*, *699*, 59–63. https://doi.org/10.1016/J.NEULET.2019.01.042

Kawatani, K., Nambara, T., Nawa, N., Yoshimatsu, H., Kusakabe, H., Hirata, K., Tanave, A., Sumiyama, K., Banno, K., Taniguchi, H., Arahori, H., Ozono, K., & Kitabatake, Y. (2021). A human isogenic iPSC-derived cell line panel identifies major regulators of aberrant astrocyte proliferation in Down syndrome. *Communications Biology 2021 4:1*, *4*(1), 1–15. https://doi.org/10.1038/s42003-021-02242-7

Kazuki, Y., Gao, F. J., Yamakawa, M., Hirabayashi, M., Kazuki, K., Kajitani, N., Miyagawa-Tomita, S., Abe, S., Sanbo, M., Hara, H., Kuniishi, H., Ichisaka, S., Hata, Y., Koshima, M., Takayama, H., Takehara, S., Nakayama, Y., Hiratsuka, M., Iida, Y., … Reeves, R. H. (2022). A transchromosomic rat model with human chromosome 21 shows robust Down syndrome features. *American Journal of Human Genetics, 109*(2), 328–344. https://doi.org/10.1016/j.ajhg.2021.12.015

Khairova, R., Pawar, R., Salvadore, G., Juruena, M. F., De Sousa, R. T., Soeiro-De-Souza, M. G., Salvador, M., Zarate, C. A., Gattaz, W. F., & Machado-Vieira, R. (2012). Effects of lithium on oxidative stress parameters in healthy subjects. *Molecular Medicine Reports*, *5*(3), 680. https://doi.org/10.3892/MMR.2011.732

Kim, C. (2015). iPSC technology-Powerful hand for disease modeling and therapeutic screen. *BMB Reports*, *48*(5), 256. https://doi.org/10.5483/BMBREP.2015.48.5.100

Kim, H. J., Denli, A. M., Wright, R., Baul, T. D., Clemenson, G. D., Morcos, A. S., Zhao, C., Schafer, S. T., Gage, F. H., & Kagalwala, M. N. (2015). REST Regulates Non–Cell-Autonomous Neuronal Differentiation and Maturation of Neural Progenitor Cells via Secretogranin II. *The Journal of Neuroscience*, *35*(44), 14872. https://doi.org/10.1523/JNEUROSCI.4286-14.2015

Kim, Y. H., Rane, A., Lussier, S., & Andersen, J. K. (2011). Lithium protects against oxidative stress-mediated cell death in α-synuclein-overexpressing in vitro and in vivo models of Parkinson's disease. *Journal of Neuroscience Research*, *89*(10), 1666–1675. https://doi.org/10.1002/JNR.22700

King, T. D., Bijur, G. N., & Jope, R. S. (2001). Caspase-3 activation induced by inhibition of mitochondrial complex I is facilitated by glycogen synthase kinase-3beta and attenuated by lithium. *Brain Research*, *919*(1), 106–114. https://doi.org/10.1016/S0006-8993(01)03005-0

Krapfenbauer, K., Yoo, B. C., Cairns, N., & Lubec, G. (1999). Differential display reveals deteriorated mRNA levels of NADH3 (complex I) in cerebellum of patients with Down Syndrome. *Journal of Neural Transmission, Supplement*, *57*, 211–220. https://doi.org/10.1007/978-3-7091-6380-1_13

Kühlbrandt, W. (2015). Structure and function of mitochondrial membrane protein complexes. *BMC Biology*, *13*(1), 1–11. https://doi.org/10.1186/S12915-015-0201-X

Kwon, M., Lee, J. H., Yoon, Y., Pleasure, S. J., & Yoon, K. (2023). The CRHR1/CREB/REST signaling cascade regulates mammalian embryonic neural stem cell properties. *EMBO Reports*, *24*(2). https://doi.org/10.15252/EMBR.202255313

Lam, X.-J., Maniam, S., Cheah, P.-S., & Ling, K.-H. (2023). REST in the Road Map of Brain Development. *Cellular and Molecular Neurobiology*, *43*(7). https://doi.org/10.1007/s10571-023-01394-w

Lander, E. S., Linton, L. M., Birren, B., Nusbaum, C., Zody, M. C., Baldwin, J., Devon, K., Dewar, K., Doyle, M., Fitzhugh, W., Funke, R., Gage, D., Harris, K., Heaford, A., Howland, J., Kann, L., Lehoczky, J., Levine, R., McEwan, P., … Morgan, M. J. (2001). Initial sequencing and analysis of the human genome. *Nature 2001 409:6822*, *409*(6822), 860–921. https://doi.org/10.1038/35057062

Landes, S. D., Stevens, J. D., & Turk, M. A. (2020). Cause of Death in Adults with Down Syndrome in the US. *Disability and Health Journal*, *13*(4), 100947. https://doi.org/10.1016/J.DHJO.2020.100947

Lee, H. C., Tan, K. L., Cheah, P. S., & Ling, K. H. (2016). Potential role of JAK-STAT Signaling Pathway in the Neurogenic-to-Gliogenic Shift in Down Syndrome brain. *Neural Plasticity*, *2016*. https://doi.org/10.1155/2016/7434191

Lee, N. R., Adeyemi, E. I., Lin, A., Clasen, L. S., Lalonde, F. M., Condon, E., Driver, D. I., Shaw, P., Gogtay, N., Raznahan, A., & Giedd, J. N. (2016). Dissociations in Cortical Morphometry in Youth with Down Syndrome: Evidence for Reduced Surface Area but Increased Thickness. *Cerebral Cortex*, *26*(7), 2982–2990. https://doi.org/10.1093/CERCOR/BHV107

Lepagnol-Bestel, A. M., Zvara, A., Maussion, G., Quignon, F., Ngimbous, B., Ramoz, N., Imbeaud, S., Loe-Mie, Y., Benihoud, K., Agier, N., Salin, P. A., Cardona, A., Khung-Savatovsky, S., Kallunki, P., Delabar, J. M., Puskas, L. G., Delacroix, H., Aggerbeck, L., Delezoide, A. L., … Simonneau, M. (2009). DYRK1A interacts with the REST/NRSF-SWI/SNF chromatin remodelling complex to deregulate gene clusters involved in the neuronal phenotypic traits of Down syndrome. *Human Molecular Genetics*, *18*(8), 1405–1414. https://doi.org/10.1093/HMG/DDP047

Li, L. B., Chang, K. H., Wang, P. R., Hirata, R. K., Papayannopoulou, T., & Russell, D. W. (2012). Trisomy correction in Down Syndrome Induced Pluripotent Stem Cells. *Cell Stem Cell*, *11*(5), 615. https://doi.org/10.1016/J.STEM.2012.08.004

Li, Q., Li, H., Roughton, K., Wang, X., Kroemer, G., Blomgren, K., & Zhu, C. (2010). Lithium reduces apoptosis and autophagy after neonatal hypoxia-ischemia. *Cell Death & Disease*, *1*(7). https://doi.org/10.1038/CDDIS.2010.33

Li, Y., Du, J., Yin, H., & Wang, Y. (2024). Efficacy and safety of adenotonsillectomy in the management of obstructive sleep apnea syndrome in children with Down syndrome: A systematic review and meta-analysis. *Journal of Sleep Research*, *33*(2), e13946. https://doi.org/10.1111/JSR.13946

Lim, C.-T., Lam, X.-J., Crystal, A.-A., Huang, T., Jusoh, N., Cheah, P.-S., & Ling, K.-H. (2024). Reduced REST Expression in Neural Progenitor Cells, Adult Cortex, and Impaired REST Nuclear Translocation in the Prefrontal Cortex of Ts1Cje Mouse Model of Down Syndrome. *Neurochemical Journal 2024 18:1*, *18*(1), 147–161. https://doi.org/10.1134/S1819712424010148

Ling, K. H., Hewitt, C. A., Tan, K. L., Cheah, P. S., Vidyadaran, S., Lai, M. I., Lee, H. C., Simpson, K., Hyde, L., Pritchard, M. A., Smyth, G. K., Thomas, T., & Scott, H. S. (2014). Functional transcriptome analysis of the postnatal brain of the

Ts1Cje mouse model for Down syndrome reveals global disruption of interferon-related molecular networks. *BMC Genomics*, *15*(1), 1–19. https://doi.org/10.1186/1471-2164-15-624

Liu, C., Oikonomopoulos, A., Sayed, N., & Wu, J. C. (2018). Modeling human diseases with induced pluripotent stem cells: from 2D to 3D and beyond. *Development (Cambridge, England)*, *145*(5). https://doi.org/10.1242/DEV.156166

Liu, J., Shen, J., Zong, J., Fan, Y., Cui, J., Peng, D., & Jin, Y. (2024). Lithium Chloride Promotes Endogenous Synthesis of CLA in Bovine Mammary Epithelial Cells. *Biological Trace Element Research*, *202*(2), 513–526. https://doi.org/10.1007/S12011-023-03679-Z

Liu, M., Qian, T., Zhou, W., Tao, X., Sang, S., & Zhao, L. (2020). Beneficial effects of low-dose lithium on cognitive ability and pathological alteration of Alzheimer's disease transgenic mice model. *NeuroReport*, *31*(13), 943–951. https://doi.org/10.1097/WNR.0000000000001499

Liu, P. Q., Tan, S., Mendel, M. C., Murrills, R. J., Bhat, B. M., Schlag, B., Samuel, R., Matteo, J. J., De La Rosa, R., Howes, K., Reik, A., Case, C. C., Bex, F. J., Young, K., & Gregory, P. D. (2005). Isogenic Human Cell Lines for Drug Discovery: Regulation of Target Gene Expression by Engineered Zinc-Finger Protein Transcription Factors.*10*(4), 304–313. https://doi.org/10.1177/1087057104272663

Lockrow, J. P., Fortress, A. M., & Granholm, A. C. E. (2012). Age-related Neurodegeneration and Memory Loss in Down Syndrome. *Current Gerontology and Geriatrics Research*, *2012*(1), 463909. https://doi.org/10.1155/2012/463909

Lockrow, J., Prakasam, A., Huang, P., Bimonte-Nelson, H., Sambamurti, K., & Granholm, A. C. (2009). Cholinergic degeneration and memory loss delayed by vitamin E in a Down syndrome mouse model. *Experimental Neurology*, *216*(2), 278. https://doi.org/10.1016/J.EXPNEUROL.2008.11.021

López-Hidalgo, R., Ballestín, R., Lorenzo, L., Sánchez-Martí, S., Blasco-Ibáñez, J. M., Crespo, C., Nacher, J., & Varea, E. (2024). Early chronic fasudil treatment rescues hippocampal alterations in the Ts65Dn model for down syndrome. *Neurochemistry International*, *174*. https://doi.org/10.1016/J.NEUINT.2024.105679

Lott, I. T., Head, E., Doran, E., & Busciglio, J. (2006). Beta-amyloid, Oxidative Stress and Down Syndrome. *Current Alzheimer Research*, *3*(5), 521–528. https://doi.org/10.2174/156720506779025305

Lu, M., Zheng, L., Han, B., Wang, L., Wang, P., Liu, H., & Sun, X. (2011). REST Regulates DYRK1A Transcription in a Negative Feedback Loop. *Journal of Biological Chemistry*, *286*(12), 10755–10763. https://doi.org/10.1074/JBC.M110.174540

Lu, T., Aron, L., Zullo, J., Pan, Y., Kim, H., Chen, Y., Yang, T. H., Kim, H. M., Drake, D., Liu, X. S., Bennett, D. A., Colaiácovo, M. P., & Yankner, B. A. (2014). REST and stress resistance in ageing and Alzheimer's disease. *Nature 2014 507:7493*, *507*(7493), 448–454. https://doi.org/10.1038/nature13163

Machado-Vieira, R., Andreazza, A. C., Viale, C. I., Zanatto, V., Cereser, V., Vargas, R. da S., Kapczinski, F., Portela, L. V., Souza, D. O., Salvador, M., & Gentil, V. (2007). Oxidative stress parameters in unmedicated and treated bipolar subjects during initial manic episode: A possible role for lithium antioxidant effects. *Neuroscience Letters*, *421*(1), 33–36. https://doi.org/10.1016/J.NEULET.2007.05.016

Malle, L., Patel, R. S., Martin-Fernandez, M., Stewart, O. J., Philippot, Q., Buta, S., Richardson, A., Barcessat, V., Taft, J., Bastard, P., Samuels, J., Mircher, C., Rebillat, A. S., Maillebouis, L., Vilaire-Meunier, M., Tuballes, K., Rosenberg, B. R., Trachtman, R., Casanova, J. L., … Bogunovic, D. (2023). Autoimmunity in Down's syndrome via cytokines, CD4 T cells and CD11c+ B cells. *Nature*, *615*(7951), 305–314. https://doi.org/10.1038/S41586-023-05736-Y

Mampay, M., & Sheridan, G. K. (2019). REST: An epigenetic regulator of neuronal stress responses in the young and ageing brain. *Frontiers in Neuroendocrinology*, *53*. https://doi.org/10.1016/J.YFRNE.2019.04.001

Mampay, M., Velasco-Estevez, M., Rolle, S. O., Chaney, A. M., Boutin, H., Dev, K. K., Moeendarbary, E., & Sheridan, G. K. (2021). Spatiotemporal immunolocalisation of REST in the brain of healthy ageing and Alzheimer's disease rats. *FEBS Open Bio*, *11*(1), 146–163. https://doi.org/10.1002/2211-5463.13036

Mandel, G., Fiondella, C. G., Covey, M. V., Lu, D. D., LoTurco, J. J., & Ballas, N. (2011). Repressor element 1 silencing transcription factor (REST) controls radial migration and temporal neuronal specification during neocortical development. *Proceedings of the National Academy of Sciences of the United States of America*, *108*(40), 16789–16794. https://doi.org/10.1073/pnas.1113486108

Mari´a, M., Andrés, E., Burger, C., Peral-Rubio, J., Battaglioli, E., Anderson, M. E., Grimes, J., Dallman, J., Ballas, N., & Mandel, G. (1999). CoREST: A functional corepressor required for regulation of neural-specific gene expression. In *Neurobiology Communicated by William J. Lennarz* (Vol. 96). https://doi.org/10.1073/pnas.96.17.9873

Martin-Perez, Y., Gonzalez-Montero, G., Gutierrez-Hernandez, A. L., Blázquez-Sánchez, V., & Sánchez-Ramos, C. (2023). Vision Impairments in Young Adults with Down Syndrome. *Vision*, *7*(3). https://doi.org/10.3390/VISION7030060

Matsumoto, T., Kim, M. H., & Kino-oka, M. (2022). Effect of Rho–associated Kinase Inhibitor on Growth Behaviors of Human Induced Pluripotent Stem Cells in Suspension Culture. *Bioengineering*, *9*(11). https://doi.org/10.3390/BIOENGINEERING9110613/S1

McCarron, M., McCallion, P., Reilly, E., Dunne, P., Carroll, R., & Mulryan, N. (2017). A prospective 20-year longitudinal follow-up of dementia in persons with Down syndrome. *Journal of Intellectual Disability Research : JIDR*, *61*(9), 843–852. https://doi.org/10.1111/JIR.12390

McDaniel, M. A. (2005). Big-brained people are smarter: A meta-analysis of the relationship between in vivo brain volume and intelligence. *Intelligence*, *33*(4), 337–346. https://doi.org/10.1016/J.INTELL.2004.11.005

Meharena, H. S., Marco, A., Dileep, V., Lockshin, E. R., Akatsu, G. Y., Mullahoo, J., Watson, L. A., Ko, T., Guerin, L. N., Abdurrob, F., Rengarajan, S., Papanastasiou, M., Jaffe, J. D., & Tsai, L. H. (2022). Down-syndrome-induced senescence disrupts the nuclear architecture of neural progenitors. *Cell Stem Cell*, *29*(1), 116-130.e7. https://doi.org/10.1016/J.STEM.2021.12.002

Metwalley, K. A., & Farghaly, H. S. (2022). Endocrinal dysfunction in children with Down syndrome. *Annals of Pediatric Endocrinology & Metabolism*, *27*(1), 15. https://doi.org/10.6065/APEM.2142236.118

Meyer, K., Feldman, H. M., Lu, T., Drake, D., Lim, E. T., Ling, K. H., Bishop, N. A., Pan, Y., Seo, J., Lin, Y. T., Su, S. C., Church, G. M., Tsai, L. H., & Yankner, B. A. (2019). REST and Neural Gene Network Dysregulation in iPSC models of Alzheimer's Disease. *Cell Reports*, *26*(5), 1112-1127.e9. https://doi.org/10.1016/J.CELREP.2019.01.023

Meyer, K., Ling, K. H., Yeo, P. L., Spathopoulou, A., Drake, D., Choi, J., Aron, L., Garcia-Corral, M., Ko, T., Lee, E. A., Tam, J. M., Perlis, R. H., Church, G. M., Tsai, L. H., & Yankner, B. A. (2023). Impaired neural stress resistance and loss of REST in bipolar disorder. *Molecular Psychiatry 2023*, 1–12. https://doi.org/10.1038/s41380-023-02313-7

Miotto, M., Rosito, M., Paoluzzi, M., de Turris, V., Folli, V., Leonetti, M., Ruocco, G., Rosa, A., & Gosti, G. (2023). Collective behavior and self-organization in neural rosette morphogenesis. *Frontiers in Cell and Developmental Biology*, *11*. https://doi.org/10.3389/FCELL.2023.1134091

Miyabara, S., Gropp, A., & Winking, H. (1982). Trisomy 16 in the mouse fetus associated with generalized edema and cardiovascular and urinary tract anomalies. *Teratology*, *25*(3), 369–380. https://doi.org/10.1002/tera.1420250314

Monaghan, C. E., Nechiporuk, T., Jeng, S., McWeeney, S. K., Wang, J., Rosenfeld, M. G., & Mandel, G. (2017). REST corepressors RCOR1 and RCOR2 and the repressor INSM1 regulate the proliferation-differentiation balance in the developing brain. *Proceedings of the National Academy of Sciences of the United States of America, 114*(3), E406–E415. https://doi.org/10.1073/PNAS.1620230114

Moore, C. S., Hawkins, C., Franca, A., Lawler, A., Devenney, B., Das, I., & Reeves, R. H. (2010). Increased male reproductive success in Ts65Dn "Down syndrome" mice. *Mammalian Genome : Official Journal of the International Mammalian Genome Society*, *21*(11–12), 543–549. https://doi.org/10.1007/S00335-010-9300-8

Mori, N., Schoenherr, C., Vandenbergh, D. J., & Anderson, D. J. (1992). A common silencer element in the SCG10 and type II Na+ channel genes binds a factor present in nonneuronal cells but not in neuronal cells. *Neuron*, *9*(1), 45–54. https://doi.org/10.1016/0896-6273(92)90219-4

Mosmann, T. (1983). Rapid colorimetric assay for cellular growth and survival: application to proliferation and cytotoxicity assays. *Journal of Immunological Methods*, *65*(1–2), 55–63. https://doi.org/10.1016/0022-1759(83)90303-4

Mulaudzi, P. E., Abrahamse, H., & Crous, A. (2023). Insights on Three Dimensional Organoid Studies for Stem Cell Therapy in Regenerative Medicine. *Stem Cell Reviews and Reports 2023 20:2*, *20*(2), 509–523. https://doi.org/10.1007/S12015-023-10655-6

Muñoz-Montaño, J. R., Moreno, F. J., Avila, J., & Díaz-Nido, J. (1997). Lithium inhibits Alzheimer's disease-like tau protein phosphorylation in neurons. *FEBS Letters*, *411*(2–3), 183–188. https://doi.org/10.1016/S0014-5793(97)00688-1

Murray, A., Letourneau, A., Canzonetta, C., Stathaki, E., Gimelli, S., Sloan-Bena, F., Abrehart, R., Goh, P., Lim, S., Baldo, C., Dagna-Bricarelli, F., Hannan, S., Mortensen, M., Ballard, D., Syndercombe Court, D., Fusaki, N., Hasegawa, M., Smart, T. G., Bishop, C., … Nizetic, D. (2015). Brief Report: Isogenic Induced Pluripotent Stem Cell Lines From an Adult With Mosaic Down Syndrome Model Accelerated Neuronal Ageing and Neurodegeneration. *Stem Cells*, *33*(6), 2077–2084. https://doi.org/10.1002/STEM.1968

Nagasaka, R., Matsumoto, M., Okada, M., Sasaki, H., Kanie, K., Kii, H., Uozumi, T., Kiyota, Y., Honda, H., & Kato, R. (2017). Visualization of morphological categories of colonies for monitoring of effect on induced pluripotent stem cell culture status. *Regenerative Therapy*, *6*, 41–51. https://doi.org/10.1016/J.RETH.2016.12.003

Nahman, S., Belmaker, R. H., & Azab, A. N. (2012). Effects of lithium on lipopolysaccharide-induced inflammation in rat primary glia cells. *Innate Immunity*, *18*(3), 447–458. https://doi.org/10.1021%2Fcn500038f

Naruse, Y., Aoki, T., Kojima, T., & Mori, N. (1999). Neural restrictive silencer factor recruits mSin3 and histone deacetylase complex to repress neuron-specific target genes. *Proceedings of the National Academy of Sciences of the United States of America*, *96*(24), 13691. https://doi.org/10.1073/PNAS.96.24.13691

Nciri, R., Desmoulin, F., Allagui, M. S., Murat, J. C., Feki, A. El, Vincent, C., & Croute, F. (2013). Neuroprotective effects of chronic exposure of SH-SY5Y to low lithium concentration involve glycolysis stimulation, extracellular pyruvate accumulation and resistance to oxidative stress. *The International Journal of Neuropsychopharmacology*, *16*(2), 365–376. https://doi.org/10.1017/S1461145712000132

Nechiporuk, T., McGann, J., Mullendorff, K., Hsieh, J., Wurst, W., Floss, T., & Mandel, G. (2016). The REST remodeling complex protects genomic integrity during embryonic neurogenesis. *ELife*, *5*(JANUARY2016). https://doi.org/10.7554/ELIFE.09584.001

Nesti, E., Corson, G. M., McCleskey, M., Oyer, J. A., & Mandel, G. (2014). C-terminal domain small phosphatase 1 and MAP kinase reciprocally control REST stability and neuronal differentiation. *Proceedings of the National Academy of Sciences of the United States of America, 111*(37), E3929–E3936. https://doi.org/10.1073/pnas.1414770111

Ng, N. S., & Ooi, L. (2021). A Simple Microplate Assay for Reactive Oxygen Species Generation and Rapid Cellular Protein Normalization. *Bio-Protocol*, *11*(1). https://doi.org/10.21769/BIOPROTOC.3877

NHS England Digital. (2022). *Prevalence of babies with Down's syndrome, Edwards' syndrome and Patau's syndrome.* https://digital.nhs.uk/data-and-information/publications/statistical/ncardrs-congenital-anomaly-statistics-annual-data/ncardrs-congenital-anomaly-statistics-report-2020/prevalence-t21-t18-t13

Nikonorova, V. G., Chrishtop, V. V., Mironov, V. A., & Prilepskii, A. Y. (2023). Advantages and Potential Benefits of Using Organoids in Nanotoxicology. *Cells*, *12*(4). https://doi.org/10.3390/CELLS12040610

Nishihara, S., Tsuda, L., & Ogura, T. (2003). The canonical Wnt pathway directly regulates NRSF/REST expression in chick spinal cord. *Biochemical and Biophysical Research Communications*, *311*(1), 55–63. https://doi.org/10.1016/j.bbrc.2003.09.158

Nistor, M., Don, M., Parekh, M., Sarsoza, F., Goodus, M., Lopez, G. E., Kawas, C., Leverenz, J., Doran, E., Lott, I. T., Hill, M., & Head, E. (2007). Alpha- and beta-secretase activity as a function of age and beta-amyloid in Down syndrome and normal brain. *Neurobiology of Aging*, *28*(10), 1493. https://doi.org/10.1016/J.NEUROBIOLAGING.2006.06.023

Noble, J. (1998). Natural history of Down's syndrome: a brief review for those involved in antenatal screening. *Journal of Medical Screening*, *5*(4), 172–177. https://doi.org/10.1136/JMS.5.4.172

Noble, W., Planel, E., Zehr, C., Olm, V., Meyerson, J., Suleman, F., Gaynor, K., Wang, L., LaFrancois, J., Feinstein, B., Burns, M., Krishnamurthy, P., Wen, Y., Bhat, R., Lewis, J., Dickson, D., & Duff, K. (2005). Inhibition of glycogen synthase kinase-3 by lithium correlates with reduced tauopathy and degeneration in vivo. *Proceedings of the National Academy of Sciences of the United States of America*, *102*(19), 6990–6995. https://doi.org/10.1073/PNAS.0500466102

Nunes, P. V., Forlenza, O. V., & Gattaz, W. F. (2007). Lithium and risk for Alzheimer's disease in elderly patients with bipolar disorder. *The British Journal of Psychiatry : The Journal of Mental Science*, *190*(APR.), 359–360. https://doi.org/10.1192/BJP.BP.106.029868

Ong, M. B. H., Davey, M. J., Nixon, G. M., Walter, L. M., & Horne, R. S. (2024). Effect of sleep disordered breathing severity in children with Down syndrome on parental wellbeing and social support. *Sleep Medicine*, *116*, 71–80. https://doi.org/10.1016/J.SLEEP.2024.02.037

Ortega, M., Toma, I. De, Fernández-Blanco, Á., Calderón, A., Barahona, L., Trullàs, R., Sabidó, E., & Dierssen, M. (2022). Proteomic profiling reveals mitochondrial dysfunction in the cerebellum of transgenic mice overexpressing DYRK1A, a Down syndrome candidate gene. *Frontiers in Molecular Neuroscience*, *15*, 1015220. https://doi.org/10.3389/FNMOL.2022.1015220

Pagnotta, S., Tramutola, A., Barone, E., Di Domenico, F., Pittalà, V., Salerno, L., Folgiero, V., Caforio, M., Locatelli, F., Petrini, S., Butterfield, D. A., & Perluigi, M. (2022). CAPE and its synthetic derivative VP961 restore BACH1/NRF2 axis in Down Syndrome. *Free Radical Biology and Medicine, 183,* 1–13. https://doi.org/10.1016/J.FREERADBIOMED.2022.03.006

Pakzad, M., Totonchi, M., Taei, A., Seifinejad, A., Hassani, S. N., & Baharvand, H. (2010). Presence of a ROCK inhibitor in extracellular matrix supports more undifferentiated growth of feeder-free human embryonic and induced pluripotent stem cells upon passaging. *Stem Cell Reviews and Reports*, *6*(1), 96–107. https://doi.org/10.1007/S12015-009-9103-Z

Pan, Y., Short, J. L., Newman, S. A., Choy, K. H. C., Tiwari, D., Yap, C., Senyschyn, D., Banks, W. A., & Nicolazzo, J. A. (2018). Cognitive benefits of lithium chloride in APP/PS1 mice are associated with enhanced brain clearance of β-amyloid. *Brain, Behavior, and Immunity*, *70*, 36–47. https://doi.org/10.1016/J.BBI.2018.03.007

Paquette, A. J., Perez, S. E., & Anderson, D. J. (2000). Constitutive expression of the neuron-restrictive silencer factor (NRSF)/REST in differentiating neurons disrupts neuronal gene expression and causes axon pathfinding errors in vivo. *Proceedings of the National Academy of Sciences of the United States of America*, *97*(22), 12318–12323. https://doi.org/10.1073%2Fpnas.97.22.12318

Parisotto, E. B., Giaretta, A. G., Zamoner, A., Moreira, E. A. M., Fröde, T. S., Pedrosa, R. C., & Filho, D. W. (2015). Persistence of the benefit of an antioxidant therapy in children and teenagers with Down syndrome. *Research in Developmental Disabilities*, *45–46*, 14–20. https://doi.org/10.1016/J.RIDD.2015.07.010

Park, D., Xiang, A. P., Mao, F. F., Zhang, L., Di, C. G., Liu, X. M., Shao, Y., Ma, B. F., Lee, J. H., Ha, K. S., Walton, N., & Lahn, B. T. (2010). Nestin Is Required for the Proper Self-Renewal of Neural Stem Cells. *STEM CELLS*, *28*(12), 2162–2171. https://doi.org/10.1002/STEM.541

Park, I. H., Arora, N., Huo, H., Maherali, N., Ahfeldt, T., Shimamura, A., Lensch, M. W., Cowan, C., Hochedlinger, K., & Daley, G. Q. (2008). Disease-specific induced pluripotent stem cells. *Cell*, *134*(5), 877–886. https://doi.org/10.1016/J.CELL.2008.07.041

Patkee, P. A., Baburamani, A. A., Kyriakopoulou, V., Davidson, A., Avini, E., Dimitrova, R., Allsop, J., Hughes, E., Kangas, J., McAlonan, G., & Rutherford, M. A. (2020). Early alterations in cortical and cerebellar regional brain growth in Down Syndrome: An in vivo fetal and neonatal MRI assessment. *NeuroImage: Clinical*, *25*, 102139. https://doi.org/10.1016/J.NICL.2019.102139

Patterson, D., & Costa, A. C. S. (2005). Down syndrome and genetics — a case of linked histories. *Nature Reviews Genetics 2005 6:2*, *6*(2), 137–147. https://doi.org/10.1038/nrg1525

Peng, H., Xie, P., Liu, L., Kuang, X., Wang, Y., Qu, L., Gong, H., Jiang, S., Li, A., Ruan, Z., Ding, L., Yao, Z., Chen, C., Chen, M., Daigle, T. L., Dalley, R., Ding, Z., Duan, Y., Feiner, A., … Zeng, H. (2021). Morphological diversity of single neurons in molecularly defined cell types. *Nature*, *598*(7879), 174. https://doi.org/10.1038/S41586-021-03941-1

Pinter, J. D., Eliez, S., Schmitt, J. E., Capone, G. T., & Reiss, A. L. (2001). Neuroanatomy of Down's syndrome: A high-resolution MRI study. *American Journal of Psychiatry*, *158*(10), 1659–1665. https://doi.org/10.1176/appi.ajp.158.10.1659

Polk, R. C. (2014). *Using the Ts65dn mouse model Of Down Syndrome to understand the genetics of congenital heart defects*. http://jhir.library.jhu.edu/handle/1774.2/36959

Ponroy Bally, B., Farmer, W. T., Jones, E. V., Jessa, S., Kacerovsky, J. B., Mayran, A., Peng, H., Lefebvre, J. L., Drouin, J., Hayer, A., Ernst, C., & Murai, K. K. (2020). Human iPSC-derived Down syndrome astrocytes display genome-wide perturbations in gene expression, an altered adhesion profile, and increased cellular dynamics. *Human Molecular Genetics*, *29*(5), 785–802. https://doi.org/10.1093/HMG/DDAA003

Puglisi-Allegra, S., Lazzeri, G., Busceti, C. L., Giorgi, F. S., Biagioni, F., & Fornai, F. (2023). Lithium engages autophagy for neuroprotection and neuroplasticity: Translational evidence for therapy. *Neuroscience & Biobehavioral Reviews*, *148*, 105148. https://doi.org/10.1016/J.NEUBIOREV.2023.105148

Puglisi-Allegra, S., Ruggieri, S., & Fornai, F. (2021). Translational evidence for lithium-induced brain plasticity and neuroprotection in the treatment of neuropsychiatric disorders. *Translational Psychiatry 2021 11:1*, *11*(1), 1–10. https://doi.org/10.1038/s41398-021-01492-7

Qi, L., Tang, Y., He, W., Pan, H., Jiang, W., Wang, L., & Deng, W. (2017). Lithium chloride promotes neuronal differentiation of rat neural stem cells and enhances neural regeneration in Parkinson's disease model. *Cytotechnology*, *69*(2), 277–287. https://doi.org/10.1007/S10616-016-0056-1

Qiu, J. J., Liu, Y. N., Wei, H., Zeng, F., & Yan, J. Bin. (2023). Single-cell RNA sequencing of neural stem cells derived from human trisomic iPSCs reveals the abnormalities during neural differentiation of Down syndrome. *Frontiers in Molecular Neuroscience*, *16*, 1137123. https://doi.org/10.3389/FNMOL.2023.1137123

Qu, Z., Sun, D., & Young, W. (2011). Lithium promotes neural precursor cell proliferation: Evidence for the involvement of the non-canonical GSK-3β-NF-AT signaling. *Cell and Bioscience*, *1*(1), 1–11. https://doi.org/10.1186/2045-3701-1-18/FIGURES/7

Quiroz, J. A., MacHado-Vieira, R., Zarate, C. A., & Manji, H. K. (2010). Novel insights into lithium's mechanism of action: neurotrophic and neuroprotective effects. *Neuropsychobiology*, *62*(1), 50–60. https://doi.org/10.1159/000314310

Nall, R. (2024). *Lithium side effects: Long term and short term*. MedicalNewsToday. https://www.medicalnewstoday.com/articles/326516

Rachidi, M., & Lopes, C. (2007). Mental retardation in Down syndrome: From gene dosage imbalance to molecular and cellular mechanisms. *Neuroscience Research*, *59*(4), 349–369. https://doi.org/10.1016/j.neures.2007.08.007

Ravanpay, A. C., Hansen, S. J., & Olson, J. M. (2010). Transcriptional inhibition of REST by NeuroD2 during neuronal differentiation. *Molecular and Cellular Neuroscience*, *44*(2), 178–189. https://doi.org/10.1016/J.MCN.2010.03.006

Ravel, A., Mircher, C., Rebillat, A. S., Cieuta-Walti, C., & Megarbane, A. (2020). Feeding problems and gastrointestinal diseases in Down syndrome. *Archives de Pédiatrie*, *27*(1), 53–60. https://doi.org/10.1016/J.ARCPED.2019.11.008

Reeves, R. H., Irving, N. G., Moran, T. H., Wohn, A., Kitt, C., Sisodia, S. S., Schmidt, C., Bronson, R. T., & Davisson, M. T. (1995). A mouse model for Down syndrome exhibits learning and behaviour deficits. *Nature Genetics*, *11*(2), 177–184. https://doi.org/10.1038/NG1095-177

Rizzuti, M., Melzi, V., Brambilla, L., Quetti, L., Sali, L., Ottoboni, L., Meneri, M., Ratti, A., Verde, F., Ticozzi, N., Comi, G. Pietro, Corti, S., & Abati, E. (2024). Shaping the Neurovascular Unit Exploiting Human Brain Organoids. *Molecular Neurobiology 2024*, 1–16. https://doi.org/10.1007/S12035-024-03998-9

Robinton, D. A., & Daley, G. Q. (2012). The promise of induced pluripotent stem cells in research and therapy. *Nature*, *481*(7381), 295–305. https://doi.org/10.1038/NATURE10761

Rueda, N., Flórez, J., Dierssen, M., & Martínez-Cué, C. (2020). Translational validity and implications of pharmacotherapies in preclinical models of Down syndrome. *Progress in Brain Research*, *251*, 245–268. https://doi.org/10.1016/BS.PBR.2019.10.001

Ruffalo, M. L. (2017). A Brief History of Lithium Treatment in Psychiatry. *The Primary Care Companion for CNS Disorders*, *19*(5), 27325. https://doi.org/10.4088/PCC.17BR02140

Sago, H., Carlson, E. J., Smith, D. J., Kilbridge, J., Rubin, E. M., Mobley, W. C., Epstein, C. J., & Huang, T. T. (1998). Ts1Cje, a partial trisomy 16 mouse model for Down syndrome, exhibits learning and behavioral abnormalities. *Proceedings of the National Academy of Sciences of the United States of America*, *95*(11), 6256–6261. https://doi.org/10.1073/PNAS.95.11.6256

Sánchez-Font, M. F., Sebastià, J., Sanfeliu, C., Cristòfol, R., Marfany, G., & Gonzàlez-Duarte, R. (2003). Peroxiredoxin 2 (PRDX2), an antioxidant enzyme, is underexpressed in Down syndrome fetal brains. *Cellular and Molecular Life Sciences: CMLS*, *60*(7), 1513. https://doi.org/10.1007/S00018-003-3048-1

Santoro, J. D., Pagarkar, D., Chu, D. T., Rosso, M., Paulsen, K. C., Levitt, P., & Rafii, M. S. (2021). Neurologic complications of Down syndrome: a systematic review. In *Journal of Neurology* (Vol. 268, Issue 12, pp. 4495–4509). Springer Science and Business Media Deutschland GmbH. https://doi.org/10.1007/s00415-020-10179-w

Santoro, S. L., Martin, L. J., & Hopkin, R. J. (2016). Screening for Hematological Disorders in Mosaic Down Syndrome: Parent Report of Experiences. *Clinical Pediatrics*, *55*(5), 421–427. https://doi.org/10.1177/0009922815589911

Sarkar, S., Floto, R. A., Berger, Z., Imarisio, S., Cordenier, A., Pasco, M., Cook, L. J., & Rubinsztein, D. C. (2005). Lithium induces autophagy by inhibiting inositol monophosphatase. *The Journal of Cell Biology*, *170*(7), 1101. https://doi.org/10.1083/JCB.200504035

Sauer, M., Was, N., Ziegenhals, T., Wang, X., Hafner, M., Becker, M., & Fischer, U. (2021). The miR-26 family regulates neural differentiation-associated microRNAs and mRNAs by directly targeting REST. *Journal of Cell Science, 134*(12). https://doi.org/10.1242/jcs.257535

Schmidt-Sidor, B., Ke, W., Th, S., & Ea, S. (1990). Brain growth in Down syndrome subjects 15 to 22 weeks of gestational age and birth to 60 months. *Clinical Neuropathology*.

Schoenherr, C. J., & Anderson, D. J. (1995). The neuron-restrictive silencer factor (NRSF): a coordinate repressor of multiple neuron-specific genes. *Science (New York, N.Y.)*, *267*(5202), 1360–1363. https://doi.org/10.1126/SCIENCE.7871435

Shabri, N. (2019). *Screening for Chromosomal Anomalies - PORTAL MyHEALTH*. http://www.myhealth.gov.my/en/screening-chromosomal-anomalies/

Shi, G., & Jin, Y. (2010). Role of Oct4 in maintaining and regaining stem cell pluripotency. *Stem Cell Research and Therapy*, *1*(5), 1–9. https://doi.org/10.1186/scrt39

Shimada, K., Motoi, Y., Ishiguro, K., Kambe, T., Matsumoto, S. E., Itaya, M., Kunichika, M., Mori, H., Shinohara, A., Chiba, M., Mizuno, Y., Ueno, T., & Hattori, N. (2012). Long-term oral lithium treatment attenuates motor disturbance in tauopathy model mice: implications of autophagy promotion. *Neurobiology of Disease*, *46*(1), 101–108. https://doi.org/10.1016/J.NBD.2011.12.050

Shimojo, M. (2006). Characterization of the nuclear targeting signal of REST/NRSF. *Neuroscience Letters*, *398*(3), 161–166. https://doi.org/10.1016/J.NEULET.2005.12.080

Shimojo, M., & Hersh, L. B. (2003). REST/NRSF-interacting LIM domain protein, a putative nuclear translocation receptor. *Molecular and Cellular Biology*, *23*(24), 9025–9031. https://doi.org/10.1128/MCB.23.24.9025-9031.2003

Shimojo, M., & Hersh, L. B. (2006). Characterization of the REST/NRSF-interacting LIM domain protein (RILP): Localization and interaction with REST/NRSF. *Journal of Neurochemistry*, *96*(4), 1130–1138. https://doi.org/10.1111/j.1471-4159.2005.03608.x

Shimojo, M., Lee, J. H., & Hersh, L. B. (2001). Role of Zinc Finger Domains of the Transcription Factor Neuronrestrictive Silencer Factor/Repressor Element-1 Silencing Transcription Factor in DNA Binding and Nuclear Localization. *Journal of Biological Chemistry*, *276*(16), 13121–13126. https://doi.org/10.1074/jbc.M011193200

Shin, M., Siffel, C., & Correa, A. (2010). Survival of children with mosaic Down syndrome. *American Journal of Medical Genetics Part A*, *152A*(3), 800–801. https://doi.org/10.1002/AJMG.A.33295

Siarey, R. J., Villar, A. J., Epstein, C. J., & Galdzicki, Z. (2005). Abnormal synaptic plasticity in the Ts1Cje segmental trisomy 16 mouse model of Down syndrome. *Neuropharmacology*, *49*(1), 122–128. https://doi.org/10.1016/j.neuropharm.2005.02.012

Song, Z., Yang, W., Zhou, X., Yang, L., & Zhao, D. (2017). Lithium alleviates neurotoxic prion peptide-induced synaptic damage and neuronal death partially by the upregulation of nuclear target REST and the restoration of Wnt signaling. *Neuropharmacology*, *123*, 332–348. https://doi.org/10.1016/J.NEUROPHARM.2017.05.021

Stagni, F., Giacomini, A., Guidi, S., Ciani, E., & Bartesaghi, R. (2015). Timing of therapies for downsyndrome: The sooner, the better. *Frontiers in Behavioral Neuroscience*, *9*(OCT). https://doi.org/10.3389/FNBEH.2015.00265

Sterling, K., Cao, R., & Song, W. (2023). Gonadotropin releasing hormone (GnRH): a hormone therapy boosts cognition in Down syndrome and dementia. *Signal Transduction and Targeted Therapy 2023 8:1*, *8*(1), 1–3. https://doi.org/10.1038/s41392-023-01321-x

Stiles, J., & Jernigan, T. L. (2010). The basics of brain development. *Neuropsychology Review*, *20*(4), 327–348. https://doi.org/10.1007/S11065-010-9148-4/METRICS

Suginobe, H., Ishida, H., Ishii, Y., Ueda, K., Yoshihara, C., Ueyama, A., Wang, R., Tsuru, H., Hashimoto, K., Hirose, M., Ishii, R., Narita, J., Kitabatake, Y., & Ozono, K. (2023). Isogenic pairs of induced-pluripotent stem-derived endothelial cells identify DYRK1A/PPARG/EGR1 pathway is responsible for Down syndrome-associated pulmonary hypertension. *Human Molecular Genetics*, *33*(1), 78–90. https://doi.org/10.1093/HMG/DDAD162

Sun, Y. M., Greenway, D. J., Johnson, R., Street, M., Belyaev, N. D., Deuchars, J., Bee, T., Wilde, S., & Buckley, N. J. (2005). Distinct Profiles of REST Interactions with Its Target Genes at Different Stages of Neuronal Development. *Molecular Biology of the Cell*, *16*(12), 5630. https://doi.org/10.1091/MBC.E05-07-0687

Suzuki, S., Namiki, J., Shibata, S., Mastuzaki, Y., & Okano, H. (2010). The Neural Stem/Progenitor Cell Marker Nestin Is Expressed in Proliferative Endothelial Cells, but Not in Mature Vasculature. *Journal of Histochemistry and Cytochemistry*, *58*(8), 721. https://doi.org/10.1369/JHC.2010.955609

Tafreshi, A. P., Sylvain, A., Sun, G., Herszfeld, D., Schulze, K., & Bernard, C. C. A. (2015). Lithium chloride improves the efficiency of induced pluripotent stem cell-derived neurospheres. *Biological Chemistry*, *396*(8), 923–928. https://doi.org/10.1515/HSZ-2014-0261

Tajes, M., Gutierrez-Cuesta, J., Folch, J., Ferrer, I., Caballero, B., Smith, M. A., Casadesus, G., Camins, A., & Pallás, M. (2008). Lithium Treatment Decreases Activities of Tau Kinases in a Murine Model of Senescence. *Journal of Neuropathology & Experimental Neurology*, *67*(6), 612–623. https://doi.org/10.1097/NEN.0B013E3181776293

Tan, K. L., Lee, H. C., Cheah, P. S., & Ling, K. H. (2023). Mitochondrial Dysfunction in Down Syndrome: From Pathology to Therapy. *Neuroscience*, *511*, 1–12. https://doi.org/10.1016/J.NEUROSCIENCE.2022.12.003

Tang, X. Y., Xu, L., Wang, J., Hong, Y., Wang, Y., Zhu, Q., Wang, D., Zhang, X. Y., Liu, C. Y., Fang, K. H., Han, X., Wang, S., Wang, X., Xu, M., Bhattacharyya, A., Guo, X., Lin, M., & Liu, Y. (2021). DSCAM/PAK1 pathway suppression reverses neurogenesis deficits in iPSC-derived cerebral organoids from patients with Down syndrome. *The Journal of Clinical Investigation*, *131*(12). https://doi.org/10.1172/JCI135763

Tapia-Ramírez, J., Eggen, B. J. L., Peral-Rubio, M. J., Toledo-Aral, J. J., & Mandel, G. (1997). A single zinc finger motif in the silencing factor REST represses the neural-specific type II sodium channel promoter. *Proceedings of the National*

Academy of Sciences of the United States of America, *94*(4), 1177. https://doi.org/10.1073/PNAS.94.4.1177

Terao, T., Nakano, H., Inoue, Y., Okamoto, T., Nakamura, J., & Iwata, N. (2006). Lithium and dementia: A preliminary study. *Progress in Neuro-Psychopharmacology and Biological Psychiatry*, *30*(6), 1125–1128. https://doi.org/10.1016/J.PNPBP.2006.04.020

Thomazeau, A., Lassalle, O., & Manzoni, O. J. (2023). Glutamatergic synaptic deficits in the prefrontal cortex of the Ts65Dn mouse model for Down syndrome. *Frontiers in Neuroscience*, *17*, 1171797. https://doi.org/10.3389/fnins.2023.1171797

Toledo, E. M., & Inestrosa, N. C. (2010). Activation of Wnt signaling by lithium and rosiglitazone reduced spatial memory impairment and neurodegeneration in brains of an APPswe/PSEN1DeltaE9 mouse model of Alzheimer's disease. *Molecular Psychiatry*, *15*(3), 272–285. https://doi.org/10.1038/MP.2009.72

Tondo, L., Alda, M., Bauer, M., Bergink, V., Grof, P., Hajek, T., Lewitka, U., Licht, R. W., Manchia, M., Müller-Oerlinghausen, B., Nielsen, R. E., Selo, M., Simhandl, C., & Baldessarini, R. J. (2019). Clinical use of lithium salts: guide for users and prescribers. *International Journal of Bipolar Disorders*, *7*(1), 1–10. https://doi.org/10.1186/s40345-019-0151-2

Torres-Carrión, P. V., González-González, C. S., Toledo-Delgado, P. A., Muñoz-Cruz, V., Gil-Iranzo, R., Reyes-Alonso, N., & Hernández-Morales, S. (2019). Improving Cognitive Visual-Motor Abilities in Individuals with Down Syndrome. *Sensors (Basel, Switzerland)*, *19*(18). https://doi.org/10.3390/S19183984

Tosh, J. L., Rhymes, E. R., Mumford, P., Whittaker, H. T., Pulford, L. J., Noy, S. J., Cleverley, K., Strydom, A., Fisher, E., Wiseman, F., Nizetic, D., Hardy, J., Tybulewicz, V., Karmiloff-Smith, A., Walker, M. C., Tybulewicz, V. L. J., Wykes, R. C., & Wiseman, F. K. (2021). Genetic dissection of down syndrome-associated alterations in APP/amyloid-β biology using mouse models. *Scientific Reports, 11*(1), 1–13. https://doi.org/10.1038/s41598-021-85062-3

Townshend, R. F., Shao, Y., Wang, S., Cortez, C. L., Esfahani, S. N., Spence, J. R., O'Shea, K. S., Fu, J., Gumucio, D. L., & Taniguchi, K. (2020). Effect of Cell Spreading on Rosette Formation by Human Pluripotent Stem Cell-Derived Neural Progenitor Cells. *Frontiers in Cell and Developmental Biology*, *8*. https://doi.org/10.3389/FCELL.2020.588941/FULL

Triarico, S., Trombatore, G., Capozza, M. A., Romano, A., Mastrangelo, S., Attinà, G., Maurizi, P., & Ruggiero, A. (2022). Hematological disorders in children with Down syndrome. *Expert Review of Hematology*, *15*(2), 127–135. https://doi.org/10.1080/17474086.2022.2044780

Tunca, Z., Ozerdem, A., Ceylan, D., Yalçin, Y., Can, G., Resmi, H., Akan, P., Ergör, G., Aydemir, Ö., Çağrisiz, C., & Kerim, D. (2014). Alterations in BDNF (brain derived neurotrophic factor) and GDNF (glial cell line-derived neurotrophic factor) serum levels in bipolar disorder: The role of lithium. *Journal of Affective Disorders*, *166*, 193–200. https://doi.org/10.1016/J.JAD.2014.05.012

Valenti, D., Braidy, N., De Rasmo, D., Signorile, A., Rossi, L., Atanasov, A. G., Volpicella, M., Henrion-Caude, A., Nabavi, S. M., & Vacca, R. A. (2018).

Mitochondria as pharmacological targets in Down syndrome. *Free Radical Biology and Medicine*, *114*, 69–83. https://doi.org/10.1016/J.FREERADBIOMED.2017.08.014

Valenti, D., de Bari, L., de Rasmo, D., Signorile, A., Henrion-Caude, A., Contestabile, A., & Vacca, R. A. (2016). The polyphenols resveratrol and epigallocatechin-3-gallate restore the severe impairment of mitochondria in hippocampal progenitor cells from a Down syndrome mouse model. *Biochimica et Biophysica Acta (BBA) - Molecular Basis of Disease*, *1862*(6), 1093–1104. https://doi.org/10.1016/J.BBADIS.2016.03.003

Wakao, S., Kitada, M., Kuroda, Y., Ogura, F., Murakami, T., Niwa, A., & Dezawa, M. (2012). Morphologic and Gene Expression Criteria for Identifying Human Induced Pluripotent Stem Cells. *PLoS ONE*, *7*(12). https://doi.org/10.1371/JOURNAL.PONE.0048677

Wang, T., Kang, W., Du, L., & Ge, S. (2017). Rho-kinase inhibitor Y-27632 facilitates the proliferation, migration and pluripotency of human periodontal ligament stem cells. *Journal of Cellular and Molecular Medicine*, *21*(11), 3100. https://doi.org/10.1111/JCMM.13222

Wang, Y. C., Liu, P., Yue, L. Y., Huang, F., Xu, Y. X., & Zhu, C. Q. (2021). NRSF deficiency leads to abnormal postnatal development of dentate gyrus and impairment of progenitors in subgranular zone of hippocampus. *Hippocampus*, *31*(9), 935–956. https://doi.org/10.1002/HIPO.23336

Wang, Y., Ni, J., Liu, Y., Liao, D., Zhou, Q., Ji, X., Niu, G., & Ni, Y. (2023). Realizing the potential of exploiting human IPSCs and their derivatives in research of Down syndrome. *BIOCELL*, *47*(12), 2567–2578. https://doi.org/10.32604/BIOCELL.2023.043781

Wang, Y. Y., Lu, Y. H., Geng, R. J., Cheng, X. Y., Huang, X. X., Lű, Q. Y., Ying, Q. A., & Yi, Z. H. (2019). Effect of lithium carbonate on oxidative stress in patients with bipolar disorder. *Journal of Shanghai Jiaotong University(Medical Science)*, *39*(5), 494–499. https://doi.org/10.3969/J.ISSN.1674- 8115.2019.05.009

Webb, S., Anderson, R. H., Lamers, W. H., & Brown, N. A. (1999). Mechanisms of deficient cardiac septation in the mouse with trisomy 16. *Circulation Research*, *84*(8), 897–905. https://doi.org/10.1161/01.RES.84.8.897

Weick, J. P., Held, D. L., Bonadurer, G. F., Doers, M. E., Liu, Y., Maguire, C., Clark, A., Knackert, J. A., Molinarolo, K., Musser, M., Yao, L., Yin, Y., Lu, J., Zhang, X., Zhang, S. C., & Bhattacharyya, A. (2013). Deficits in human trisomy 21 iPSCs and neurons. *Proceedings of the National Academy of Sciences of the United States of America*, *110*(24), 9962–9967. https://doi.org/10.1073/PNAS.1216575110

Whitbourne, K. (2024). *Down Syndrome: Causes, Symptoms, Diagnosis, and Treatment*. WebMD. https://www.webmd.com/children/understanding-down-syndrome-basics#1-2

Williams, A. D., Mjaatvedt, C. H., & Moore, C. S. (2008). Characterization of the cardiac phenotype in neonatal Ts65Dn mice. *Developmental Dynamics : An Official Publication of the American Association of Anatomists*, *237*(2), 426–435. https://doi.org/10.1002/DVDY.21416

Wilton, G. J., Woodhouse, R., Vinuela-Navarro, V., England, R., & Woodhouse, J. M. (2021). Behavioural Features of Cerebral Visual Impairment Are Common in Children With Down Syndrome. *Frontiers in Human Neuroscience*, *15*, 673342. https://doi.org/10.3389/FNHUM.2021.673342

Wiseman, F. K., Al-Janabi, T., Hardy, J., Karmiloff-Smith, A., Nizetic, D., Tybulewicz, V. L. J., Fisher, E. M. C., & Strydom, A. (2015). A genetic cause of Alzheimer disease: mechanistic insights from Down syndrome. *Nature Reviews. Neuroscience*, *16*(9), 564–574. https://doi.org/10.1038/NRN3983

Wu, N., Luo, Q., Huang, Y., Wan, L., Hou, X., Jiang, Z., Li, Y., Qiu, J., Chen, P., Yu, K., Zhuang, J., & Yang, Y. (2023). Lithium Chloride Exerts Anti-Inflammatory and Neuroprotective Effects by Inhibiting Microglial Activation in LPS-Induced Retinal Injury. *Investigative Ophthalmology and Visual Science*, *64*(3). https://doi.org/10.1167/IOVS.64.3.35

Wu, Y., West, N. R., Bhattacharyya, A., & Wiseman, F. K. (2022). Cell models for Down syndrome-Alzheimer's disease research. *Neuronal Signaling*, *6*(1), 20210054. https://doi.org/10.1042/NS20210054/231069

Xia, M. Y., Zhao, X. Y., Huang, Q. L., Sun, H. Y., Sun, C., Yuan, J., He, C., Sun, Y., Huang, X., Kong, W., & Kong, W. J. (2017). Activation of Wnt/β-catenin signaling by lithium chloride attenuates d-galactose-induced neurodegeneration in the auditory cortex of a rat model of aging. *FEBS Open Bio*, *7*(6), 759. https://doi.org/10.1002/2211-5463.12220

Xu, L., Huo, H. Q., Lu, K. Q., Tang, X. Y., Hong, Y., Han, X., Fu, Z. X., Fang, K. H., Xu, M., Guo, X., & Liu, Y. (2022). Abnormal mitochondria in Down syndrome iPSC-derived GABAergic interneurons and organoids. *Biochimica et Biophysica Acta (BBA) - Molecular Basis of Disease*, *1868*(6), 166388. https://doi.org/10.1016/J.BBADIS.2022.166388

Xu, R., Brawner, A. T., Li, S., Liu, J. J., Kim, H., Xue, H., Pang, Z. P., Kim, W. Y., Hart, R. P., Liu, Y., & Jiang, P. (2019). OLIG2 Drives Abnormal Neurodevelopmental Phenotypes in Human iPSC-Based Organoid and Chimeric Mouse Models of Down Syndrome. *Cell Stem Cell*, *24*(6), 908-926.e8. https://doi.org/10.1016/j.stem.2019.04.014

Yam, W. K. L., Tse, P. W. T., Yu, C. M., Chow, C. B., But, W. M., Li, K. Y., Lee, L. P., Fung, E. L. W., Mak, P. P. Y., & Lau, J. T. F. (2008). Medical issues among children and teenagers with Down syndrome in Hong Kong. *Down's Syndrome, Research and Practice : The Journal of the Sarah Duffen Centre*, *12*(2), 138–140. https://doi.org/10.3104/REPORTS.2005

Yasuda, S., Liang, M. H., Marinova, Z., Yahyavi, A., & Chuang, D. M. (2009). The mood stabilizers lithium and valproate selectively activate the promoter IV of brain-derived neurotrophic factor in neurons. *Molecular Psychiatry*, *14*(1), 51–59. https://doi.org/10.1038/SJ.MP.4002099

Yu, F., Zhang, Y., & Chuang, D. M. (2012). Lithium reduces BACE1 overexpression, β amyloid accumulation, and spatial learning deficits in mice with traumatic brain injury. *Journal of Neurotrauma*, *29*(13), 2342–2351. https://doi.org/10.1089/NEU.2012.2449

Zamponi, E., Zamponi, N., Coskun, P., Quassollo, G., Lorenzo, A., Cannas, S. A., Pigino, G., Chialvo, D. R., Gardiner, K., Busciglio, J., & Helguera, P. (2018). Nrf2 stabilization prevents critical oxidative damage in Down syndrome cells. *Aging Cell, 17*(5), e12812. https://doi.org/10.1111/ACEL.12812

Zeineddine, D., Hammoud, A. A., Mortada, M., & Boeuf, H. (2014). The Oct4 protein: more than a magic stemness marker. *American Journal of Stem Cells*, *3*(2), 74.

Zhang, J., He, L., Yang, Z., Li, L., & Cai, W. (2019). Lithium chloride promotes proliferation of neural stem cells in vitro, possibly by triggering the Wnt signaling pathway. *Animal Cells and Systems*, *23*(1), 32. https://doi.org/10.1080/19768354.2018.1487334

Zhang, X., Guo, J., Wei, X., Niu, C., Jia, M., Li, Q., & Meng, D. (2018). Bach1: Function, Regulation, and Involvement in Disease. *Oxidative Medicine and Cellular Longevity, 2018.* https://doi.org/10.1155/2018/1347969

Zhang, X., Heng, X., Li, T., Li, L., Yang, D., Zhang, X., Du, Y., Doody, R. S., & Le, W. (2011). Long-term treatment with lithium alleviates memory deficits and reduces amyloid-β production in an aged Alzheimer's disease transgenic mouse model. *Journal of Alzheimer's Disease*, *24*(4), 739–749. https://doi.org/10.3233/JAD-2011-101875

Zhao, Q., Liu, H., Cheng, J., Zhu, Y., Xiao, Q., Bai, Y., & Tao, J. (2019). Neuroprotective effects of lithium on a chronic MPTP mouse model of Parkinson's disease via regulation of α-synuclein methylation. *Molecular Medicine Reports*, *19*(6), 4989–4997. https://doi.org/10.3892/MMR.2019.10152/HTML

Zuccato, C., Belyaev, N., Conforti, P., Ooi, L., Tartari, M., Papadimou, E., MacDonald, M., Fossale, E., Zeitlin, S., Buckley, N., & Cattaneo, E. (2007). Widespread Disruption of Repressor Element-1 Silencing Transcription Factor/Neuron-Restrictive Silencer Factor Occupancy at Its Target Genes in Huntington's Disease. *Journal of Neuroscience*, *27*(26), 6972–6983. https://doi.org/10.1523/JNEUROSCI.4278-06.2007

Zuccato, C., Tartari, M., Crotti, A., Goffredo, D., Valenza, M., Conti, L., Cataudella, T., Leavitt, B. R., Hayden, M. R., Timmusk, T., Rigamonti, D., & Cattaneo, E. (2003). Huntingtin interacts with REST/NRSF to modulate the transcription of NRSE-controlled neuronal genes. *Nature Genetics*, *35*(1), 76–83. https://doi.org/10.1038/NG1219

LIST OF PUBLICATIONS

Publications:

Lam, X.-J., Xu, B., Yeo, P.-L., Cheah, P.-S., & Ling, K.-H. (2023). Mitochondria dysfunction and bipolar disorder: From pathology to therapy. *IBRO Neuroscience Reports, 14,* 407–418. https://doi.org/10.1016/J.IBNEUR.2023.04.002

Lam, X.-J., Maniam, S., Cheah, P.-S., & Ling, K.-H. (2023). REST in the Road Map of Brain Development. *Cellular and Molecular Neurobiology*, *43*(7). https://doi.org/10.1007/s10571-023-01394-w

Lim, C.-T., **Lam, X.-J.**, Crystal, A.-A., Huang, T., Jusoh, N., Cheah, P.-S., & Ling, K.-H. (2024). Reduced REST Expression in Neural Progenitor Cells, Adult Cortex, and Impaired REST Nuclear Translocation in the Prefrontal Cortex of Ts1Cje Mouse Model of Down Syndrome. *Neurochemical Journal,* *18*(1), 147–161. https://doi.org/10.1134/S1819712424010148

Huang, T., **Lam, X.-J.**, Lim, C.T, Jusoh, N., Fakurazi, S., Cheah, P.S. & Ling, K.H. (2024). Understanding Perspectives and Research Trends in Down Syndrome Neuropathogenesis: A Bibliometric Analysis. *Journal of Intellectual Disabiity.* https://doi.org/10.1177/17446295241299160

Lam, X.-J., Maniam, S., Ling, K.H. & Cheah, P.S. (2025). Lithium Restores Nuclear REST and Mitigates Oxidative Stress in Down Syndrome iPSC-derived Neurons. *Neuroscience, 567,* 86–95. http://dx.doi.org/10.1016/j.neuroscience.2024.12.061

Proceedings:

Lim, C.-T., **Lam, X.-J.**, Crystal, A.-A., Huang, T., Jusoh, N., Cheah, P.-S., & Ling, K.-H. (2023). Dysregulation Of REST During Brain Development of The Ts1cje Mouse Model for Down Syndrome. *IBRO Neuroscience Reports, 15,* S112. https://doi.org/10.1016/j.ibneur.2023.08.110

Honors and Awards:

Best Oral Presenter Award (as presenter) – Lim CT, Lam XJ, Crystal AA, Huang T, Jusoh N, Cheah PS & Ling KH. "REST dysregulation in the Down Syndrome Ts1Cje mouse brain". 22 – 24 November 2022, 3rd International Anatomical and Biomedical Scientific Conference

2nd Best Oral Presenter Award (as co-author) – Lim CT, Lam XJ, Crystal AA, Huang T, Jusoh N, Cheah PS & Ling KH. "REST dysregulation in the brain of Ts1Cje mouse model of Down Syndrome". 30 September – 3 October 2022, 30th Malaysian Society of Neurosciences Annual Scientific Meeting

3rd Best Oral Presenter Award (as presenter) – Lam XJ, Maniam S, Ling KH & Cheah PS. "Neuroprotective potential of lithium-mediated REST restoration in Down syndrome induced pluripotent stem cell (iPSC)-derived Neurons". 29 – 30 September 2023, 31st Malaysian Society of Neurosciences Annual Scientific Meeting

Conferences:

30th Annual Scientific Meeting of the Malaysian Society of Neurosciences (as delegate): 30 September 2022 – 2 October 2022, at Kuala Lumpur, Malaysia.

3rd International Anatomical and Biomedical Scientific Conference (as oral presenter): 22 – 24 November 2022, virtual.

26th Thai Neuroscience Society Conference (as poster presenter): 9 June 2023, at University Naresuan, Thailand.

Neuroscience: Breach the Research Barrier (as delegate): 15 June 2023, at Universiti Putra Malaysia

11th IBRO World Congress of Neuroscience (as poster presenter): 9 – 11 September 2023, at Granada, Spain.

31st Annual Scientific Meeting of the Malaysian Society of Neurosciences (as oral presenter): 29 September – 1 October 2023, at Sarawak, Malaysia.

School:

IBRO/APRC Associate School of Neuroscience 2023: "Neuroscience and Brain Disease: From translation to intervention" : 6 – 11 June 2023, at University Naresuan, Thailand.